POLITECNICO DI MILANO

Scuola di Ingegneria Industriale e dell'informazione

Corso di Laurea in Ingegneria Energetica

Design and optimization of operating theater ventilation and contamination control system through an experimentally validated CFD model

Relatore: Prof. Cesare Maria JOPPOLO

Co-relatore: Ing. Francesco ROMANO

Tesi di Laurea di:

Chiara DI SANTIS Matr. 783814

Anno Accademico 2012 - 2013

Acknowledgements

A questo punto del mio percorso è per me spontaneo, più che doveroso, fare alcuni ringraziamenti a chi ha accompagnato, con conoscenze tecniche o semplicemente con la sua vicinanza, la messa a punto del mio lavoro di tesi e la grande avventura di questi cinque anni al Politecnico di Milano. Innanzitutto ringrazio il professor Joppolo per la sua fiducia e per avermi fatto scoprire che anche l'ingegneria ha un suo lato profondamente umano ed 'artistico'. Più che doveroso è un grazie all'ingegner Francesco Romano che mi ha saputo accompagnare e sostenere durante tutto il periodo della tesi offrendomi, senza remore, molto del suo tempo. La mia gratitudine va, oltre i confini fisici italiani, al professor Luca Marocco che con pazienza ha seriamente considerato le mie richieste di aiuto, trasmettendomi, oltre che una conoscenza intelligente e ricca, anche una grande passione per il suo lavoro. Ringrazio tutto il gruppo di Fluent e in particolare Claudio Basilico per le preziose consulenze fornitemi soprattutto nei momenti iniziali della tesi quando le mesh minavano la mia pazienza. Grazie alla SagiCofim S.p.a. per avermi considerato sempre professionalmente valida e per avermi supportata in particolar modo durante la fase sperimentale mettendo a dispozisione strumenti e tempo.
Uscendo dal mondo puramente didattico ringrazio la mia famiglia che ha accettato di avere un' ingegnera in casa e che mi ha dato piena libertà appoggiandomi in tutte le scelte e grazie a Giovanni che mi ha aiutata a non perdere la bussola e a non cedere alla tentazione inevitabile dello sconforto. Un ultimo ma grande grazie a tutti gli amici incontrati in questi cinque anni che mi hanno permesso di stare davanti alla realtà con uno sguardo sempre meno rivolto verso me stessa e mi hanno aiutata a diventare un po' più grande.

Homo sum,
humani nihil a me
alienum puto

Publio Terenzio Afro

Contents

List of Figures

List of Tables

Abstract

The design of a heating, ventilating and air conditioning (HVAC) system for an operating room is aimed to prevent the risk of infections during surgical operations while maintaining an adequate comfort condition for the patient and the surgical staff. For this reason, it is very important to design an efficient HVAC system. Nowadays new technologies are applied in this field and the CFD modeling represents a very important tool in order to simulate the real behavior of the air flow entering in an operating theater and its ability of removal of particles generated and aero-transported. In fact, its advantages consist in facility of the implementation, saving of money and time comparing with the experimental campaign, and possibility to test in short time other configurations to find an optimum in the design of operating theaters. The aim of this work is the creation of a CFD model of an existing operating theater which is mainly used for the cardiac-surgery, equipped with a partial unidirectional ventilation system and classified, ISO 5 'in operational' conditions, according to the UNI EN ISO 14644-1. The supply air comes from a ceiling filter system composed by 23 absolute filters H14, in accordance with the UNI EN 1822 and assures the unidirectional flow on the surgical table and in the area in which the staff operates. For the internal configuration of the operating theater and the qualification test conditions, it was followed the German standard DIN 1964-4. This is complete for many aspects, and moreover, it gives accurate indications to conduct the test, so that it is repeatable. After the design of 3D-model, meshing simulation of one of the configuration prescribed by the DIN 1964-4, by means the CAD and simulation tools of ANSYS, a validation stage, with an experimental campaign, has followed, in order to create a consistent model adoptable in the future. With the validated model, it was possible to test other configurations different by the real ones in order to show some critical aspects to take into account during the usage of the operating theater and during its design.

Keywords: Operating theater, Contamination control, Ventilation, CFD simulation, Model validation, Experimental tests

Italian version

La progettazione di un sistema di riscaldamento, ventilazione e condizionamento dell'aria (HVAC) per una sala operatoria, è volto a prevenire il rischio di infezione durante le operazioni chirurgiche per il paziente e per l'equipe medica e a mantenere un'adeguata condizione di comfort per gli stessi. La corretta progettazione di un sistema HVAC, dunque, è di primaria importanza. Ai nostri giorni, in questo campo, sono state introdotte nuove tecnologie, e la modellazione CFD, per simulare il reale comportamento dei flussi d'aria e la sua abilità nel rimuovere il particolato generato e aerotrasportato, rappresenta uno strumento fortemente innovativo. Infatti, tra i suoi vantaggi si evidenziano la semplicità di implementazione, il risparmio di costo e tempo rispetto alle tradizionali campagne sperimentali, e la possibilità di testare, in breve tempo, altre configurazioni per trovare un punto di ottimo durante la progettazione di una sala operatoria. Il cuore del lavoro è stato quindi la creazione di un modello CFD di una sala operatoria esistente che è prevalentemente utilizzata per operazioni di cardiochirurgia, dotata di sistema di ventilazione unidirezionale parziale e, conformemente alla UNI EN ISO 14644-1, classificata ISO 5. L'aria di mandata proviene da un plafone filtrante composto da 23 filtri assoluti H14, secondo la UNI EN 1822 e garantisce flusso unidirezionale nell'area del tavolo operatorio in cui agisce lo staff medico. Per le condizioni di test e la configurazione della sala, si è scelto di seguire la normativa tedesca DIN 1964-4. Questa, a differenza delle altre, fornisce condizioni di test precise così da renderlo ripetibile. Dopo la fase di modellazione 3D, meshatura e simulazione di una delle due configurazioni previste dalla DIN 1964-4, per mezzo degli strumenti CAD e di simulazione di ANSYS, è seguita la fase di validazione mediante una campagna sperimentale, al fine di creare un modello consistente, fruibile nel futuro. A valle della validazione, è stato possibile testare altre configurazioni alternative a quella reale, al fine di rilevare alcuni aspetti critici da considerare durante l'utilizzo della sala operatoria e in fase di progettazione.

Parole chiave: Sala operatoria, Controllo della contaminazione, Ventilazione, Simulazione CFD, Validazione del modello

Estratto

La progettazione di un sistema di riscaldamento, ventilazione e condizionamento dell'aria (HVAC) per una sala operatoria, è volto a prevenire il rischio di infezione durante le operazioni chirurgiche per il paziente e per l'equipe medica e a mantenere in secondo luogo un'adeguata condizione di comfort per gli stessi. Le infezioni da sito operatorio (o Surgical Site Infections, SSI) sono le terze per frequenza che colpiscono i ricoverati in ospedale (circa il 14-16% di tutti i casi di infezione dei pazienti ricoverati). Fin dagli anni '60, quando la tecnologia delle cleanroom fu applicata per la prima volta nelle sale operatorie, fu evidente che, avere un buon livello di pulizia e un flusso d'aria ben organizzato, potesse ridurre l'incidenza delle SSI. Il numero di infezioni post-chirurgiche è strettamente connesso all'incremento della durata di degenza e, conseguentemente, all'incremento degli oneri economici per la struttura ospedaliera stessa. L'interesse intorno a questa materia ha senza dubbio una portata rilevante. Ci sono numerosi aspetti che potrebbero condizionare l'insorgere di tali infezioni, vale a dire: fattori legati al paziente (come la suscettibilità alle infezioni), fattori legati al campo chirurgico (come il pennacchio termico dal sito), fattori legati alla camera (come la pulizia della sala operatoria) e fattori legati all'HVAC (come i ricambi orari e la direzionalità dei flussi). La contaminazione del sito chirurgico è una causa inevitabile dell'insorgere delle infezioni da sito operatorio. In accordo con la letteratura, si può affermare che la sorgente primaria di contaminazione in una sala operatoria è la presenza umana. Le particelle rilasciate dal corpo mediante la normale attività di respirazione, traspirazione e sudorazione, in aggiunta a quelle dovute alla desquamazione della cute o rilasciate dai capi di abbigliamento, sono tra le più frequenti cause di infezione in caso di presenza di ferite chirurgiche esposte durante una normale operazione. Esse rappresentano un pericolo poichè circa il 5-10% possono essere veicolo di batteri. Per quanto detto, l'aria nella sala operatoria deve essere il più possibile asettica, e deve esibire una umidità e temperatura controllate; inoltre i flussi d'aria devono essere diretti in modo tale da evitare la ricircolazione dei microbi aerotrasportati dalle particelle e da non recare disturbo all'equipe medica operante. A causa delle condizioni della qualità dell'aria

interna, le sale operatorie costituiscono la più costosa tra le applicazioni nel campo dell'assistenza sanitaria (raggiungendo anche il 33% dei costi totali). Gli alti consumi energetici sono dovuti agli elevati carichi per il riscaldamento, raffrescamento e per la ventilazione per un funzionamento continuo nelle 24 h. Vista la complessità del tema, lo sviluppo della tecnologia ha permesso di studiare la problematica della ventilazione nelle sale operatorie mediante strumenti alternativi a quelli puramente sperimentali. In particolare un contributo consistente si sta traendo negli ultimi anni dalla tecnica di simulazione fluidodinamica, comunemente nota con l'acronimo CFD (Computational Fluid Dynaycs). L'importanza scorta nell'utilizzo di questo mezzo consiste principalmente nella scommesa di poter arrivare a evitare gli oneri di costo e di tempo che una campagna sperimentale comporta. Seguendo questa intuizione, il lavoro qui presentato è volto allo studio della movimentazione dei flussi d'aria per la rimozione del particolato aerotrasportato all'interno di una sala operatoria realmente esistente. Lo scopo del lavoro consiste dunque nella costruzione di un modello virtuale della sala operatoria che sia validato da una campagna sperimentale in modo da poter essere fruibile nel futuro per considerazioni in fase progettuale o per evidenziare criticità che alcuni comportamenti inadeguati potrebbero causare. Al fine di studiare il comportamento del plafone filtrante esistente nella sala operatoria in esame, si è deciso di procedere organizzando all'interno dell'ambiente simulato un test per la verifica del grado di protezione della zona critica in cui si svolge l'operazione chirurgica. Per questo scopo si sono consultate numerose normative europee in merito ai sistemi HVAC per le sale operatorie e per gli ambienti ad esse asserviti. Molti degli standard e delle normative europee sulla progettazione, controllo e manutenzione dei sistemi di ventilazione e controllo della contaminazione nelle sale operatorie, fanno diretto riferimento alla menzionata UNI EN ISO 14644, per quanto rigurda la contaminazione particellare. Tra tutti gli standard e le linee guida esistenti circa lo svolgimento di test per la verifica del grado di protezione del sistema di ventilazione e controllo della contaminazione ambientale, la norma tedesca DIN 1964-4 risulta più completa e particolareggiata nella descrizione della procedura di conduzione del suddetto test. Ciò permette di effettuare la verifica del grado di protezione in condizioni ripetibili e quindi anche agevolmente confrontabili.

Caso di studio

La sala operatoria in esame è denominata B2 e fa parte di un blocco operatorio di un ospedale sito nell'hinterland milanese. Essa è stata ultimata nel 2010 ed è utilizzata prevalentemente per operazioni di cardiochirurgia. La

sala è a pianta quadrata con 7 m di lato, resa ottagonale nei sui spigoli, per un totale di 46.5 m^2 e un volume utile di 144 m^3 (l'altezza è 3 m). La geometria entro cui è stata sviluppata l'analisi è stata fornita dalla Sagicofim S.p.a, azienda costruttrice ed installatrice del plafone filtrante; esso è collocato a soffitto e le sue dimensioni sono 2800×2800 mm. I filtri che sono installati in esso sono filtri assoluti classificati, secondo la UNI EN 1822, come H14. In tutti il plafone consta di 23 filtri collocati nel plenum di mandata. Le dimensioni di ogni singolo filtro sono 575 x 575 mm. La caratteristica di questo plafone è la differenziazione della velocità dell'aria di mandata: i 3 filtri centrali mandano aria a 0.45 m/s, 6 filtri intorno ad essi mandano aria a 0.35 m/s, i restanti mandano aria a 0.25 m/s. Le riprese dell'aria sono due per spigolo, per un totale di 8. Per ogni spigolo abbiamo una ripresa posta a 300 mm dal soffitto di dimensioni 300×600 (WxL) e una posta a 300 mm dal pavimento di dimensioni 300×900. Il sistema di ventilazione della sala operatoria considerata è stato progettato in modo che sia classificata ISO 5 nella configurazione 'in operational' secondo la UNI EN 14644-1, per cui, conformemente alla norma UNI 11425 si tratta di una sala operatoria a elevatissima qualità dell'aria. Come già accennato, per la conduzione del lavoro si è fatto riferimento alla norma tedesca DIN 1964-4. Esse presenta in modo dettagliato quale debba essere la configurazione della zona critica sotto il plafone filtrante, per condurre i test di verifica. In particolare oltre al tavolo operatorio sono presenti 5 manichini (dummies) rappresentati come cilindri la cui sommità presenta una calotta semi emisferica. Di questi 4 sono di altezza 180 cm mentre uno è di 120 cm. I primi raffigurano l'equipe medica mentre l'ultimo l'anestesista in posizione seduta. Un sesto dummy, rappresentato come un semplice cilindro di altezza 150 cm rappresenta il macchinario. Nella sala sono posizionati poi 6 cilindri di altezza 30 cm e diametro 25 cm raffiguranti i diffusori di particolato sintetico per la conduzione delle prove in modalità 'operational simulato'. É specificata la portata d'aria complessiva uscente da essi e la concentrazione di particolato presente in essa. Inoltre come è già stato presentato, la norma differenzia due casi diversi per la valutazione della qualità del plafone rispetto alla contaminazione prodotta all'interno della zona critica o all'esterno di essa, distinguendo due disposizioni diverse dei generatori di particolato. Essendo presenti nella stanza anche due lampade scialitiche, di esse verrà tenuto conto anche in fase di simulazione oltre che in fase di misurazione durante le prove sperimentali. Infatti, mentre la base di esse non è direttamente investita dal flusso unidirezionale, i bracci e le parti che emettono luce sono posizionate in prossimità della zona critica e possono essere motivo di distorsione delle linee di flusso oltre che fonte di calore. Per la costruzione del modello 3D relativo al nostro caso studio ci siamo avvalsi del Design Modeler fornito da Ansys. Seguendo

le specifiche costruttive relative alla sala operatoria, è stato possibile creare la stanza nella sua interezza. Rimanendo conformi alla normativa DIN 1964-4 è stato possibile disporre all'interno della camera i manichini (o dummies), il tavolo operatorio e i generatori di particolato. Sul soffitto sono stati posti i 23 filtri componenti il plafone, in modo del tutto corrispondente al caso reale. Allo stesso modo sono state riprodotte fedelmente le posizioni delle riprese ai 4 spigoli della camera. Sono state incluse le due porte con gli spifferi che esse lasciano con il pavimento e le lampade scialitiche. Per quanto riguarda il posizionamento dei diffusori di particolato, poichè si è scelto di verificare entrambe le configurazioni indicate dalla norma, sono stati creati due diversi modelli 3D. Una volta conclusa la modellazione CAD il progetto è stato importato nel meshatore di Ansys. In tutti i casi gli elementi della mesh sono di tipo tetraedrico. Il fluido di lavoro aria secca con proprietà chimico-fisica costanti, mentre il particolato utilizzato è il DEHS conformemente alla UNI EN 1822-2. Le simulazioni sono state condotte mediante Fluent (ANSYS) in regime transitorio per permettere una buona convergenza dei risultati e superare alcune limitazioni del programma. Il modello di turbolenza utilizzato è il $\kappa-\varepsilon$ Realizable mentre sono state usate Scalable Wall Function per definire il comportamento del fluido in prossimità della parete. Per l'accoppiamento pressione-velocità si è usato uno schema SIMPLE e per tutte le simulazioni si è raggiunta la convergenza con discretizzazioni del secondo ordine.

Validazione del modello

Al fine di validare il modello sono state effettuate le prove sperimentali all'interno della sala operatoria sopra descritta. Si è scelto di effettuare il test per la verifica del grado di protezione, per entrambe le configurazioni indicate dalla norma: per comodità, A1, è detta la configurazione che prevede il test di verifica della classe di protezione in presenza di contaminazione proveniente dall'esterno della zona critica e A2 è detta quella con contaminazione proveniente dall'interno di essa. Per poter rendere disponibile la sala in un tempo ragionevole ma permettere anche di entrare più nel dettaglio durante la fase di validazione, si sono effettuate misure aggiuntive di temperatura, velocità e concentrazione di particolato, in punti significativi all'interno della sala per la sola configurazione con generazione proveninete dall'interno della zona critica (chiamato caso A1). I risultati ottenuti sono stati confrontati con quelli rilevati in fase di simulazione. Le due simulazioni, nelle configurazioni standard della sala con la contaminazione interna ed esterna, sono risultarte in larga parte fedeli nella descrizione del fenomeno reale. In particolare, i valori di contaminazione aerotrasportata sopra il tavolo operatorio

sono confrontabili con quelli ottenuti durante la campagna sperimentale. Uno scostamento è presente solo per i dati campionati nella zona del torace, nel centro del tavolo operatorio. Questo fatto è stato ricondotto alla presenza dei manichini utilizzati durante il test composti da materiale in parte deteriorato e quindi soggetto a desqumazione. Per giungere a tale conclusione è stato effettuato un apposito test con la generazione di particolato artificiale spenta e con i manichini funzionanti. Per quanto riguarda i valori di temperatura dell'aria essi non superano il 3% di scostamento dalle misure sperimentali. I valori di velocità dell'aria invece presentano molte corrispondenze e alcune anomalie (errori al massimo pari al 24%) giustificabili da alcune evidenze. Infatti, il layout della sala reale non è esattamente analogo a quello simulato. All'interno dello spazio operatorio infatti sono presenti macchinari d'ausilio all'attività chirurgica non previsti in fase di sperimentazione. Essi, in alcuni punti, costituituiscono vere e proprie barriere al flusso deviandone il regolare percorso. Per questo motivo si è ritenuto ragionevole considerare esclusivamente i punti di flusso indisturbato per condurre in modo appropriato la fase di validazione. Anche i valori di concentrazione della contaminazione particellare subiscono l'influenza dei componenti chirurgici aggiuntivi sopra menzionati, in aggiunta al deterioramento dei manichini già descritto. Inoltre è da notare un altro fatto. Il tavolo operatoria, una volta giunti sul sito chirurgico, è risultato disassato circa 10 cm rispetto alla mezzeria della stanza. Ciò significa che i tre filtri ad alta velocità presenti nel plafone soprastante non vanno a lavare in modo ottimo la contaminazione presente sul tavolo. Globalmente la fase di validazione è stata ritenuta soddisfacente e ha rilevato alcune criticità di cui sarà opportuno tener conto in future modellazioni.

Analisi di altre configurazioni della sala

Il lavoro, dopo la fase di validazione, è proceduto con la simulazione di configurazioni alternative della sala. Questo ha come scopo fondamentale il mettere in luce alcuni scenari che potrebbero verificarsi durante l'utilizzo scorretto della sala operatoria. Sono state quindi effettuate quattro simulazioni aggiuntive con:

- un angolo della sala con entrambe le riprese occluse (caso B2);
- l'ingresso principale dotato di porta scorrevole aperta (caso C2);
- una nuova configurazione del plafone filtrante con un unico supporto per entrambe le lampade scialitiche collocato nel centro in sostituzione di un filtro ad alta velocità (caso D1 e D2).

Il caso B2 è stato condotto al fine di evidenziare come reagisca il sistema di ventilazione quando entrambe le riprese nell'angolo opposto a quello più prossimo all'ingresso principale sono ostruite. Si è scelto questo angolo perchè è quello solitamente più ingombro durante lo svolgimento dell'operazione chirurgica. Le simulazioni hanno evidenziato la presenza di un ricircolo di aria, e quindi di particolato trasportato, nei pressi dell'angolo che presenta l'ostruzione delle griglie, ma il sistema di ventilazione è comunque in grado di garantire la pulizia sul tavolo operatorio. In caso C2, simulato con la porta scorrevolo principale completamente aperta, ha evidenziato l'ovvio trascinamento dei flussi d'aria verso l'esterno della sala operatoria, ma questa tendenza rigurada in paricolare le portate d'aria uscenti dai filtri a velocità minori. Per questo motivo sul tavolo operatorio è comunque garantita l'assenza di particolato. Le simulazioni D1 e D2 sono state condotte con la configurazione del plafone con un unico supporto centrale per entrambe le lampade scialitiche, in sostituzione di un filtro con diffusione dell'aria ad alta velocità. Esse non differenziano particolarmente per la fluidodinamica ed, in entrambe i casi, si è osservata la formazione di un vortice all'interno della zona critica, in prossimità del tavolo operatorio. L'assenza del filtro centrale e la presenza dei bracci delle lampade sotto il flusso unidirezionale ha comportato questa situazione che potrebbe essere fortemente rischiosa nel caso in cui parte della contaminazione si trovasse nei pressi di tale vortice: essa sarebbe condotta in breve tempo in prossimità del paziente. Cone le condizioni ideali di contaminazione generata in fasi di simulazione non si è tuttavia riscontrata contaminazione sul tavolo operatorio.

Conclusioni

In conclusione si puossono ritenere interessanti i risultati ottenuti circa la comparazione tra dati sperimentali e simulati. Le simulazioni hanno riprodotto in modo considerevolmente corrispontente l'effettivo comportamento dei flussi d'aria visualizzati in fase di prova mediante smoke test. Sono necessarie delle migliorie sia nella simulazione che per quanto rigarda la realizzazione dei componenti per lo svolgimento delle prove in sala operatoria.

Introduction

The design and testing process of an operating theater (OT) is a complex task to carry out only by using a single knowledge or a simple standard or guideline. Operating theater is a space where many different medical operations take place and therefore it is necessary to approach the problem in a multidisciplinary way by using both the best techniques coming from engineering and medical sciences. Of course, engineering science can only afford part of the problems which arise in an OT, such as problems related with environmental control or medical devices. The design of a heating, ventilating and air conditioning (HVAC) system for an operating room is aimed to prevent the risk of infections during surgical operations while maintaining an adequate comfort condition for the patient and the surgical staff [1].
Hospital-Acquired Infections (HAI), or in medical literature known as nosocomial infection, are infections whose development are favored by a hospital environment, such as one acquired by a patient during a hospital visit or one developing among hospital staff. HAI are estimated to affect approximately 10-11% of all patients as a result of care and treatment. Andersson [2] in her thesis mentions that the most common infections are, in descending order, the urinary tract, the lower respiratory tract, surgical wounds, followed by the blood stream. The Surgical Site Infections (SSI), on the contrary are infections that normally are acquired on site during a surgical operation and can be classified into three main categories: superficial, deep incisional and organ depending on the type of operations. SSIs infections are found to be associated with increased postoperative length of stay, increased costs, hospital re-admission rates and the use of antimicrobial agents. However, the adverse effect related to SSI varies depending on the category of surgery and type of SSI. Andersson [2] found that the greatest increase in length of stay was observed for cardiovascular surgery, with a mean extension of 13.7 days. Rui et al. [3] stated that, in 1980, it was estimated that an SSI increased a patient's hospital stay by approximately 10 days and an additional cost of 2000 $. The interest to intervene in a significant way to reduce the causes of these contingency is obvious.
There are many aspects that could influence these infections: factors related

to the patient (as the susceptibility to infections), others related to the surgical site, factors related to the HVAC system and the contamination control within the OT environment. The contamination on surgical site is a unavoidable reason of the occurrence of SSIs. The developments in the control of infections include implementation of new methods of sterilization and surgical techniques, the construction of shield, the study of optimization and renovation of ventilating system. According to the literature it can be stated that the primary sources of contamination in an operating theater are the scales of the skin and the particles (biologically active or inert) released by the human body during the normal activity of breathing, transpiration and sweating plus the particles released from standard personnel clothing. Such particles are placed in a dimensional range of 0.5-10 μm and, settling on the surgical site, they could be origin of potential infections [3]. A person releases about 10 million particles/day (between 0.5-5 μm). The release rate is 10'000 particles/min for a normal walk. About 5-10% of these particles may carry bacteria. The patient is not usually a significant contaminant source because his or her movements are minimal [4]. For this reason, clothing is an important issue for medical personnel. A simple head cover (hood plus face mask) made of disposable non-woven materials is commonly used, while it has also been suggested to use a complete helmet aspirator system in order to reduce emission of bacteria from the head. The routine use of surgical face masks is a common infection control measure in an OT, although the influence of their use has yet to be conclusively demonstrated [5].
In many aspects, an OT environment can be seen as a special cleanroom where are carried out different types of processes (operations) by different personnel (medical staff). Therefore, almost all the national and European standards which deal with operating theaters and related controlled environments have common roots from the standards and procedure used for cleanrooms, as the ISO 14644 [20] for particle contamination and the ISO 14698 [29] for microbiological contamination. In the last years many national standards have been written with the aim to rule the design and the performance test procedure of operating theaters from the point of view of airborne contamination control. However, there is no complete consensus and uniformity among the various design standards and even more there is a large inequality when dealing with the real performance tests to carry out in OT in order to measure the protection level of the entire OT system in operational conditions. Contamination performance test in OTs are quite time consuming and expensive. Even more OTs are places where time occupancy, availability, reliability and cleanliness guarantee are important parameters, especially in emergency cases, therefore the time available for carrying out real contamination and ventilation performance tests is always short and as

in many cases in reality null.

Based on what aforementioned the scope of the present master thesis work consists of in the design of a virtual model of an operating theater which is able to simulate the ventilation and contamination control performance of a real operating room following the specifications of a test procedure. The computational fluid dynamics technique was chosen as the right tool in order to carry out the proposed work. The advantages of using CFD tools are many, first of all it is cheaper and less invasive than the traditional experimental test campaign in contamination controlled environments as the operating room, secondly it gives the possibility to forecast and study different solution and case scenarios without interfering with the usage of a real and important space as it is an OT. In this case it is possible to study the level of performance of the OT ventilation system in different scenarios and validate the simulated results with the data obtained during the test for the validation process. As first step of this work, a brief introduction on the operating theaters performances and techniques has been given in Chapter 1. Chapter 2 focuses on the main standards, procedure and technical specifications issued by national and international institutions on the field of operating theaters and their contamination control. This chapter also gives an overview of the pro and con of those documents especially when treating the experimental contamination performance test. Chapter 3 introduces the operating theater chosen as reference OT for the CFD model and for carrying out the real test according to the procedure chosen in Chapter 2 while Chapter 4 explains the CFD model theory, assumptions and setting used during the simulations carried out in this work. Finally, Chapter 5 describes the various scenarios of the OT simulated and their results. For two of the scenarios treated there is also a data validation with the real measurement carried out in the reference OT using the same layout and setting suggested by the test procedure chosen.

Chapter 1

The operating theaters and their performances

In the matter of what mentioned before, the air in an OT must be as clean as possible, at a reasonably constant temperature and humidity, and must have relatively low velocity in order to avoid drafts and swirls that promote the recirculation of particles which may carry microbes and may disrupt the procedures during an operation.
The work by Blower and Crew [7] and Charneley in the late 1960s [8] and Whyte et al. and Lidwell et al. [9] at the beginning of the 1980s has shown the important correlation between the airborne wound contamination and ventilation system. In particular, they established the linear relationship between the level of bacterial air contamination and the frequency of "deep sepsis" following joint replacement surgery. The ventilation rate is expressed as the volumetric air flow input, divided by the volume of the space, e.g. number of air changes per hour (ACH).
The basic aim of ventilation system in OT is to prevent airborne microbial contaminants from entering the surgical wound of patient above the surgical table. The secondary aim is to provide reasonable working conditions for the OT staff in order to avoid causes of discomfort and therefore an increase of particle release from the staff. The first intent is obtained by the filtration of the air, air distribution, air dilution and room pressurization. The comfort of surgical staff is obtained by proper conditions of temperature and humidity and by a suitable technical clothing system.
The desirable conditions of temperature, humidity, filtration level, particle concentration, air velocity etc., can be reached by proper design, installation, operation and maintenance of the equipment, such as the HVAC equipment and lighting systems of the space and the other medical tools within an OT. Due to their demanding indoor air quality conditions, operating theaters con-

stitute the most expensive sector of the healthcare establishment mandating an efficient management, reaching 33% of the total cost. The other energetic consumptions are due to high heating, refrigerating and ventilating load for a continuous operation in 24 hours a day and seven days a week [10]. Even though during non-activity periods the entire ventilation system can work on set-back conditions, e.g. reducing airflow rate.

A contamination controlled environment is characterized by the definition of the following parameters:

- temperature, relative humidity and air inlet-velocity: they should ensure the indoor thermohygrometric conditions evaluated like correct for the correct conduction of the process and the wellness of the staff;
- supply air: it should be in the right quantity and should exhibit a proper degree of filtration to maintain airborne particles concentration under the limits of the contamination class considered like suitable for the product/process to realize, in the environment, in operational condition. The same is for the microbiological concentration expressed in CFU (Colony Forming Unit) per cubic meter of air, under the set value. Moreover, supply air must take into account also for the airflow filtration necessary for maintaing the OT environment in overpressure with respect to the adjacent ambients;
- ambient pressure: it should be maintain over pressure in order to avoid infiltrations of uncleaned contaminated air from surrounding environments.

1.1 Temperature and humidity

Indoor air temperature must be maintained into the recommended range to ensure acceptable conditions. The international standards, introduced in the next chapter, usually indicate a range between 20-14°C. In practice it's impossible to create acceptable conditions for the 100 % of the occupants because, the working staff could have different perceptions due to different activity levels, because of the different positions occupied because of the subjectivity of comfort level perception. The asymmetry of the thermal radiation of the lights above the surgical staff is a potential cause of discomfort. Also the medical clothing has a direct impact on the thermal comfort of the personnel. It is worn by the surgical staff to control the airborne contamination and limit the androgen particle emission but it should be comfortable to ensure the execution of the medical activity without causing the generation of particulate by means of the increase of personnel sweat.

The air humidity must be maintained at an acceptable level because it is closely related to the environmental hygiene and to the thermal comfort conditions perceived by personnel. The humidity control is often obtained treating the ventilation air, increasing (humidification) or decreasing (dehumidification) its water content. An high level of humidity promotes the growth and the transfer of bacteria which could be transported through the air on the water molecules (or another type of particle with dimensions bigger than the bacteria's ones). In addition, an elevated rate of humidity creates thermal discomfort. On the other hand, a low humidity degree increases the rate of blood coagulation which is undesirable during a surgical operation. Furthermore, the humidity level in the air could facilitate the deposition or coagulation of water film of small drops in air ducts and settling in building materials, thus generating the optimal conditions for the proliferation of bacteria and microbes which may be carried by the particles.

Different type of OTs have different conditions which are imposed by the national regulation. For example, in the Table 2.2,there is an extract of the ambient parameters prescribed by the Italian standard UNI 11425:2011 [11] for three type of operating theaters.

Table 1.1: Ambiental parameters in the operating theaters (UNI 11425) [11]

Ambienti	Temperatura [°C]		Umidità relativa [%]		Sovrapressione rispetto all'esterno	Aria esterna	Aria di ricircolo	Classi di pulizia secondo UNI EN ISO 14644-1	Livello di filtrazione finale	Livello di pressione sonora
	Inverno	Estate	Inverno	Estate	[Pa]	[vol/h]	[-]			[dBA]
Sale operatorie a elevatissima qualità dell'aria	≥ 20	≤ 24	≥ 40	≤ 60	15[1)]	15	SI[2)]	ISO 5	H 14	45[3)]
Sale operatorie a elevata qualità dell'aria					15[1)]	15	SI[2)]	ISO 7	H 14	45[3)]
Sale operatorie a qualità dell'aria standard					15[1)]	15	-[4)]	ISO 8	H 14	45[3)]

1.2 Ventilation

As mentioned before, an appropriate ventilation is the primary goal to ensure a safety and controlled condition of internal air quality. Its scope is:

- to reduce particle concentration (which may carry bacteria and virus) up to acceptable concentrations;
- to remove anesthetic gases and smells released during a surgical operation which may disturb the surgical staff and the patients;
- to provide for comfortable working conditions to ease the performance of surgical staff during an operation.

The legislation (DPR 14^{th} January 1997 [12]) requires, for the operating theater, a number of changes of fresh air greater or equal to 15 volumes per hour (ACH), to control particle contamination, by means of continuous dilution process of contaminants which arise inside the OT environment In addition, this amount of fresh air volume is required to maintain the over pressure conditions among the adjoining environments. In the matter of this, it is necessary to underline that usually the operating theater is maintained at a positive pressure relative to corridors and neighboring areas, and rarely underpressure.

A low limit value of fresh air flow is set up during the operational condition of the room, and, considering this, is possible to realize a recirculation with the following cases:

- the recirculated air comes from the same room or from rooms closely related with its, in order to avoid cross-contamination between different environments;
- the recirculated air undertakes the same filtration stages as the fresh air;
- the unjustified increase of fresh air compared with the imposed limit value represents an additional load for the filtering system and entails increasing energetic costs for thermohygrometric treatment.

The trend of air fluxes are related to the positioning of return grilles and of supply air diffusers to collect and control the spread of contaminants, and to delete sacs of polluted air to provide for achieving the desired environmental conditions. The return grilles as the supply diffuser too, exist in different dimensions and geometries in relation with the available space. Balaras et al. [9] supported the idea that, according to the international and national standards, the return grilles should be two at least on the lateral wall: one near the floor in order to remove the anesthetic gases which are heavier than air or particles which are conveyed by air or personnel movements towards floor. The second one, should be positioned near the ceiling, in order to remove in an efficient way anesthetic gases lighter than air, particles or other chemical substance which could be aero-transported by the air during the surgical operation. In addition, they concluded that the optimum layout of the air-return outlets is to have return grilles at every corner of the OT, one at the floor and one at the ceiling level. The air flows should ensure that the direction of the air is from the most demanding (in terms of air quality) towards the ones which required less strict conditions in terms of contamination control. An important fact is to avoid the formation of air sacs where the dirty air is recirculated in the theoretical cleaner areas. The

main air flux shouldn't meet obstacles in particular in the direction where is produced the most relevant contamination around the operating table.

The ventilating systems should work continuously during the surgical operations and also when the operating theaters are not used, or, at least, they should work at a lower ventilating rate, in order to maintain the level of cleanliness of OT environment. Many different parameters may influence the efficacy of the ventilation system adopted in an OT. The airflow velocity at the supply diffusers has been shown to be one of the most important factors when it comes to control distortions in airflow patterns produced, for example, by OR lamps. Chow et al. [13] showed that, if the supply velocity is higher than 0.38 m/s, the buoyant forces from sugical lamps and equipment have a minimal effect on airflow patterns and the transportation of contaminants can proceed undisturbed towards the return outlets grilles. In contrast, an experimental study [3], simulating different air velocities with the same supply area, have demonstrated that increasing the air velocity beyond a certain rate resulted in an increase in CFU deposition. Moreover, if the supply air velocity rate exceeds 0.3 m/s, this results in the development of a vortex above the patient. Nowadays, in the field of operating theaters, four different categories of ventilating system are commonly used:: turbulent airflow, upward displacement airflow, unidirectional airflow and mixed airflow.

1.2.1 Turbulent airflow

The respect of the maximum allowed contaminant concentration derives from the correct combination of quantity and quality of supply air, from the quality of the mixing obtained through the diffusers' throw in relation with the fluid dynamical obstacles (staff, equipment...) and, obviously from the characteristics and distribution of contamination sources.

The inlet flow will be characterized by a proper level of cleanliness thanks to HEPA filters stages installed before diffuser. Air flow will have an high velocity in a way to induce, in the air of the room, convective motions at large scales to increase the diffusion of supply air with the still air present in the room. The principle of functioning of this type of ventilation is based on the concept of the perfect mix of air. Supported by this assumption, the contamination diffusion within an enclosed environment has no preferential direction. Ideally, there is a constant concentration of contaminants (inert, biological, gaseous and radioactive) in each point of the ventilated room. Also the thermohygrometric conditions are considered to be constant throughout the room. A simplified scheme of a turbulent airflow OT is shown in Figure 1.1.

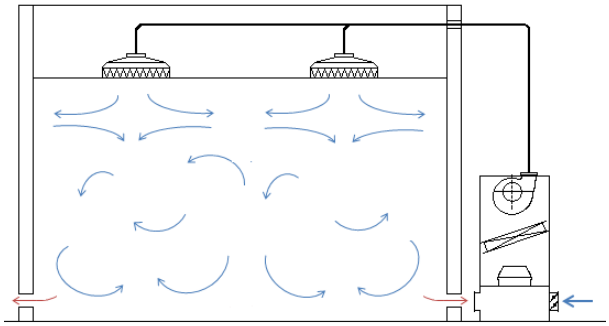

Figure 1.1: Example of turbulent diffusion of air

How can be seen in Figure 1.1, the air is injected from the ceiling and a high inductive air flow is created, in order to ensure a good mixing of the air.

1.2.2 Upward displacement airflow

The upward air-displacement system supplies cool air (2-3°C below ambient temperature) above the floor in each corner of the room. Via thermal convection, the air is subsequently evacuated through return air outlets located at the corners of the ceiling. How it can be seen in Figure 1.2, the air is injected at the level of the floor and gradually it is warmed up by the thermal loads produced in the room by personnel, equipment, computers, lamps and so on. The air, carrying the thermal load, drags along the contaminant released in the room and, reached the ceiling is extracted by the return grilles located in proximity of the ceiling.

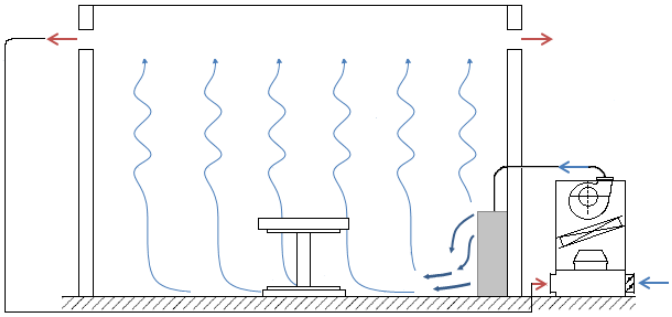

Figure 1.2: Example of upward air-displacement system

Regarding the capacity of the upward displacement system, it has been demonstrated that it is more effective in removing particles compared with the turbulent system. An experimental study [14] comparing turbulent and

upward displacement ventilation system confirms that the upward displacement system is more efficient in removing small particles (<10 μm), whereas no differences were found between the two ventilation systems for particles larger than 10 μm.

1.2.3 Unidirectional airflow

The unidirectional airflow is a flow which is developed in a preferential direction, if it is not obstructed by the equipment in the room. The principle of functioning of this type of ventilation is based on the concept of the piston flux, ideally characterized by parallel flow pattern along air moves away. The idea is to "wash out or swipe away" the contaminants from the clean zone and prevent contaminated air entering in it. This type of diffusion system is used when low values of contamination above large areas are required. This type of ventilation can be arranged for an horizontal or vertical injection of the air. Because it is of interest in this work, it is explain the vertical unidirectional airflow.
From the constructive point of view, this arrangement uses an array of HEPA filters, acting as final filter diffusers, which reaches out over the entire wall or ceiling in order to create a downward flow (in case of diffusers on the ceiling). This flow drags off the impurities inside the entire volume of the room before their settling on the surfaces of the room. At the end, how can be seen in Figure 1.3, the air is extract by the grilles in proximity of the floor, having in this way a vertical unidirectional aiflow.

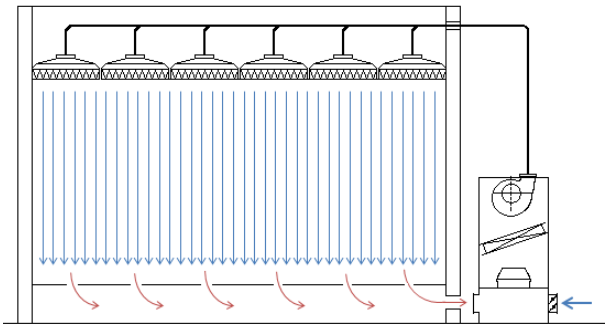

Figure 1.3: Example of vertical unidirectional air diffusion

The air velocity must be maintained at low levels to avoid the development of currents and turbulence which could cause mixes and spreads of bacterias and airborne particulate. For this reason this type of ventilation is usually called 'laminar flow'. This is a improper way to call this ventilation

because the motion regime is turbulent indeed, but it wants to emphasize the low velocity of the airflow patterns, to avoid the mixing.
People, surgical lamps and the equipment could be obstructions for the air flow and they are an heat source modifying the hypothesis of isothermal momentum field. The advantage in using this type of configuration is the minimization of the infections, moving a consistent volume of clean air in a unidirectional and uniform way. The convective streams of air due to heat or to the human motion are minimized. When an air flow encounters a solid object, it goes around that and the unidirectional-flow pattern is distorted in the close proximity of the object. Hypothetically, contaminants are flushed out as soon as they are released by the source without migration to other areas. In any case, for medical applications, this system should be vertical to remove the contamination and to minimize the path length toward the exhaust grilles [15].
In an horizontal setting of unidirectional flow, the swept effect is from one side to another of two vertical walls.

1.2.4 Mixed airflow

This solution is intermediate between the two solutions afore mentioned, both from the point of view of costs and of design. This type of flow takes place when only a part of the room is involved by a unidirectional flow. In particular, the operating bed, the cart carrying the instrumentation and the operating area of the staff are put under the 'piston' flow generated by ceiling filter with HEPA filter installed. The other parts are invested by a turbulent air stream, as it can be seen in Figure 1.4. The air is extracted by the return grilles, usually located at the corners of the room.

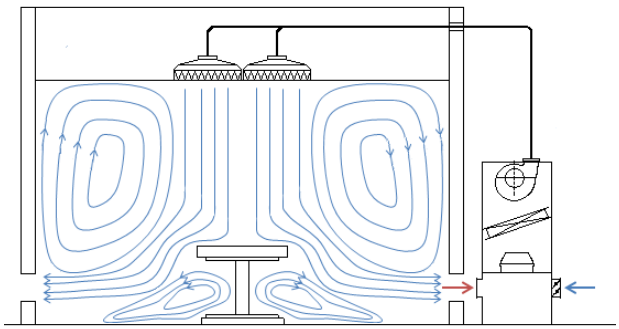

Figure 1.4: Example mixed air diffusion

This solution is possible because the surgical operations take place in a

confined critical area in which the personnel should stand following adequate procedures. The external area around the critical one is characterized by less strict conditions of contamination, because this system configuration make this zone dirtier than the one under the ceiling filter. This technical solution is organized with a unidirectional air stream under a turbulent motion outside, therefore inside the room there are alternate zones with maximum and minimum level of particle concentration, and therefore of cleanliness level or, from a medical point of view, different risk of contamination.

It is important to evaluate the connection system-process to avoid that the less clean areas influence the cleaner ones over the prescribed limits.

1.3 Filtration

Talking about the ventilation in operating theaters, it is important to make an introduction about air filtration. As mentioned before, because the operating site is a contamination controlled environment, the levels of concentration of pollutants are subject to strong constraints imposed by regulations in relation to the requested level of cleanliness and for matter of safety. In order to obtain the desired performances, it is necessary to install in the HVAC system a proper number of filtration stages, usually three, before the air enters in the critical area of an OT. Before introducing the description of these three filters it is necessary to introduce two International standards about the filtration.
In the following two sections the UNI EN 1822:2010 [16], the reference standard about the high and very high efficiency filters, and the UNI EN 779:2012 [17], the standard for the general ventilation filters, are briefly summarized.

1.3.1 UNI EN 779:2012

The European Standard UNI EN 779:2012 [17] refers to particulate air filters for general ventilation. These filters are classified according to their performance as measured in this test procedure. In order to obtain results for comparison and classification purposes, particulate air filters shall be tested against two synthetic aerosols, a fine aerosol for measurement of filtration efficiency as a function of particle size within a particle size range 0.2 μm to 3 μm, and a coarse one for obtaining information about test dust capacity and, in the case of coarse filters, filtration efficiency with respect to coarse loading dust (arrestance). This European Standard applies to air filters having an initial efficiency of less than 98 % with respect to 0.4 μm particles. Filters shall be tested at an air flow rate between 0.24 m^3/s (850 m^3/h) and

1.5 m^3/s (5400 m^3/h).
Filters are classified according to their average efficiency or average arrestance under the following test conditions:

- the air flow shall be 0.944 m^3/s (3 400 m^3/h) if the manufacturer does not specify any rated air flow rate;
- 250 Pa maximum final test pressure drop for Coarse (G) filters;
- 450 Pa maximum final test pressure drop for Medium (M) and Fine (F) filters.

If the filters are tested at 0.944 m^3/s and at maximum final test pressure drops, they are classified according to Table 1.2. The filters described in this regulation go up from the class G to the class F, and are characterized by different filtering efficiencies. They are preferred for heavy dust load as prefilters in order to intercept the highly concentrated dust in air coming from outdoor, entering in Air Handling Units.

Table 1.2: Classification of air filters according to the UNI EN 779 [17]

Group	Class	Final test pressure drop Pa	Average arrestance (A_m) of synthetic dust %	Average efficiency (E_m) of 0,4 µm particles %	Minimum Efficiency [a] of 0,4 µm particles %
Coarse	G1	250	$50 \le A_m < 65$	-	-
	G2	250	$65 \le A_m < 80$	-	-
	G3	250	$80 \le A_m < 90$	-	-
	G4	250	$90 \le A_m$	-	-
Medium	M5	450	-	$40 \le E_m < 60$	-
	M6	450	-	$60 \le E_m < 80$	-
Fine	F7	450	-	$80 \le E_m < 90$	35
	F8	450	-	$90 \le E_m < 95$	55
	F9	450	-	$95 \le E_m$	70

[a] Minimum efficiency is the lowest efficiency among the initial efficiency, discharged efficiency and the lowest efficiency throughout the loading procedure of the test.

In Table 1.2 there are two parameter by which filters are classified:

1. A_m, determined for the filters of class G, is the average arrestance, the ratio of the total amount of loading dust retained by the filter to the

total amount of dust fed up to final test pressure drop. It is calculated with the following equation:

$$A_m = \frac{1}{M} \times [\sum_{j=1}^{N} M_j \times Aj] * 100\ [\%] \tag{1.1}$$

$$A_j = \left(1 - \frac{m_j}{M_j}\right) \tag{1.2}$$

where:
M, is the total mass of dust fed equal to $\sum_{j=1}^{N} M_j$ $[g]$
M_j, is the mass of dust fed to the filter during loading phase j $[g]$
m_j, is the mass of dust passing the filter at the dust loading phase j $[g]$
A_j, is the arrestance in loading phase j, [%]
n, is the number of dust loading phases

2. E_m, determined for the filters of class M and F, is the weighted average of the efficiencies of 0.4 μm particles for the different specified dust loading levels up to final test pressure drop. It is determined by the following relation:

$$E_{m,i} = \frac{1}{M} \times \sum_{j=1}^{N} \left(\frac{E_{i,(j-1)} + E_{i,j}}{2} \times Mj\right) \times 100 \tag{1.3}$$

$$E_{i,j} = \frac{E_{1,i} + \cdots + E_{6,i}}{6} \tag{1.4}$$

where:
$E_{m,i}$, is the average efficiency for particle size range i for all dust loading stages [%]
$E_{i,j}$, is the average efficiency for size range i after the dust loading phase j [%]
M, is the total mass of dust fed equal to $\sum_{j=1}^{N} M_j$ $[g]$
M_j, is the mass of dust fed to the filter during the loading j $[g]$
n, is the number of dust loading phases

After this, in the standard there is the explanation of the instrumentation and of the procedure to conduct the efficiency test. It is also shown how to calculate the average efficiency and the measure of uncertainty of the test for a particular size range. At the end of the test it is necessary to write a test report, which shall include a description of the test method and any deviations from it. The report shall include also: summary of the results,

measured efficiencies and their uncertainties, calculated efficiencies, data and results of air flow rate and pressure drop measurements, data and results of dust loading measurements.
This type of filters are usually located in the AHU to cover the first two filtration stages for the dirty air coming from outdoor.

1.3.2 UNI EN 1822:2010

This European Standard applies to high efficiency particulate and ultra low penetration air filters (EPA, HEPA and ULPA) used in the field of ventilation and air conditioning and for technical processes, e.g. for applications in cleanroom technology, pharmaceutical industry and hospital facilities. It is composed of five parts:

– Part 1: *Classification, performance testing, marking* - This part of EN 1822 establishes a procedure for the determination of the efficiency on the basis of a particle counting method using a liquid (or alternatively a solid) test aerosol, and allows a standardized classification of these filters in terms of their efficiency, both local and integral efficiency [16]. This part is very important and it contains the classification of the high efficiency filters. Because of its central relevance, the high efficiency filter classification is reported in the Table 1.3:

Table 1.3: Classification of EPA, HEPA, ULPA filters according to the UNI EN 1822-1 [16]

Filter Group	Integral value		Local value [a] [b]	
Filter Class	Efficiency (%)	Penetration (%)	Efficiency (%)	Penetration (%)
E 10	≥ 85	≤ 15	---[c]	---[c]
E 11	≥ 95	≤ 5	---[c]	---[c]
E 12	≥ 99,5	≤ 0,5	---[c]	---[c]
H 13	≥ 99,95	≤ 0,05	≥ 99,75	≤ 0,25
H 14	≥ 99,995	≤ 0,005	≥ 99,975	≤ 0,025
U 15	≥ 99,999 5	≤ 0,000 5	≥ 99,997 5	≤ 0,002 5
U 16	≥ 99,999 95	≤ 0,000 05	≥ 99,999 75	≤ 0,000 25
U 17	≥ 99,999 995	≤ 0,000 005	≥ 99,999 9	≤ 0,000 1

[a] See 7.5.2 and EN 1822-4.

[b] Local penetration values lower than those given in the table may be agreed between supplier and purchaser.

[c] Group E filters (Classes E10, E11 and E12) cannot and shall not be leak tested for classification purposes.

One of the most important factor of the UNI EN 1822 [16], is the so

called MPPS (Most Penetrating Particle Size) which indicates the particle size at which the filter media and the filter itself reach the lowest particle filtration efficiency. Usually, the MPPS of a media filter made of glass microfiber paper is between 0.12 and 0.25 μm. To find out the MPPS, it is necessary to deliver the total efficiency curve of the filtering material according to the UNI EN 1822-3 [16]. The HEPA filters are made of fibers and they take advantage from the mechanical filtration which takes place while the inlet air pass through the filter, by means of the settling and retention of particulate on the fibers which form the filtering media. The operation of mechanical filtration is based on different mechanisms which could take place individually or coupled: sieve effect, direct interception, diffusion interception and inertial impact. At the same time these mechanisms are influenced by other important factors like crossing velocity of fibers, particle diameter, fiber diameter and density. Combining the effects of different mechanisms, because they have different impacts with the variation of the particle diameter in transit, it is possible to find a cut-off diameter related to the minimum efficiency, the MPPS. In the Figure 1.5 the global effect of mechanical filtration is resumed and it is shown the point corresponding to the MPPS.

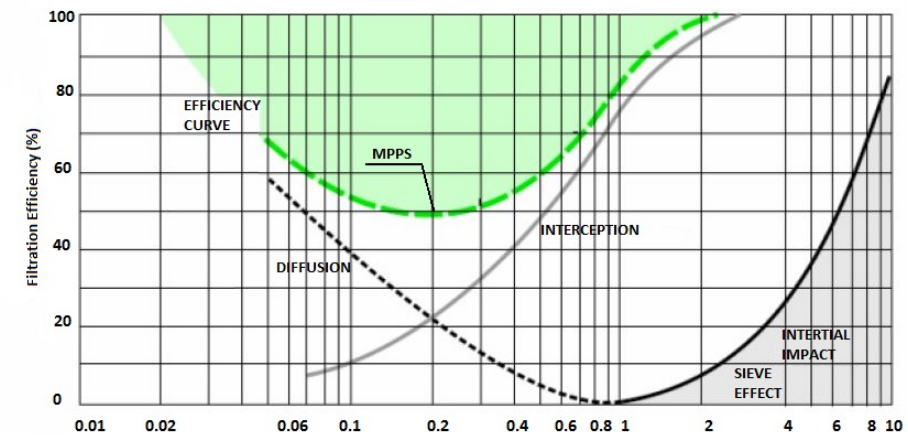

Figure 1.5: the global effect of mechanical filtration mechanisms [19]

The efficiency is expresses by means of two values: the average efficiency on all the surface of the filter and the local efficiency, the lowest efficiency found out in a specific point of the filter. How can be seen in the table 1.3, the filters of class H, with which the terminal air diffusers of an operating theater is equipped, have to ensure a very high

efficiency.

- Part 2: *Aerosol production, measuring equipment, particle counting statistics* - This part of EN 1822 describes the measuring instruments and aerosol generators used in the course of this testing. With regard to particle counting it specifies the statistical basis for the evaluation of counts with only small numbers of counted events [16].

- Part 3: *Testing flat sheet filter media* - This part of EN 1822 applies to testing sheet filter media used in high efficiency air filters. The procedure includes methods, test assemblies and conditions for carrying out the test, and the basis for calculating results [16].

- Part 4: *Determining leakage of filter elements (scan method)* - This part of EN 1822 applies to the leak testing of filter elements. The scan method which is described in detail regarding procedure, apparatus and test conditions in the body of this standard is valid for the complete range of group H and U filters and is considered to be the reference test method for leak determination [16]. The test on the high efficiency filters, are stricter and heavier than the ones of the general ventilation, because of the high performances that they reach.

- Part 5: *Determining the efficiency of filter elements* - This part of the EN 1822 series deals with measuring the efficiency of filter elements, specifying the conditions and procedures for carrying out tests, describing a specimen test apparatus and its components, and including the method for evaluating test results [16].

The main European standards (the Italian, German, French etc.), indicate three air filtration stage for the incoming air. The first two filtration stages must be installed in the HVAC device and the third one installed at the end, in proximity of the ceiling of the OT. For the first filtration stage at least filter class F5 (or if it is possible F7, according to the UNI EN 779:2012 [17]) should be provided. For the second filtration stage, filter class F9 should be provided, while for the third filtration stage suspended matter filters of filter class at least H13 (according to the UNI EN 1822-1 [16]) should be provided. It is important that the filtration system should be equipped with pressure difference manometers for each filtration stage for constantly monitoring its performance and for reason of safety (in case of possible filter damage or breakage). In general, for hygienic reasons, the maximum service life time should be limited up to 12 months for the first filtration stage and up to

24 months for the second one. For the third filtration stage a considerably longer service life can be achieved.

In the Figure 1.6 there is an HEPA filter like the ones installed in the operating theater studied in this work of thesis. It is a terminal filter classified, according to the UNI EN 1822-1 [16]. It is one of the twenty-three filters located in the ceiling filtering system, which will be well described in the chapter three.

Figure 1.6: HEPA filter H14 (source: Sagicofim) [18]

Because of the vibrations or the accidental hits and the fast variation of temperature have an impact on the retention of particles, it's necessary to pay attention during the installation of the filter. In any case, after the in situ filter installation on the ceiling filter, an integrity filter leak test, over all the HEPA filter installed, must be carried out, in order to fulfill with standards. The leak test is necessary in order to assure the total filtration integrity and efficiency af the filter plus filter case and installation. Furthermore, in case of long stops of the chamber, it is opportune doing inspections to verify the presence of bacterial growth on the surfaces of the filters. It's very important because the filter could became source of bioareosol and because the colonies could make larger the spaces between the fibers [19].

Chapter 2

Normative references

The design and testing process of an operating theater is a complex task to carry out only by using a single knowledge or a simple standard or guideline. Operating theater is a complex place where many different medical operations take place and therefore it is necessary to approach the problem in a multidisciplinary way by using both the best techniques from engineering and medical sciences. Of course, engineering science can only afford part of the problems which arise in an OT, such as problems related with indoor environmental conditions control or medical devices. Interest of this work is the study of the environmental control of an OT with particular interest to the airborne contamination control techniques and standards. In many aspects, an OT can be seen as a special cleanroom where are carried out different types of processes (operations) by different personnel (medical staff). Therefore, almost all the national and European standards which deal with operating theaters and related environments have common roots from the standards used for cleanrooms, as the ISO 14644 [20] for particle contamination. In the proceeding of this chapter after a brief introduction of the international standard UNI EN ISO 14644 [20], a discussion on the most important national standards relating with operating theater design and testing has been given. Particular attention is given to the choice of the experimental test, among those proposed by the national standards, to be used as reference test for the validation of the simulations done with the CFD model.

2.1 UNI EN ISO 14644

The standard UNI EN ISO 14644 [20] was conceived from the FED-STD-209E ('*Airborne Particulate Cleanliness Classes in Cleanrooms and Clean Zones*'). The need of a single standard to classify the cleanrooms and to determine the way to conduct tests in those, led to the composition of the

first ISO document in 1999 with the ISO 14644-1. In 2001 was published the ISO 14644-2 and consequently was canceled the old standard FS-209E. Since 2001 the standard was updated and completed and since 2012.
The operating theater is indeed a contamination controlled environment. As defined in the UNI EN ISO 14644-1 [20], it is a:

> *"Room in which the concentration of airborne particles is controlled, and which is constructed and used in a manner to minimize the introduction, generation, and retention of particles inside the room, and in which other relevant parameters, e.g. temperature, humidity, and pressure, are controlled as necessary"*

For this reason, this relation has a particular importance. It is composed of 10 parts which will be described below:

- Part 1 (2001): *Classification of air cleanliness* - This part of the UNI EN ISO 14644 covers the classification of air cleanliness in cleanrooms and associated controlled environments exclusively in terms of concentration of airborne particles. Only particle populations having cumulative distributions based on threshold (lower limit) sizes ranging from 0.1 μm to 5 μm are considered for classification purposes. This part of UNI EN ISO 14644 does not provide for classification of particle populations that are outside of the specified particle size range, 0.1 μm to 5 μm. Concentrations of ultrafine particles (particles smaller than 0.1 μm) and macroparticles (particles larger than 5 μm) may be used to quantify these populations in terms of U descriptors and M descriptors, respectively.
  The level of concentration of airborne particulate required is distinguish according to the number of class specified by the highest quantity of number of particles per cubic meter of the air acceptable. Nine classes of cleanliness are allowed (see the table 2.1). This standard defines the class by means of a number 'N' (0.1 is the smallest permitted increment of N) and, in function of the diameter of the particle, permits to evaluate the maximum admissible concentration (upper limit) for this class, expressible by the following formula:

$$C_n = 10^N \cdot \left(\frac{0.1}{D}\right)^{2.08} \tag{2.1}$$

  where:

  C_n, is the maximum admissible concentration $[pp/m^3]$

N, is the ISO classification number which shall not exceed a value of 9. Allowable increment of ISO classification number equal to 0.1

D, is the considered particle size [μm], it is between 0 and 5 μm

0.1, is the minimum reference particle diameter [μm]

Table 2.1: Selected airborne particulate cleanliness classes for cleanrooms and clean zones [20]

ISO classification number (N)	Maximum concentration limits (particles/m^3 of air) for particles equal to and larger than the considered sizes shown below (concentration limits are calculated in accordance with equation (1) in 3.2)					
	0,1 µm	0,2 µm	0,3 µm	0,5 µm	1 µm	5 µm
ISO Class 1	10	2				
ISO Class 2	100	24	10	4		
ISO Class 3	1 000	237	102	35	8	
ISO Class 4	10 000	2 370	1 020	352	83	
ISO Class 5	100 000	23 700	10 200	3 520	832	29
ISO Class 6	1 000 000	237 000	102 000	35 200	8 320	293
ISO Class 7				352 000	83 200	2 930
ISO Class 8				3 520 000	832 000	29 300
ISO Class 9				35 200 000	8 320 000	293 000
NOTE Uncertainties related to the measurement process require that concentration data with no more than three significant figures be used in determining the classification level						

The indications for the definition of the level of air cleanliness are given, concerning the suspended particles for all environments and for all areas considered as critical according to the level of risk that the surgical activities and other procedures imply. This part of ISO 14644 cannot be used to characterize the physical, chemical, radiological, or viable nature of airborne particles [20]. The classification of a cleanroom, according to UNI EN ISO 14644-1 [20], can be given in three different possible occupancy states: as-built, at rest and operational.

– Part 2 (2000): *Specifications for testing and monitoring to prove continued compliance with ISO 14644-1* - This part of ISO 14644 specifies requirements for periodic testing of a cleanroom or clean zone to prove its continued compliance with ISO 14644-1 for the designated classification of airborne particulate claeanliness. These requirements invoke the test described in ISO 14644-1 for classification of cleanroom or clean zone. Additional tests are also specified, to be carried out in accordance

with the requirements of this part of ISO 14644. Optional tests, to be applied at the user's discretion, are also identified. This part of ISO 14644 also specifies requirements for monitoring of cleanroom or clean zone to provide evidence of its continued compliance with ISO 14644-1 for the designated classification of airborne particulate cleanliness [20].

– Part 3 (2006): *Metrology and test methods* - This part of ISO 14644 specifies test methods for designated classification of airborne particulate cleanliness and for characterizing the performance of cleanrooms and clean zones. Performance tests are specified for two types of cleanrooms and clean zones: those with unidirectional flow and those with non-unidirectional flow, in three possible occupancy states: as-built, at-rest and operational. The test methods recommend test apparatus and test procedures for determining performance parameters. Where the test method is affected by the type of cleanroom or clean zone, alternative procedures are suggested. For some of the tests, several different methods and apparatus are recommended to accommodate different end-use considerations. Alternative methods not included in this part of ISO 14644 may be used if based on agreement between customer and supplier [20].

– Part 4 (2004): *Design, construction and start-up* - This part of ISO 14644 specifies requirements for the design and construction of cleanroom installations but does not prescribe specific technological or contractual means to meet these requirements. It provides a checklist of important parameters of performance. Construction guidance is provided, including requirements for start-up and qualification [20].

– Part 5 (2005): *Operations* - This part of ISO 14644 specifies basic requirements for cleanroom operations. It is intended for those planning to use and operate a cleanroom. Aspects of safety that have no direct bearing on contamination control are not considered in this part and national and local safety regulations must be observed. This document considers all classes of cleanrooms used to produce all types of products [20].

– Part 6 (2008): *Terms and definitions* - This part of ISO 14644 establishes a vocabulary of terms and definitions related to cleanrooms and associated controlled environments. This part is a compendium of the terms and definitions given in the other parts of ISO 14644 [20].

– Part 7 (2005): *Separative devices (clean air hoods, gloveboxes, isolators and mini-environments)* This part of ISO 14644 specifies the mini-

mum requirements for the design, construction, installation, test and approval of separative devices [20].

– Part 8 (2007): *Classification of airborne molecular contamination* - This part of ISO 14644 covers the classification of airborne molecular contamination (AMC) in cleanrooms and associated controlled environments, in terms of airborne concentrations of specific chemical substances (individual, group or category) and provides a protocol to include test methods, analysis and time weighted factors within the specification for classification. This part of ISO 14644 currently considers only concentrations of AMC between 100 and 10^{12} g/m^3 under cleanroom operational conditions. This part is not relevant for application in those industries, processes or production, where the presence of airborne molecular substances is not considered a risk to the product or process. It is not the intention of this part to describe the nature of airborne molecular contaminants [20].

– Part 9 (2012): *Classification of surface cleanliness by particle concentration*- It establishes the classification of cleanliness levels on solid surfaces (such as walls, ceilings, floors, working environments, tools, equipment and products) by particle concentration in cleanrooms and associated controlled environment applications. The surface particle cleanliness (SPC) classification is limited to particles between 0.05 μm and 500 μm. Recommendations on testing and measuring methods, as well as information about surface characteristics are also given [20].

– Part 10 (2013): *Classification of surface cleanliness by chemical concentration*- It defines the classification system for cleanliness of surfaces in cleanrooms with regard to the presence of chemical compounds or elements (including molecules, ions, atoms and particles). It is applicable to all solid surfaces in cleanrooms and associated controlled environments such as walls, ceilings, floors, working environment, tools, equipment and devices [20].

2.2 The Italian standards

2.2.1 UNI 11425:2011

This is the first Italian standard regarding the design, construction, commissioning, monitoring, qualification, management of the plants and of components which contribute to the environmental contamination control and to

the maintenance of preset thermohygrometric conditions in ward for the surgical activities. It is applied to the new constructions and to the renovations of buildings or/and plants. Furthermore, this standard provides the minimal requirements to verify the operational conditions of existing operating theaters.

The UNI 11425 [11] defines the VCCC (Ventilation and air-Conditioning system for Contamination Control) plants for Surgery operating theaters like a '*process*' plants and for this reason they must exhibit the specific requirements to ensure the quality of the process, as stated also in the UNI EN ISO 14644 [20] and the EU-GMP [22] and FDA [23] guidelines, like: reliability and performance control, the personnel and environmental safety and the control reproducibility. It is specified that the proper process requirements are primary compared with the standards about the thermohygrometric comfort; the VCCC plants of surgery operating theaters have the scope to maintain:

- the biological and inert total airborne particulate concentration under the allowed limits;
- the thermohygrometric conditions adequate to guarantee the normal process execution;
- The chemical pollutants concentration under the permitted limits;
- stable and measurable pressure gradients within environments with different protection requirements against contaminants;
- Time-constant values of set parameters.

The UNI 11425:2011 [11] indicates, for different surgical applications, the respective cleanliness levels:

- at least ISO 5: for operating theaters used to specialist surgeries like organ transplantation, implant of prosthesis, neurosurgery and complex oncology and other complex surgeries which last more than 60 minutes;
- at least ISO 7: for operating theaters used to surgeries without implant of foreign materials, but which require an high protection level, like arthroscopic surgery, vascular surgery, neurosurgery and obstetrics, implantation of pacemakers and, in general, minimally invasive surgery;
- at least ISO 8: for operating theaters used to low-invasive surgery and short duration.

The classification is based on the maximum allowed number of total particles of a specify diameter per meter cube of air, in *simulated operational condition*, set by the project documentation, conforming to the UNI EN ISO 14644-1 [20]. For the operating theaters the reference diameter is 0.5 μm. In the Table 2.2 there is an extract of a resuming table with the description of some cases of operating theater conditions.

Table 2.2: Environmental parameters in the operating theaters (UNI 11425) [11]

Ambienti	Temperatura [°C]		Umidità relativa [%]		Sovrapressione rispetto all'esterno	Aria esterna	Aria di ricircolo	Classi di pulizia secondo UNI EN ISO 14644-1	Livello di filtrazione finale	Livello di pressione sonora
	Inverno	Estate	Inverno	Estate	[Pa]	[vol/h]	[-]			[dBA]
Sale operatorie a elevatissima qualità dell'aria	≥ 20	≤ 24	≥ 40	≤ 60	15[1)]	15	SI[2)]	ISO 5	H 14	45[3)]
Sale operatorie a elevata qualità dell'aria					15[1)]	15	SI[2)]	ISO 7	H 14	45[3)]
Sale operatorie a qualità dell'aria standard					15[1)]	15	- [4)]	ISO 8	H 14	45[3)]

The UNI 11425 [11] also establishes some plant restrictions, such as: the mean velocity near the critical area, close to operating table, which should be always under 0.3 m/s to avoid the development of air sacs and eddies. About the AHU (Air Handle Unit) there is a description of the insulation, air tightness, materials and other design advice. Moreover there is a description of the internal surfaces finishing of the surgical operating theaters and for every part in this design constraints are fixed in order to provide an adequate internal cleanliness.

In the UNI 11425 [11] issues are raised, regarding energy saving. In order to reduce the energy consumption, the VCCC plants could provide to a recirculated air flow like a part of the supply air flow. In case of a single plant serving more than one room, it is necessary to pay attention to the cross-contamination [11, 21] among different OTs and VCCCs system.

2.2.2 EX-ISPESL: Guidelines on health and safety in health care facilities: 2009

These guidelines are intended to guide the implementation of the legislation on the activity in operating theater and connected environments.
The first part it is about the structural characteristics and the general technology. The description of the VCCC system has a particular importance. It has to maintain the thermohygrometric conditions suitable to permit the

execution of the work of the surgical staff and the comfort of the user; in addition it has to supply the fresh air and remove the contamination and control its concentration. The system should also maintain a pressure gradient with the adjoined environments.
In order to reach the described goals, in this guideline [24], the ISPESL fixes some requirements to follow during the design stage. This standard quotes other Italian regulations like the D.P.R 14/1/1997 [12] in merit of the amount of fresh air to supply in an operating theater: greater than 15 ACH. The part the different way to supply the air in an operating theater are also described. The ISPESL refers to the UNI EN ISO 14644-2:2001 [20] for the referential base performances of operating theaters and fixes the aspects to monitor and control in the operating theater:

- Filters: the pressure drops of the filtering system it is recorded with differential manometers;
- Airflow and air changes per hour: they might be at least 15 ACH (according to the DPR 14^{th} January 1997 [12]);
- Pressure difference: it might be at least 5 Pa (according to the UNI EN ISO 14644-4:2004 [20]);
- Temperature and relative humidity: the temperature might be in the range of $20 - 24°C$ and the relative humidity between 40% and 60%;
- Noise level: the reference values of the French, German, Swiss, Austrian and English regulations are used;
- Lightning;

Furthermore there are some performance tests to carry out periodically in the operating room:

- Recovery time: it is a test to determine the system ability to remove the suspending particle contamination. These performances are calculated using the recovery time of 100:1. It is defined as the time required to decrease the initial concentration of a 100 factor. The reference particle size for this test is 1 μm. The test is well described in the UNI EN ISO 14644-3:2006 [20];
- Monitoring of microbiological contamination in at-rest and operational conditions: it is fixed a limit value, near the operating theater, of $\leq$180 CFU/m^3, in operational condition for a turbulent flow system and $\leq$20 CFU/m^3 for a unidirectional flow system; how to conduct the at rest

test is also explained.

– Particle contamination and classification (according to the UNI EN ISO 14644-1 [20]): to ensure the air quality it is necessary a periodic control of contamination. In order to do this it is necessary a DPC (Discrete particle counter) or OPC (Optical particle counter) able to record the particle count and the size, distinguish the particle size in order to give the total concentration of a particular size of particles. The instrumentation must be equipped with a valid calibration certificate. During an experimental test for proofing the OT performance, the OPC probe is positioned at fixed points within the OT environment. The OPC probe shall be oriented toward the air flow and each sample it shall extracts at least a volume of:

$$V = \frac{20}{C} * 1000 \tag{2.2}$$

where:
V, is the minimum sampling volume for each sampling point $[l]$
C, is the class limit with the grater dimension considered pp/m^3
20, is the number of particles which might be count if the particle concentration is at the class limit pp/m^3

The test is conducted in at rest conditions and the suggest particle size is 0.5 μm. Are also recommended a number of sampling point at least equal to:

$$N_L = \sqrt{A} \tag{2.3}$$

where:
N_L, is the minimum sampling points $[-]$
A, is the surface of the operating theater (in plant) or of the critical zone $[m^2]$, where for critical zone can be considered the area under the ceiling filter or the area near the operating table.

The periodicity of the test are different for the operating theater $\leq$ISO 5 (every six month) and $\leq$ISO 7 (every twelve month).

A particular section is dedicated to the behavior procedure and to the individual protection device (comprehensive of the material of the technical clothes) to use in an operating theater.

2.3 The English standard: HTM 03-01-Part A: 2007

The part of interest in the English memorandum is the chapter 7 [25], about the specialized ventilation systems and the chapter 8 about the validation of specialized ventilation systems.
In the first part of chapter 7, it is described each goal of a ventilation system in healthcare premises. These are: air-movement control, temperature and humidity control, removal and dilution of waste anesthetic gases, fire aspects and door protection.
About the design of the air terminals and air distribution within the room, it is indicated that for all vertical UCV (Ultra-Clean Ventilation) systems, the design discharge velocities will be, 2 meters above floor level at the operating position, of 0.38 m/s for partial-wall system (0.3 m/s for full-wall system) and between 0.2 and 0.3 m/s 1 meter above the floor level. The following part is related to the ventilation of operating department ancillary areas.
A consistent part is dedicated to the UCV system. This system is based on the need to dilute contaminants and control both the condition and movement of air in a operating room. Air is discharged above the operating zone and, while not truly laminar, its downward displacement purges the clean zone of any contaminants and particles generated within it. Ultra-clean air is defined as that air containing not more than 10 CFU/m^3. It also specified that an inherent feature of a UCV system is its large air flow, so it is essential to recirculate the air supplied to the operating theatre and/or to recover its energy in order to optimize operating costs.
Like in the French regulation it is reported the different indicator-lights for a good control of the conditions in the room.
The following part regards the different type of extract systems; they are precisely described, with the indication of typical arrangements and peculiar utilization, in case of the use of corresponding supply-systems.
In the chapter 8 are well described the equipment tests. These are about:

- *Filter challenge*: it must separate the control on general ventilation filters and HEPA filters; for the second category, the complete installation must be tested using the method set out in UNI EN 14644:3-4 'Method of Testing for the Determination of Filter Installation Leaks'. The challenge tests may be carried out using either DOP (Di-octyl Phthalate), to provide the challenge and a photometer to detect leaks and a DPC (Discrete Particle Counter) to detect leaks

- *Bacteriological sampling*: bacteriological sampling will not normally be required for either general or local exhaust ventilation (LEV) systems

unless otherwise specified. The level of airborne bacteria introduced by the supply air should be checked by closing all doors and leaving the operating room empty with the ventilation system running for 15 minutes. An active air sampler set to take at least a 1 m^3 sample volume and mounted in the center of the room approximately 1 m above floor level should then be activated remotely. Aerobic cultures on non-selective media should not exceed ten bacterial and/or fungal colony forming units per cubic meter (CFU/m^3).

– *Air movement*: The use of smoke to gain an understanding of the overall performance of the system may prove useful at this stage in the validation process but cannot be relied on to produce a contractually definitive measure of performance.

– *Plant capacity and control*

– *Noise level*

An important section of this chapter is about the UCV validation procedure. The conditions of humidity and temperature to the test are specified (19-23°C and 30-65% RH). Fore vertical units, a test grid should be constructed on the floor within the ultra-clean terminal footprint as projected by the inside dimensions of the side walls or boundary air curtain (each square of the grid are of 280 mm each side and the inner zone should comprise a minimum grid of 6x6 test square). An example of test grid is shown in the figure 2.1.

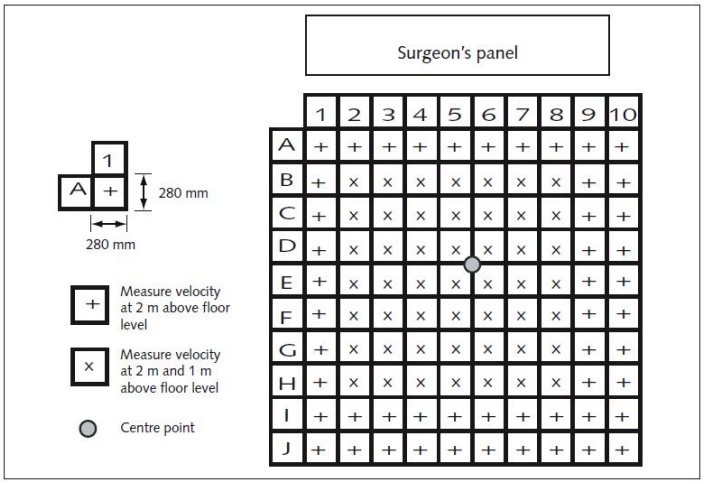

Figure 2.1: Example of a test grid for a 2.8 m x 2.8 m UCV terminal (from HTM 03-01-Part A [25])

A very relevant test described in the HTM 03-01-Part A [25] is the UCV entrainment test, only for vertical systems. In this, a source of particles is produced outside of the UCV terminal and is used to challenge the system. A particle detector (OPC or photometer) is placed within the ultra-clean air flow and used to determine the percentage penetration of the test particles at predefined locations under the UCV terminal footprint. The source and detector are moved in tandem around the UCV canopy and pairs of readings taken, from which the percentage penetration at specified locations is calculated. The degree of penetration should be below specified maximum limits if entrainment is to be declared not significant. This test may be carried out using either the DOP, to provide the challenge source at the specified release position and a photometer to measure the entrainment or ducting non-HEPA-filtered air to the specified release position and use a DPC to measure the entrainment. The test should be performed without any equipment in place beneath or closely adjacent to the UCV terminal. Theatre lights should be moved to a central position beneath the terminal and raised to 2 m above floor level so as not to interfere with the peripheral air flows.
The tracer particles are mainly within the size range 0.3–5 μm and thus capable of remaining airborne for a substantial time. A concentration of approximately 10^5 particles per cubic meter of source air has been shown to be adequate. The source unit should be a fan/blower or other method that takes non-HEPA-filtered air and expels it via a delivery head at the specified release position to provide the particle challenge. The challenge air should be delivered vertically downwards from the lowermost edge of the partial wall, on the outside of the UCV canopy, parallel to the air flow coming from the diffusers.
The detector may be a photometer or a DPC. The instrument should be capable of sampling a minimum of 28.3 l/min of air, in the case of the DPC, provide readings for particle size ranges from 0.3 μm to 5 μm and greater. The instrument should be compliant with the requirements of UNI EN ISO 14644-1 [20] and ISO 21501-4 [26].
The test positions should be at the center of each test square, as defined for the velocity test. For rectangular UCV terminals, measurements of penetration are to be taken at the four corner test squares of the test grid and at intermediate positions along the line of test squares between the corners. Furthermore, a single measurement should be taken at the geometric center of the UCV terminal footprint.
The center of the challenge particle source should be aligned with the center of the designated test. The test person should stand within the UCV terminal footprint but not in the same quadrant as the detector head.
The English regulation recommends the following standards to achieved:

- at each test position in the outer zone, penetration is to be less than 10% of the challenge;
- at each test position in the inner zone, penetration is to less than 1% of the challenge;
- at the center test position, penetration is to be less than 0.1% of the challenge.

2.4 The Swedish technical specification: SIS-TS 39:2012

The intention behind the Swedish technical specification, SIS-TS 39:2012 [27], is to provide a guidance concerning the way in which the airborne contamination of surgical sites and medical devices can be minimized in operating rooms and adjacent rooms. The aim is to prevent post-operative infections caused by airborne microorganisms. This technical specification gives functional requirements, guidance concerning the technical design of ventilation system and describes methods for evaluating the capacity of ventilation system to remove microorganisms form the air. The interaction between clothing system and air flow is also described. The first part takes into account the microbiological requirements for different type of operating room, set-up rooms, rooms with direct connection to an operating room, as well as where and how the microbiological samples should be taken.
In the following part there is a detailed description of technical building requirements (floor, ceiling, wall, doors, windows, etc,...) and of technical ventilation requirements, about:

- Air flows (outdoor and recirculated air flows): the total air flow is dimensioned to dilute the concentration of airborne bacteria-carrying particles and it has been calculated on the number of people in the room and their source strength. The microbiological requirement for air in operating rooms for infection-prone clean surgery is $\leq$10 CFU/m^3 when clean air suits are worn;
- Positive pressure differences: it must be maintained and set to $\geq$ 5 Pa;
- Air filters: two pre-filters must be placed before the final filter and must fulfill class F7 in stage 1 and class F9 in stage 2 in accordance with UNI EN 779 [17]; the final filter must fulfil class $\geq$ H14 in accordance with UNI EN 1822-1[16];

- Air humidity: it must not exceed 70% RH except in exceptional cases;
- Temperature: it must be adjustable, normally in the range of 22±4 $°C$;
- Noise level: it should be included in the specification of requirements for operating rooms and set-up room;
- Static electricity: it depends on the type of equipment used.

The table 2.3 summarizes the guidelines concerning operating rooms

Table 2.3: Guidelines concerning operating rooms [27]

No.	Property	Level	Governing document
6.2	Total air flow	For the dimensioning of air flow, see Figure 1a – d	
6.4	Outdoor air flow	Minimum 0.56 m^3/s	
6.6	Pressure differences	≥5 Pa positive pressure	
6.7	Air filter (final filter)	≥H14	Requirements in accordance with EN 1822-1 Installation control, method in accordance with SS-EN ISO 14644-3
	Air filter (pre-filter)	F7 Stage 1 F9 Stage 2	Requirements in accordance with SS-EN 779
6.8	Air humidity	Recommendation ≤70% RH	
6.9	Room temperature	22 °C ±4 °C	
6.10	Noise level	In accordance with the specification of requirements	AFS 2005:16

The SIS-TS 39:2012 [27] gives also a wide description of some functional tests to be carried out in an OT and ancillary premises like:

- *Air flow test:* it shall be carried out in accordance with the UNI EN ISO 14644-3;
- *Pressure difference*: at least 5 Pa;
- *Leakage test:* it shall be carried out on filters using integrity testing and pressure drop across final filters in accordance with UNI EN ISO 14644-3;
- *Air movement studies:* air movement visualization shall be carried out initially upon completion of the operating room in order to visualize air

movements in the operating room. Stagnation zones or the formation of vortices where contaminants may accumulate should be avoided. The air movement study shall clearly indicate that turbulent mixing is achieved, or that air is moving from a clean zone to an adjacent area by sweeping action of the parallel flow;

– *Entrainment of airborne particles into clean zones:* in order to test whether the entrainment of airborne particles into a zone (operating table and surgical instrument table) is occurring, a Limitation of Risk method (LR method) shall be carried out. The basic level of airborne particles shall be measured in the clean zone and a particle challenge shall be applied to the room from outside the clean zone consisting of at least 10^7 particles (≥ 0.5 μm) per m^3. It is introduced the definition of a risk factor, which shall be <0.01% (10^{-4}) of the challenge concentration:

$$LR = \frac{C_k}{C} \tag{2.4}$$

where:
LR, is the Risk Factor $[-]$
C, is the concentration in the particle challenge area $[pp/m^3]$
C_x, is the concentration in clean zone $[pp/m^3]$

– *Recovery time:* it is a test to determine the system ability to remove the suspending particles. The recovery time is defined as the time required to decrease the initial concentration of a 100 factor. It shall be ≤ 20 min; tests shall be carried out in accordance with UNI EN ISO 14644-3 [20].

In the Appendix B of this technical specification, there is a part regarding the procedures during experimental measurements. In particular, it is written that the ventilation and lighting must be operated normally. Operating lamps must be turned on and positioned in their normal position, and the operating table and instrument tables must be in their usual positions. Furthermore, the measuring probe of the particle counter must face vertically upwards and be positioned in the middle of the operating table at around 1.5 m above floor level. The evaluation should normally be carried out in an empty room without the operating personnel present. Further information can be obtained by performing the test under simulated surgical operations. In another section of appendix B it is described in three steps the LR method introduced before. Firstly, the main air movements are visualized (with the aid of artificial smoke), and any vortices or stagnation areas are identified.

The second step consists in the particle challenge test, which identifies potential risk situations. The particle challenge test with simultaneous particle measurement is performed with the measuring probe of the particle counter facing upwards and places in the center of the operating table, 1.2 m above floor level at the same time as particles are generated along the lower periphery of the clean zone. Particles should be generated until a local concentration exceeds 10^7 particles equal to or larger than 0.5 μm per cubic meter.
In the third step a risk factor is calculated. The risk factor is defined as the ratio between the maximum measured concentration (number of particles $\geq$ 0.5 μm per meter (or foot) in the clean area and the particle challenge level. Due to insufficient measuring accuracy at high concentrations, the value of 10^7 particles $\geq$ μm per cubic meter must be used as the particle challenge level when calculating the risk factor. It is necessary to have an appropriate particle source for the local generation of particles to a concentration of more than 10^7 particles per cubic meter (or 300'000 particle per cubic foot). It is necessary also a particle counter (DPC) for the calculation and size determination of airborne particles $\geq$ 0.5 μm.The sampling flow must be 1 cubic foot per minute, or 28.3 l/min.
The position of particles diffusers is different according to the shape of the clean zone: it could be rectangular or circular , but in both case there are 4 aerosol diffusers distributed around the outer perimeter of the clean zone (approximately 0.5 m wide and between 0.1 and 1.2 m above the floor level).

2.5 The French regulation: NF S90-351: 2013

The NF S90-351 [28] is the French regulation and wants to specify the necessities of health care safety for the design, construction, utilization and maintenance of treatment facilities and air quality system in health care buildings. An important section of this standard is about the expressions of needs, expected performance and constraints to maintain the operating theater in a safety condition. It is necessary to establish the flow chart to describe precisely the different circuits of personal carers, external staff, visitors, patients, waste products and materials. The contaminants are distinguished in three distinct families: particulate, microbiological and chemical. For the first class, the particulate, depending on the system considered, potential contaminants must be described by nature (inert or radiologically active) and the desired level of cleanliness and the considered particle size must be specified (for example ISO 5, ISO 7, ISO 8 at 0.5 mum). For the microbiological contaminants the microbiological class (M 1, M 10, M 100) must be indicated. For the chemical contaminants the nature (solid, liquid, gas), the

TLV (Threshold Limit Value) and the TWA (Time Weighted Average) of exposition must be specified.
In the design phase the regulation underlines that the project studies must take into account all the relevant requirements of the control and elimination of the contamination and the necessary time to carry out the particles. These requirements are focused on the following points: filtration characteristics, fresh and recirculated air flow, velocity profiles of supply air, noise level, positioning elements for adjusting the temperature and speed, monitoring parameters system (of temperature, pressure, etc..), alarm device in case of pressure losses.
According to the *risk class* of the room it is indicated the periodicity of the monitoring actions.
There are four risk classes: the number 1 has the less strict conditions, the number 4 has the most critical ones. In the NF S90-351 [28] there is the classification of each hospital environment according to the risk classes.
For the most critical zones, the criteria to measuring the performance of the air cleanliness are indicated, according to the UNI EN ISO 14644-1:2001 [20] (see table 2.1). In addition, for the particle size of 0.5 μm, there is a description of three classes of particle removal velocity. It is specified the time (in minutes) to obtain a reduction equal to 90% of the particles in the critical area.

- $CP_{(0.5)}20$, in which the time to obtain this reduction is ≤ 20 minutes;
- $CP_{(0.5)}10$, in which the time to obtain this reduction is ≤ 10 minutes;
- $CP_{(0.5)}5$, in which the time to obtain this reduction is ≤ 5 minutes.

In this section three microbiological classes are introduced, we have:

- $M\,100$, in which the maximum concentration of viable particles per cubic meter of air is 100 CFU/m^3;
- $M\,10$, in which the maximum concentration of viable particles per cubic meter of air is 10 CFU/m^3;
- $M\,1$, in which the maximum concentration of viable particles per cubic meter of air is less than 1 CFU/m^3.

The characteristics of each risk class for OT (except the first one) are summarized and are shown in the table 2.4, and the acoustic performances are fixed.

Table 2.4: Reference values of performance of OT 'at rest' condition (from NF S 90-351 [28])

Classe de risque	Classe de propreté particulaire	Cinétique d'élimination des particules	Classe de propreté micro-biologique	Pression différentielle (positive ou négative)	Plage de températures	Régime d'écoulement de l'air de la zone à protéger	Autres spécifications, valeur minimale
4 [a]	ISO 5	CP 5	M1	15 Pa ± 5 Pa	19 °C à 26 °C	Flux unidirectionnel	Zone sous le flux Vitesse d'air de 0,25 m/s à 0,35 m/s taux d'air neuf du local ≥ 6 volumes/heure
3	ISO 7	CP 10	M10	15 Pa ± 5 Pa	19 °C à 26 °C	Flux unidirectionnel ou non unidirectionnel	taux de brassage ≥ 15 volumes/heure
2	ISO 8	CP 20	M100	15 Pa ± 5 Pa	19 °C à 26 °C	Flux non unidirectionnel	taux de brassage ≥ 10 volumes/heure

[a] Le taux de brassage, dans le cas particulier d'un flux unidirectionnel, doit être fixé indépendamment pour la zone située sous le flux et pour l'ensemble du local considéré.

According to the UNI EN 779 [17] and UNI EN 1822 [16], it is described the filtration chain from the AHU to the ceiling of operating theater. This regulation gives an accurate description of the construction requirements for vertical walls, doors, ceiling, floor and filtering ceiling system. There is also a detailed part about qualification and maintenance procedures. Moreover, it is presented the environmental control of air and surfaces procedures for which it is necessary to individuate:

- Critical control points
- The type of sample (single instant, compound);
- The required resources (time, material, financial, human);
- Planning of the collection of samples (conditions, nature, location, number, frequency) at the critical points;
- The equipment and/or devices of samples.

Depending on the type of control, the regulation indicates a schematic representation of sample points which may be used throughout all the OT area and within the critical area under the ceiling filter footprint, is shown in Figure2.2.

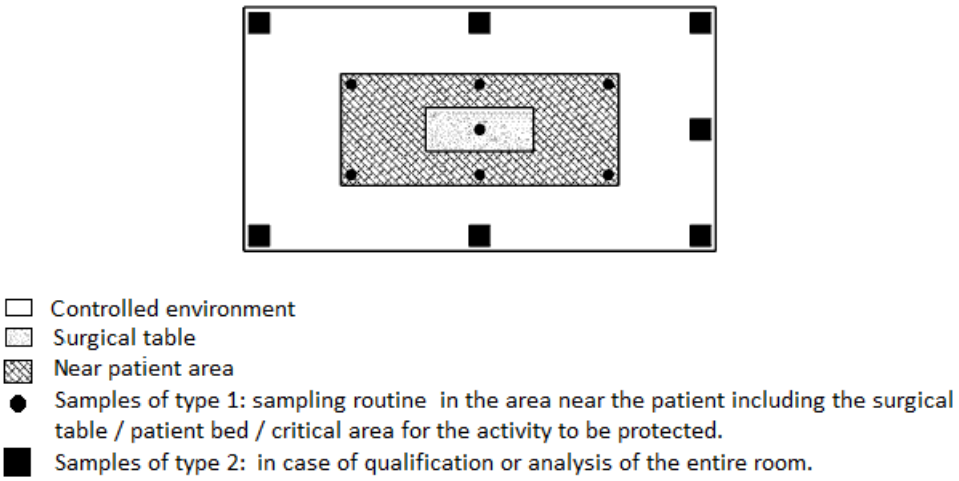

Figure 2.2: Particular case of operating rooms - Schematic representation of the sampling points including microbiological tests (from NF S 90-351 [28])

These sampling points are taken in accordance with UNI EN ISO 14644 parts 1 and 2 [20] for the risk analysis of particulate contamination and UNI EN ISO 14698 parts 1 and 2 [29] for microbiological risk analysis.

2.6 The American standard: ANSI/ ASHRAE/ASHE Standard 170-2013

The purpose of the ANSI/ASHRAE/ASHE Standard 170-2013 [30] is to define ventilation system design requirements that provide environmental control for comfort, asepsis, and odour in health care facilities.
In the first pages it is introduced a classification of surgeries. Three type of surgeries are individuated:

- *Class A- Procedure room*: provides minor surgical procedures performed under topical, local or regional anesthesia without preoperative sedation;
- *Class B- Operating room*: provides minor or major surgical procedures performed in conjunction with oral, parenteral or intravenous sedation or performed with the patient under analgesic or dissociative drugs;
- *Class C- Operating room*: provides major surgical procedures that require general or regional block anesthesia and/or support of vital bodily functions.

Subsequently the systems and equipment are introduced. The most relevant described, are:

- Heating and cooling sources and the AHU (Air-Handling-Unit);
- Outdoor air intakes and exhaust discharges;
- Filters with the individuation of three different banks;
- Air distribution devices;
- Energy recovery systems.

Standard suggests that the design of ventilation system shall provide air movement that is generally from clean to less clean areas. The goals are to provide for comfort as well as for asepsis and odor control in areas of a health care facility that directly affect patient care. The table 2.5 shows the design parameters for different type of health care facilities depending on their functions as stated in the American standard.

Table 2.5: Extract from Table 7.1 of the Standard 170-2013 with the design parameters for different type of spaces and functions[30]

Function of Space	Pressure Relationship to Adjacent Areas (n)	Minimum Outdoor ach	Minimum Total ach	All Room Air Exhausted Directly to Outdoors (j)	Air Recirculated by Means of Room Units (a)	RH (k), %	DesignTemperature (l), °F/°C
SURGERY AND CRITICAL CARE							
Class B and C operating rooms, (m), (n), (o)	Positive	4	20	N/R	No	20 – 60	68–75/20–24
Operating/surgical cystoscopic rooms, (m), (n), (o)	Positive	4	20	N/R	No	20 – 60	68–75/20–24
Delivery room (Caesarean) (m), (n), (o)	Positive	4	20	N/R	No	20 – 60	68–75/20–24
Treatment room (p)	N/R	2	6	N/R	N/R	20 – 60	70–75/21–24
Trauma room (crisis or shock) (c)	Positive	3	15	N/R	No	20 – 60	70–75/21–24
Laser eye room	Positive	3	15	N/R	No	20 – 60	70–75/21–24
Class A Operating/Procedure room (o), (d)	Positive	3	15	N/R	No	20 – 60	70–75/21–24
DIAGNOSTIC AND TREATMENT							
Gastrointestinal endoscopy procedure room	Positive	2	6	N/R	No	20 – 60	68–73/20–23

It is specified that the operating rooms (class B and C), operating/surgical cryoscopic rooms and caesarean delivery rooms shall be maintained at positive pressure with respect to all adjoining spaces at all times. A pressure differential shall be maintained at value of at least 2.5 Pa. Each room shall have individual temperature control. The airflow in these rooms shall be unidirectional, downwards and the average airflow from the diffusers shall be between 127 and 178 $L/s/m^2$. The diffusers shall be concentrated to provide

an airflow pattern over the patient and surgical team. The area of the primary supply diffuser array shall extend a minimum of 305 mm beyond the footprint of the surgical table on each side. No more than 30% of the primary supply diffuser array area shall be used for nondiffuser users such as lights, gas columns, etc. Additional supply diffusers may be required to provide additional ventilation to the operating room to achieve the environmental requirements of the table 2.5 relating to temperature, humidity, etc.
About the return air, the American regulation fixes a minimum of two low exhaust grilles spaced at opposite corners or as far apart as possible, with the bottom of three grilles installed approximately 203 mm above the floor. In addition to the required low return grilles, such grilles may be placed high in the walls.
Attention, in the standard, was also given for the planning, construction and system start up for HVAC systems serving surgery and critical-care spaces.
In the Appendix A, there is a short informative about the operations and maintenance procedures in health care facilities, in the particular case of the operating rooms, it is indicated that:

- Each operating room should be tested for positive pressure semi-annually or on an effective preventative maintenance schedule;
- when HEPA filters are present within the diffuser of operating rooms, the filter should be replaced based on pressure drop;
- operating and caesarean delivery room ventilation systems operate at all times, except during maintenance and conditions requiring shutdown by the building's fire alarm system.

For the final filters and filter frames, it is indicated that they should be visually inspected for pressure drop and leakage, monthly. Filters should be replaced based on pressure drop with filters that provide the efficiencies specified.

2.7 The German standard: DIN 1964-4:2008

This German guideline applies to heating, ventilation and air-conditioning (HVAC) systems in buildings and rooms where hospital specific procedures and activities, and interventions on humans are carried out. Examples are: hospital buildings in general, ambulant clinics, physicians'premises with rooms for surgery, facilities for internal and external sterilization services, centralized sterilization units. This guideline shall be applied to new systems and renovations.

The first parts of this standard concern on the classification of operating rooms, the structuring of planning, construction and operation requires, the description of design criteria and components. The last part deals with the system qualification. It is important to explain the term 'critical area'. The critical area is a zone around the surgical table in which the medical staff operates. In this section the arrangements of the room during the qualification test are introduced. There are two configurations for the test which simulate the operational conditions:

1. Test to evaluate the protection class of the critical area against the external particle loads;

2. Test to evaluate the protection class of the critical area against the internal particle loads;

For each configuration the German standard specify the arrangement of the test elements with proper drawings. Entering in the details:

1. The first one is addressed to verify the protection of critical area against the external loads (from the area out of the critical zone)

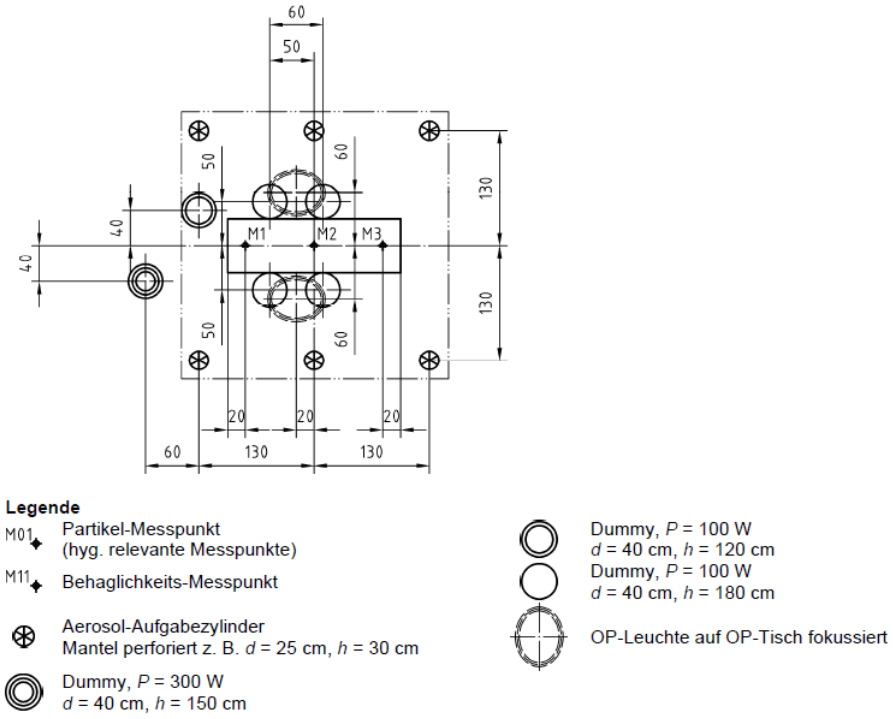

Figure 2.3: Reference load set-up for testing the protection against load entry from outside (from DIN 1964-4 [32]). External contamination layout

2. The second one is addressed to verify the protection of critical area against the internal loads (from the area under the filtering supply diffusers)

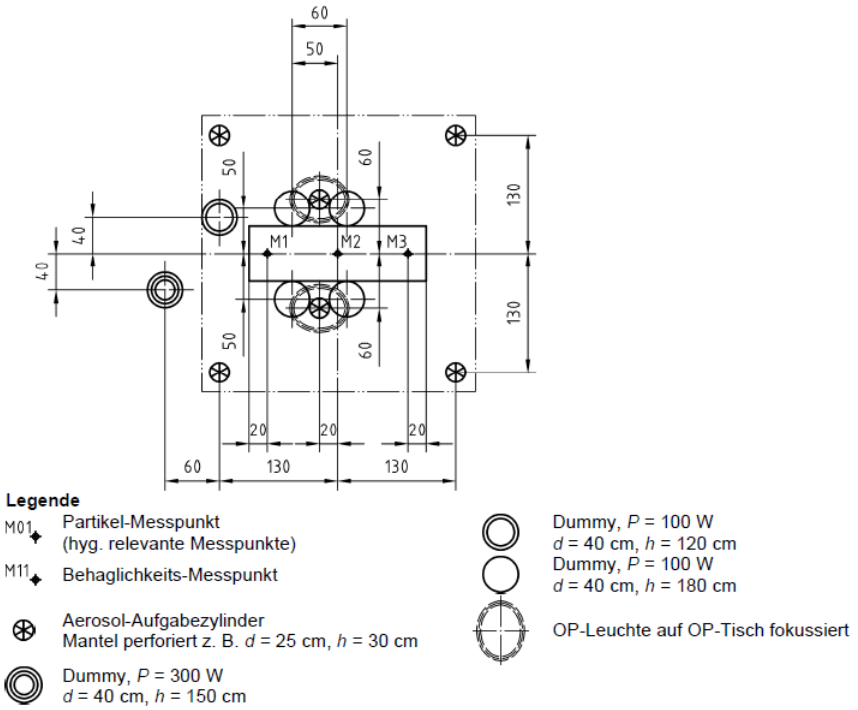

Figure 2.4: Reference load set-up for testing the protection against load entry from inside (from DIN 1964-4 [32]). Internal contamination layout

The two configurations described before are used as fixed experimental set-up (external and internal contamination), in order to experimentally evaluate the protection class in OT. How it can be seen there are five members of the surgical staff, the medical equipment, six aerosol diffusers, the surgical table and two surgical lamps 60° inclined. The protection class of the surgical site is calculated measuring the particulate concentration in the protected area, while in the operating theater is injected a reference particle load with the same intensity during each measurement. The reference artificial particle load consists, as for the Swiss standard, of an aerosol flow that is constant in time, emitted into the room at six specified locations by aerosol diffusers, whit a diameter of 25 cm and 30 cm high. The reference source strength (Q_{ref}) cannot be measured directly, but is determined as the product of the aerosol concentration (C_{Aer}) times the total aerosol volume flow (V_{Aer}):

$$Q_{ref} = C_{Aer} \cdot V_{Aer} \tag{2.5}$$

$$C_{ref} = \frac{Q_{ref}}{A_{ref} \cdot v_{ref} \cdot 3600} \tag{2.6}$$

where:
Q_{ref}, the reference source strength $[pp/h]$
C_{Aer}, the particulate concentration in the aerosol $[pp/m^3]$
V_{Aer}, the aerosol volumetric flow $[m^3/h]$
C_{ref}, the reference concentration $[pp/m^3]$
A_{ref}, the reference area covered by unidirectional flow $[m^2]$
v_{ref}, outlet air velocity of unidirectional flow $[m/s]$

During the measurements it is introduced into the OT a thermal load due to the presence of medical staff and the equipment. In particular there are:

- 5 dummies representing the medical staff which release 100 W of thermal load each one. They are 4 with a diameter of 40 cm and height of 180 cm and the other one with a diameter of 40 cm and height of 120 cm, representing the anesthetist;

- 1 machinery which releases 300 W of thermal load, with a diameter of 40 cm and an height of 150 cm.

Therefore, there is a total thermal load of 800 W within the operating theater.

The calculation of the protection class (SG) is recommended over stating particle concentrations measured in the protected area (C_x). It is calculated as:

$$SG_x = -\log\left(\frac{C_x}{C_{ref}}\right) \tag{2.7}$$

where:
C_X, the particle concentration measured in the x-location of the room $[pp/m^3]$
C_{ref}, the particle reference concentration of a value of $35.3 \cdot 10^6$ pp/m^3

The particle measuring points are called M_{01}, M_{02}, M_{03}; they are located little above the surgical table in the center of the it (medically relevant points). The comfort measuring points M_{11}, M_{12}, M_{13}, in which are measured temperature and relative humidity, are 85 cm above the surgical table in the center of it, as shown in the Figure 2.5.

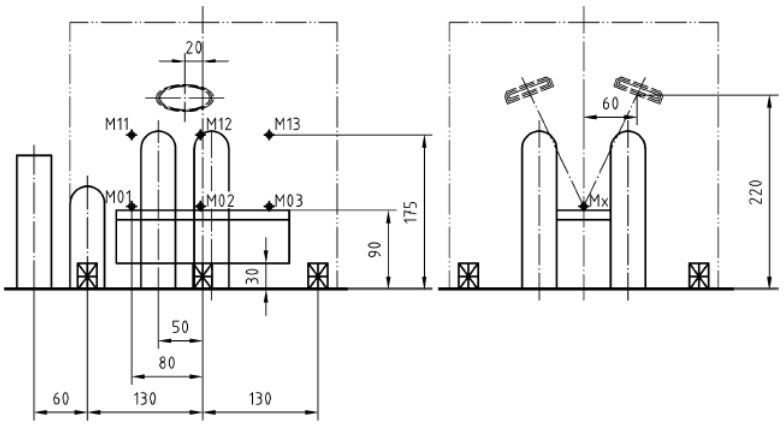

Figure 2.5: Reference load set-up for testing the protection against load entry from outside, two front views (from DIN 1964-4 [32])

At each measuring point M_{0x} it is necessary to carry out, and record immediately, at least ten successive measurements for one minute each, using a standard particle monitoring system OPC with a sample air volume flow equal to 28.3 l/min. After that, it shall be calculated and documented the mean protection class, called SG, as given by equation 5.3 from the mean value of all individual measurements at each measuring point, respectively. The protective effect against particle challenge load entry from outside and inside characterizes an operating room taking into consideration all of its flow-affecting ventilation, heating and medical installations and fittings. The range of values of the protective effect, maximally as a right-of-comma position to indicate are shown in the table 5.2.

Table 2.6: The range of values of the protection class, SG

Excellent	5.0
Very moderate	1.0
No protective	0

Other tests prescribed by this guideline, according to the UNI EN ISO 14644-3 [20], are the recovery test and the sealing seat and filter integrity test by particle measurement. For the recovery test the ventilation system must assure in 25 minutes a concentration of 3'520 pp/m^3 of particles with a diameter of 0.5 μm in 'at rest' condition. In the A4 appendix of the standard there is a description of the ULF (Unilateral Flow) supply-air diffuser for medical applications: the diffuser size must be 9.0 m^2 or above. The A5 appendix talks about the return-air terminal devices and their positions.

They must be located, if they are on the perimetral wall, near the ceiling and, arbitrarily, near the floor too [32].

2.8 The Swiss guideline: SWKI 99-3:2003

The SWKI 99-3:2003 [31] is the Swiss reference guideline for the construction, operation and monitoring of ventilation systems in hospitals. In the first part of the guideline there is a description and classification of hospital rooms based on an assessment of the risk of infection and the resuming Table 2.7 it is shown.

Table 2.7: Extract of the SWKI 99-3:2003 [31])

Use of room	***Remarks/requirements***	***Protective measure***
Operating room for implant surgery, where foreign material is implanted • *orthopaedic surgery* • *cardio/vascular surgery* • *neuro surgery*	*Contamination of the operating environment and the foreign material by airborne bacteria shall be prevented by taking appropriate measures. The fundamental measure is ventilation, supplemented by draping, clothing and disinfection.*	***Run ULF at 100 % air volume flow rate***
Operating room for surgery on sterile areas, no foreign material implanted • *neuro surgery* • *cardiosurgery* • *arthroscopy* • *keyhole surgery* • *room for caesarean sections* *Surgical MRI* *such as MRI-supervised surgery on brain tumours*	*The patient's skin is the primary source of infection risks. Germs carried in via the air may still be a problem. Requirements are therefore somewhat stricter than for interventions in areas already contaminated.*	***Run ULF at reduced air volume flow rate, if possible***
Operating room for interventions in areas already contaminated by bacteria • *visceral surgery* • *urology* • *ENT*	*Germs carried into the operating environment via the air are secondary compared with existing local flora. However, airborne germ concentrations should be as low as possible.*	

It is also specified that the the minimum size of the ULF system diffuser should the 9 m^2; smaller diffusers may be provided in specialized clinics where only those types of surgery are expected to be performed which do not require operation of a large air diffuser in the ceiling of the operating theater. In the section regarding the acceptance of operating rooms with ULF supply-air diffusers, the standard specifies the environmental conditions in term of:

– Supply-air temperature: 18 to 24 $°C$

– Minimum mean supply-air velocity: 0.24 m/s

- Minimum supply-air velocity: 0.20 m/s
- Maximum deviation of local supply-air temperature form the mean: $\pm$ 1 K
- Temperature deficit of supply air with respect of the room: 1 K
- Sound pressure level: the sound pressure level measured in the center of the area at 1.75 m above floor shall not exceed 48 db(A)

Furthermore, it is indicated, in accordance with the UNI EN ISO 14644-3 [20], to conduct two tests on the filters: one to monitor if the filters are leak-free, the second is the seal-tight test. Furthermore, there is the introduction of the hygienic acceptance test which consists of two partial test. First, proof shall be furnished that the aseptic area is sufficiently protected form its environment by means the unilateral air flow. To do this, a reference load source at a flow rate of 108 m^3/h (30 l/s) is injected by six aerosol diffusers during and this flow has to exhibit a particles concentration of $35 \cdot 10^8$ pp/m^3 with particles of a minimum diameter of 1 μm. The proof of sufficient protective effect has been furnished when the particle concentration of the fraction 1 μm does not exceed 3'500 pp/m^3 at each medically relevant measuring point in the critical area. The second partial test using a modified arrangement of the reference-load source is performed to verify any upward flow of contaminated room air from the floor into the critical area.
In the Annex F (just an informative), it is well described the way to conduct the tests. Beside the specifications introduced in the text of the regulation, it is added that, during the test, it must be considered a thermal load form the surgical staff (100 W for four members) and the equipment (300 W) and, in addition, it is indicated that the surfaces of the surgical lamps shall be less than 37°C. The internal arrangement of the room in both configurations is the same of the German one.

The guideline also fixes the requisite in the stage of planning, construction and operation. How it can be seen, this guideline is very similar to the German one except regarding the diameter of the generated particles and their concentration.

2.9 Conclusions about the regulations

These regulation are very similar for many aspects and comparable among them. The emphasis and the interest for this work is on the description of the quality test. In particular a good reference standard should explain in the details the quality test in operational or simulated operational conditions,

and consequently, the location of the aerosol diffusers and the their number, the amount of air release from them and the reference concentration to generate, the place where the particles could be counted, how to simulate the presence of the surgical staff and similar information.
The Italian standard UNI 11425:2011 [11] doesn't describe how to organize a test for the verification of the VCCC system quality. It describes the different type of health care facilities and defines their performance levels and parameters empathizing that this facilities are process-plant and so they are characterized by concepts like reliability, safety, reaching of the expected performances. The ISPESL [24] is more detailed and lists some important test to carry out in an operating theater; it describes how to calculate an appropriate number of sampling point but doesn't suggest where they are and how to conduct a test in simulated operational conditions, but only in at rest conditions.
The English standard HTM-03-01-Part A:2007 [25] is complete under many aspect. In the appendix it is also reported a complete classification of different health care facilities. There is a specification of reference particle diameter and concentration, and are defined the measurement points to compare with the challenge concentration. On the other hand, it is declared that tests should be carried out without surgical staff, which could be an element disturbing the flow path lines and particles releasing and entrainment.
The Swedish technical specification SIS-TS 39:2012 [27] introduces a reference diameter and a challenge concentration with which it is possible to calculate a quality index called Limitation Risk (LR). A brief description of disposition of the particle generation and is also indicated. Besides, it is not necessary a test under simulated surgical operations and, at any rate, it is not indicated how to conduct this test. Furthermore it isn't specified the location of the measuring points.
The French regulation NF S90-351:2013 [28] is detailed in many aspects, in particular in the classification of the different type of hospital environments and the respective parameters, in the description of the aerauliques solutions and in the information about the maintenance and qualification. A defection in the NF S90-351:2013 [28] is the deficiency of a complete description of the way to implement a qualification test in repetitive conditions for entrainment.
The American ANSI/ASHRAE/ASHE Standard 170-2013 [30] is more generic that the European ones except in fixing the operative conditions and the supply air velocities. It is poor in the quality test description; furthermore this part is briefly outlined in an appendix that is just an informative and it is not prescriptive. The Swiss regulation SWKI 99-3:2003 [31] is very similar to the German one. It was edited almost at the same time of the German regulation DIN 1964-4 [32] and the two standards are different just for some

technical considerations, for example about the diameter of the particles to sample in order to define the cleanliness class of the operating theater (the SWKI requires the sampling of particles with diameter $\geq 1\ \mu m$, whereas the German one doesn't fix a particular diameter) and for the reference concentration. But, in both cases, it is well described the way to conduct the quality test. Both of them illustrate with some layout scheme the arrangement of the room during the test. The German regulation has a reference a value concentration more realistic and practical to conduct a test. Furthermore it explains very well how to calculate a quality index (SG) to have an easy measure of the quality level of the critical zone. For this reason the DIN 1964-4:2008 [32] was chosen to create a CFD model of the considered OT in order to dispose of a validated model to use as a good alternative to the expensive and invasive experimental campaign. Thanks to the German standard, it was possible to study the performance of the ventilation system in respect of the contamination removal with a *'simulated operational'* condition, in the real operating theater and in the simulated one, with repetitive conditions.

Chapter 3

Case of study: operating theater B2 at San Gerardo Hospital in Monza

In chapter 2, it was discussed the role of the different national and international standards, guidelines and memorandum on the way of designing, constructing and testing health care premises and in the particular case of this work the protection class from airborne contamination of operating rooms and their critical areas. After having perceived the main differences among all the documents previously treated with their pro and con, it was agreed that the technical documents that best fits the needs and prescriptions of the work planned in this master thesis work was the standard DIN 1964-4:2008. In fact, this standard gives a complete description of the setting layout and procedure of the experimental test which has to be carried out in order to test an operating theater from the point of view of contamination control. This chapter gives a brief description of the real operating room chosen as reference OT for the experimental test and more important for the simulations in CFD carried out. Experimental tests are compulsory and in some way fundamental to compare and to validate the results of the CFD simulations delivered with the same geometry, boundary conditions and settings used for the experimental performance tests.

3.1 Operating theater geometry

The operating theater chosen as reference OT for this work is part of an operating block of an Italian hospitals in the neighborhood of Milan. It was completed in the 2010 and it is mainly used for cardiovascular surgery. Hereinafter, this OT will be called OT B2, as it is named in reality. The OT

B2 has a surface in plant equal to 46.5 m^2, more in detail 7×7 m, with a net height of 3 m for a total net volume of 144 m^3. The OT B2 is provided with a unidirectional ceiling diffuser composed of 23 HEPA H14 filters, , conforming to the UNI EN 1822[16]. The geometry and technical data of the ceiling filter was given by SagiCofim S.p.a., a company which has designed, produced and installed the ceiling filter diffuser in the considered operating theater. In the figure 3.1 there is a photo taken in the operating theater B2 in which it is possible to see the ceiling filter diffuser, the surgical lamps and the table.

Figure 3.1: Photo taken in the operating theater B2

More in detail, the ceiling diffuser, mod. Dif OT/LS 5/555, has total dimension of 3000×3000 mm. The dimensions of each filter are 575×575 mm, but the effective filtration area is of 521×521 mm. A plenum installed before the H14 filter array equalized the pressure upstream and let an uniform distribution of the air flow rate The main characteristic of this ceiling filter system is the differentiation of supply air velocity, even though the air path is unidirectional facing downwards. More in detail, the three central filters under the operating table release air at a velocity of 0.45 m/s and therefore they are indicated as High Speed (HS) filters, while six filters around the first three HS filters emit air at a velocity of 0.35 m/s, Medium Speed (MS). The periphery of the ceiling diffuser is equipped with H14 filters with a low air velocity (LS) equal to 0.25 m/s as shown in the Figure 3.2.

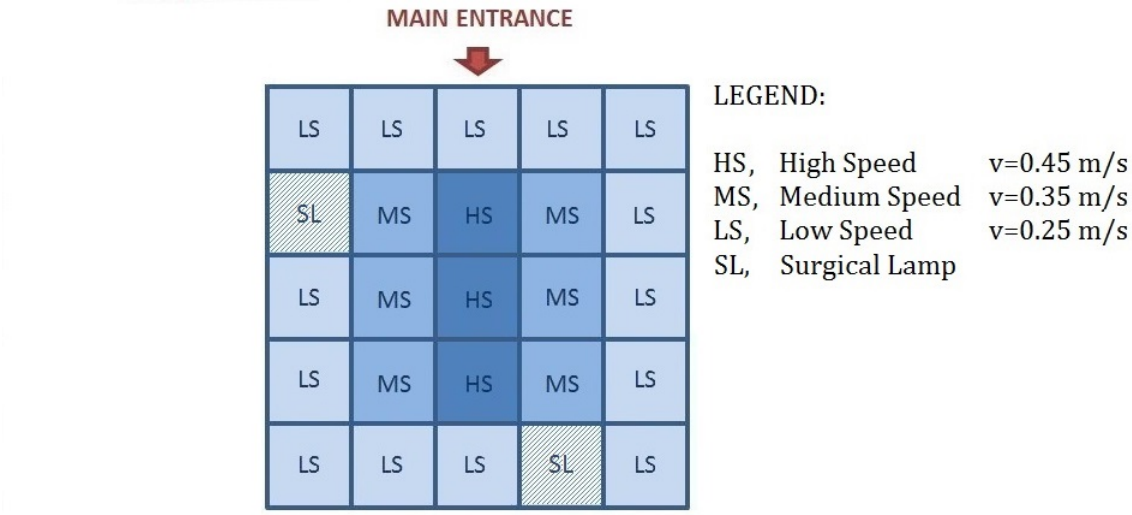

Figure 3.2: Lay-out of filters distribution in the DIF-OT ceiling filter under ventilation [18]

The various ways to bend the fibers of the filtering media originate the different crossing velocities of air through the filters and therefore the different supply air velocity described before. This type of configuration helps the process of sweeping effect of the critical area from airborne contaminants conveying contaminants both downward and towards the external part of the critical area.

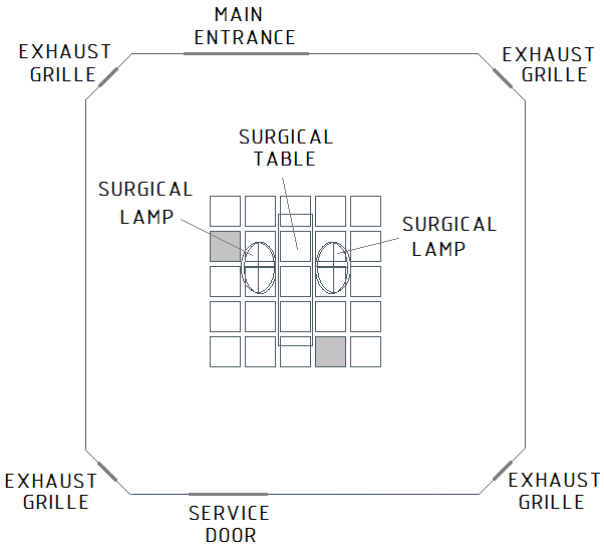

Figure 3.3: Plant of the operating theater B2

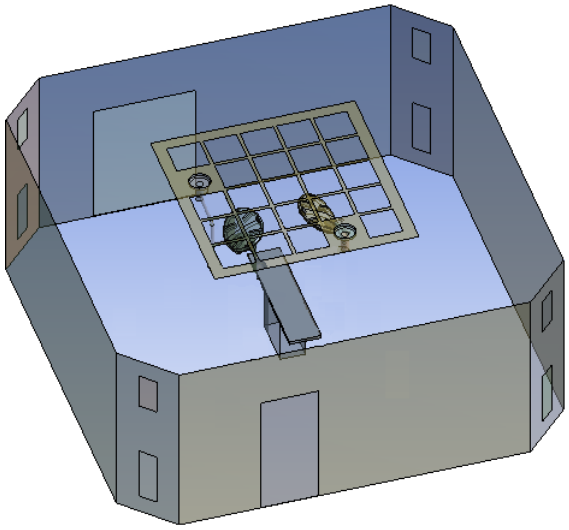

Figure 3.4: Isometric 3D rendering of the OT B2 under evaluation

As It can be seen from Figure 3.3 and 3.4, while the supply air come from the ceiling diffuser the exhaust air is conveyed outside the OT via a set of exhaust grilles located at the corners of the OT. For each corner there are two exhaust grilles located at different positions. The first one is positioned at 300 mm of distance from the floor and has a dimension of 300×900 mm, while the second one, of dimension equal to 300×600 mm, is at 300 mm of distance from the ceiling. Figure 3.5 indicates the dimension and the position of the two exhaust grilles in a corner.

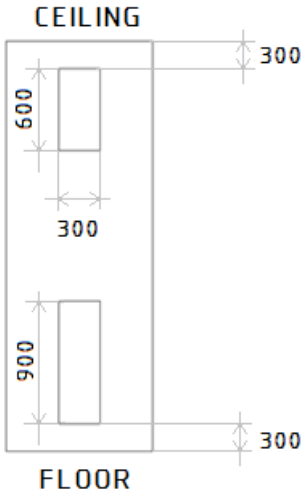

Figure 3.5: Exhaust grilles positions and dimensions in the OT B2

3.2 Operative conditions of the Operating Theater

The ventilation system of the OT B2 was designed in order to ensure an ISO 5 class in the '*operation occupational state*', conforming to the UNI EN 14644-1 [20]. In fact, it is an operating theater with an very high quantity of supply air in accordance with the UNI 11425:2011 [11]. Its operative conditions are summarized in Table 3.1.

Table 3.1: Environmental parameters for the operating blocks, table B.2, UNI 11425:2011 [11]

Ambienti	Temperatura [°C]		Umidità relativa [%]		Sovrapressione rispetto all'esterno	Aria esterna	Aria di ricircolo	Classi di pulizia secondo UNI EN ISO 14644-1	Livello di filtrazione finale	Livello di pressione sonora
	Inverno	Estate	Inverno	Estate	[Pa]	[vol/h]	[-]			[dBA]
Sale operatorie a elevatissima qualità dell'aria	≥ 20	≤ 24	≥ 40	≤ 60	15[1)]	15	SI[2)]	ISO 5	H 14	45[3)]
Sale operatorie a elevata qualità dell'aria					15[1)]	15	SI[2)]	ISO 7	H 14	45[3)]
Sale operatorie a qualità dell'aria standard					15[1)]	15	-[4)]	ISO 8	H 14	45[3)]

In order to maintain the performances in terms of air quality are injected 6800 m^3/h (corresponding to 47 ACH). Of these, 2500 m^3/h (corresponding to 17 ACH) of fresh air while the rest of the air flow rate is just recirculated air. Moreover, in order to maintain the overpressure of 15 Pa required by the regulation, 6600 m^3/h are extracted from the exhaust the eight grilles, to avoid the risk of contaminant infiltrations from adjacent environments (e.g. ancillary rooms and corridors). The design conditions of the supply air at the ceiling filter are [29]

Relative Humidity	50 % ±5
Temperature	20°C

3.3 'Simulated operational' configuration

As stated before, the DIN 1964-4 [28] was chosen as reference standard for the implementation of the experimental validation of the different OT scenarios simulated in this work. This standard was chosen because of it deals exactly with proper and full precise arrangement for challenging the contamination level of the OT critical area during repetitive experimental tests in the occupational state '*in operation*' more precisely '*simulated operational state*'.

The simulated test as stated in chapter 2, has the main goal to simulate the level of protection from external contamination of the critical area during a simulated surgical operation. Therefore, it is necessary to simulate the normal arrangement of a real surgical operation. Around the operating table are positioned 5 dummies, cylinders with an hemispherical 'head'. Four of these dummies have an height of 180 cm , they represent the surgical staff, while a dummy of 120 cm height represents the anesthetist seated close to the head of the patient. Another dummy represents the surgical equipment, 150 cm high.

The artificial challenge contamination, made of artificial oil, can be generated within the OT in two different scenarios, internal and external configurations which refer to relative position of the aerosol diffusers with respect to the operating table dummies and ceiling filter footprint as deeply explained in chapter 2.

Chapter 4

CFD model and simulations

In this chapter, at the beginning, will be shown the state of art of the CFD simulation connected with the operating theater. Later, it will be described the theory at the base of the CFD, the different type of turbulent models to overcome the problems connected to the solution of Navier-Stokes equations and the modeling of multiphase flow. In the last section it will be introduced each stage from the construction of the 3D model to the simulation setting for the simulations carried out. In order to conduct the simulations three tools of ANSYS© have been used: Design Modeler, Meshing and Fluent. All engineering simulation starts with geometry to represent the design. This geometry has been produced in a Computer-Aided Design (CAD) system: ANSYS Design Modeler software. The next step is the mesh generation. It is one of the most critical aspects of engineering simulation. Too many cells may result in long solver runs, and too few may lead to inaccurate results. ANSYS Meshing technology has been used to create an opportune mesh for the simulations. When the mesh is ready it has to be imported in Fluent. ANSYS Fluent software contains the broad physical modeling capabilities needed to model flow, turbulence, heat transfer, etc. In the this chapter there is a more detailed description of the steps carried out for this work.

The direct measurement and the numerical computation are two basic approach used in the analysis of the air fluxes and of the airborne particulate concentration in a operating theater. Obviously the most realistic information could be obtained from the experimental data, but in order to evaluate the performances of air fluxes relative to a ventilating system design for a contamination controlled environment, the CFD simulation is an extremely useful tool. With developments in Computational Fluid Dynamics (CFD) technology, comprehensive airflow analysis of the entire room space has become manageable. The developments were based on the work of Launder

and Spalding in the early 1970s. Within the context of fluid mechanics, the determination of room airflow and particulate distribution requires to solve the continuity and momentum equations in three dimensions. The CFD is based on numerical techniques which solves a set of conservation equations. These governing equations of fluid flow represent mathematical statements of the conservation laws of physics:

- The mass of a fluid is conserved
- The rate of change of momentum equals the sum of the forces on a fluid particle (Newton's second law)
- The rate of change of energy is equal to the sum of the rate of heat addition to and the rate of work done on a fluid particle (first law of thermodynamics)

The equations are solved with numerical methods. In outline the numerical algorithm consists of the following steps:

- Integration of governing equations of fluid flow over all the (finite) control volumes of the domain;
- Discretisation: conversion of the resulting integral equations into a system of algebraic equations;
- Solution of the algebraic equations by an iterative method [34].

In the prediction of air fluxes in an operating theater, the flux equations must to take into account the turbulence and the buoyancy force.

The degree of detail and result accuracy, depend on the correctness of the input boundary conditions (such as room pressure, heat flux from lamps and equipment, contaminant release rate, etc.) and the fineness of the numerical grid (subdivision of room space).

4.1 Models and applications for operating theaters

As introduced previously, the '70s CFD techniques has begun to combine the technologies related to the design and monitoring of ventilation in operating theaters. In the application of these techniques some limitations shall be taken into account such as the dependence of the solution by the type of grid adopted, the slowness and the uncertainty of convergence and the need for skilled operators able to correctly interpret the results. With the

improvements and ease of use of the simulation tool software, the difficulties were gradually reduced. There are also other limitations related more to the physical basis, in particular the use of empirical coefficients in the equations and in the wall functions. The CFD models, as powerful tools, have successfully been applied in the HVAC field. Many researches have been carried out on predicting detailed room air flow patterns, indoor temperature distributions, and pollutant transportation in indoor environment. Meantime, CFD is a useful tool in design practice for the verification and comparison of preliminary building design alternatives. In contrast to full scale ventilation performance test, the CFD method is a relatively inexpensive and alternative method. It is applicable to provide complete information concerning indoor environment and space ventilation control performance of a new developed control strategy before it is constructed [35]. Several studies about the application of CFD technologies in ventilation were carried out. Swift et al. [36] discussed the impact of different air distribution strategies on infection control and the effects of the lighting and the obstructions on laminar air flow system (declared as the best one). Memarzadeh and Manning [37] used Computational Fluid Dynamics analysis to show that when the design is appropriate, laminar flow conditions are the best choice among a large comparison of air flows and ventilation systems in order to control the risk of contaminant deposition in a surgical operating room. Memarzadeh and Jiang [38] used CFD to test the ceiling height impact on the level of contaminants present at the surgical site in an operating theater using airflow modeling and particle tracking methodologies. Kameel et al. [39] created a validated three-dimensional computational scheme used to predict the air flow regimes, relative humidity and heat transfer characteristics under actual room geometrical and operational conditions; their paper demonstrates the usefulness of utilizing such numerical procedures to adequately predict the behavior of air conditioned in operating theatres. Brohus et al. [40] investigated the influence of two disturbances in an operating room: the door opening during an operation and the activity level of the staff. The same topic was carried out by Shuyun et al. [41], Tung et al. [42] in the specific application in local operating theaters. The study of Srebrica et al. [43] demonstrated that the accuracy of CFD simulations strongly depends on the appropriate setting of boundary conditions and numerical simulation parameters. In more detail, their work explored the influence of three boundary conditions: contaminant source area size, convective-radiative heat fluxes and shape-size of human simulators. All of these works were carried out with a parallel validation of the conceived CFD models. In literature, there is very few material about the application of CFD technologies to the European Standard SWKI 99-3 [31] and DIN 1964-4 [32]. Zoon et al. [44] reported the experimental test in which

was applied the DIN 1964-4 [32] standard to a Dutch operating theater but there isn't a complete and comprehensive study with CFD methods. The present work want to follow the advantages of CFD technologies applying these to a real case tested with the German standard, DIN 1964-4 [32]. In fact, as explained before, this is the most complete and appropriate standard to test the performance of a ventilation system in an operating theater.

4.1.1 The-3D model: mesh, boundary conditions and other remarkable aspects

In this section the stages at the base of the modeling process will be introduced. The first stage is the conception of the room in order to design the right 3D model. It is important to include each aspect which are involved with the process that is studied. The degree shall allow to reach the prefixed goals. The are some simplification to model the room because it is impossible to include each obstacle. There is now the description of some simplifications ordinarily adopted. The standing surgical staff members are usually modeled by vertical cylinders by the side of the surgical table. The staff member models are considered as surfaces emitting a constant heat flux. The surgical lights are also modeled as a rectangular boxes or with better approximations above the patient, whose bottom or up surfaces are at set temperature or emit a set heat flux. It can be added other emitting bodies (of heat flux and particles) like the equipment. For this work thanks to the indication of the German regulation, the choice of the internal arrangement was easy. Among the local disturbances, the surgical lamps are considered a critical factor for the operation of the unidirectional flow system. Chow et al. [13] showed that the position of the lamps influences the protection level that the ventilation system provides to the surgical site. Also the influence of the different forms of surgical lamps was studied with the use of computational simulations and experimental campaigns. In fact, the simulations were not able to detect an appreciable difference between the various forms used, and it was verified that the size of the lamps influences significantly the performance of the downward flow.
At the beginning, the computational domain is discretized (subdivided) into a mesh of many elements. The mesh is generated with appropriate meshing tool. The distribution of the element size in the computational domain is determined from a mesh independence study by systematically changing the mesh density in all space directions both globally and locally to obtain a mesh that can give a numerical solution independent by the number of elements with an acceptable accuracy. Regular elements are used to fill most parts of the domain while properly refined element layers are assigned around

input, output, and solid surfaces to capture the high rates of change of momentum and heat transfer which take place there. In CFD exists parameters to evaluate the mesh quality such as: Aspect Ratio and Equiangle Skewness. The first one monitors the difference between two adjoining elements which couldn't be too much high not to cause a strong increase in the phenomenon of numerical diffusion. The Aspect Ratio (AR) is the ratio of longest to the shortest side in a cell. Ideally it should be equal to 1 to ensure best results. For multidimensional flow, it should be near to one. Also local variations in cell size should be minimal, i.e. adjacent cell sizes should not vary by more than 20%. Having a large aspect ratio can result in an interpolation error of unacceptable magnitude. The Equiangle Skewness of a mesh is an indicator of the mesh quality and suitability. A skewness' of 0 is the best possible one and a skewness of 1 is almost never preferred. Large skewness compromises the accuracy (from 0.94 and 1) of the interpolated regions.

After the meshing process it is necessary to load the mesh in the CFD-program to simulate the therm-fluid-dynamics conditions of the indoor environment. During the setting stage, it is important to choice the proper turbulent methods and the wall-model. An other aspect to consider is that the degree of detail and accuracy of the results depend on the correctness of the boundary conditions of the input (for example, the pressure of the room, the heat flux from the lamps and the surgical staff, the release rate of contaminants from the sources, etc.). The common boundary conditions are:

- prescribed mean velocities (or velocity profiles) on supply diffusers
- no-slip on walls and solid surfaces
- constant temperatures on diffusers
- constant temperature or constant heat flux on body surfaces
- constant temperatures on lamp surfaces
- thermal insulation on walls, on the floor and ceiling (or constant T)
- zero-value of contaminant concentration in the supply air
- constant contaminant flux released by the surgical staff

The patient is treated differently by the staff. It goes through various processes of sterilization before being operated and during the operation is maintained in a state of unconsciousness and its physical functions remain at a low level. Furthermore particles emitted from the patient hardly reach the

surgical site because they are immediately invested by the unidirectional flow [3]. This often leads to neglect the physical presence of the patient during the simulations, including those carried out in operating conditions. The major applications of CFD in ventilation are mainly for stationary flows, and these flows have not significant limitations. An unsteady flow occurs when the initial state (stationary) is disturbed by a change of the boundary conditions. An example of this is when a door between two rooms is opened: the boundary conditions of the flow field vary and are influenced by the different positions of the door and by the stabilization of the pressure. There are also other transient disturbances of the flow caused by human activity: the movements of staff and equipment are among the many possibilities that could lead to an infection from airborne particulate. For example, the position of the surgical lamps and their brightness level (i.e. the output power) can be adjusted by the staff during the operation. They are not directly controllable by an engineer specializing although there are clear instructions for their use. During the iterations it is necessary to monitor the convergence. It is possible monitoring the residuals of the running equations or plotting the trend of some properties or physical dimensions like mass flows, pressure at inlet etc. At the end of the simulation it will be important to view the results in the so-called 'post-processing' stage. It is interesting to plot the contours of velocity, temperature and distribution of contamination; it is possible to download the data useful for validation.
The scheme in the Figure 4.1 shown each stage at the base of the the modeling process.

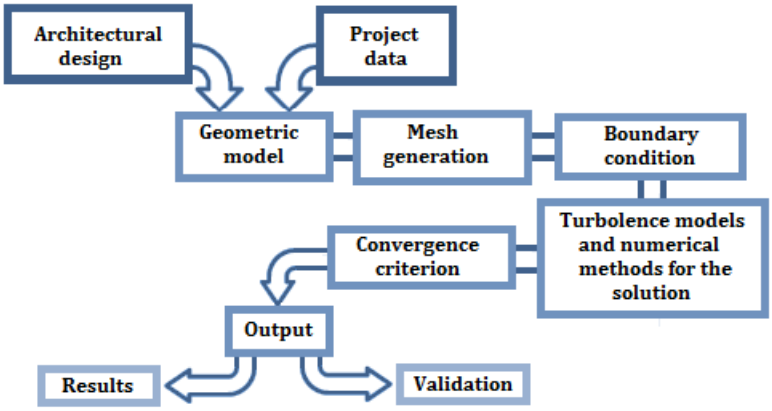

Figure 4.1: Flux diagram for a typical CFD-process [45]

The CFD modeling is undoubtedly a more and more popular approach. It can provide a greater and more immediate understanding of the aerial spread of particles and the efficiency of control strategies. However, it is necessary

to consider that there are, at least, three source of uncertainty :

- *Model uncertainty* : includes all (the errors) and uncertainties that are related to the physical model,the boundary conditions, the material properties and represent the difference between the real flow and the exact solution of the mathematical model;
- *Human uncertainty* : includes all the possible errors that the CFD analyst may (consciously or not)introduce in the discretisation of the real problem;
- *Numerical uncertainty* :includes all the convergence uncertainties, round off and discretisation error. Moreover,in order to define appropriate models it is necessary a validation stage, taking into account each uncertainty shown in the previous list.

4.2 Basic theory on CFD

4.2.1 Turbulence models

The governing equations of mass, momentum and energy, for a Newtonian fluid are the Navier-Stokes equation:

$$\frac{\partial \rho}{\partial t} + \mathrm{div}(\rho \mathbf{u}) = 0 \tag{4.1}$$

$$\frac{\partial (\rho u)}{\partial t} + \mathrm{div}(\rho u \mathbf{u}) = -\frac{\partial p}{\partial x} + \mathrm{div}(\mu \mathrm{grad} u) + S_{Mx} \tag{4.2}$$

$$\frac{\partial (\rho v)}{\partial t} + \mathrm{div}(\rho v \mathbf{u}) = -\frac{\partial p}{\partial y} + \mathrm{div}(\mu \mathrm{grad} v) + S_{My} \tag{4.3}$$

$$\frac{\partial (\rho w)}{\partial t} + \mathrm{div}(\rho w \mathbf{u}) = -\frac{\partial p}{\partial z} + \mathrm{div}(\mu \mathrm{grad} w) + S_{Mz} \tag{4.4}$$

$$\frac{\partial (\rho c T)}{\partial t} + \mathrm{div}(\rho c T \mathbf{u}) = -p \mathrm{div}\mathbf{u} + \mathrm{div}(k \mathrm{grad} T) + \Phi + S_T \tag{4.5}$$

Where:

ρ, is the density of the fluid $[kg/m^3]$
$\mathbf{u}$, is the velocity vector t, is the time $[m/s]$
u, v, w, are the components of the velocity vector $[m/s]$
p, is the pressure $[Pa]$
μ, is the turbulent viscosity $[kg/m \cdot s]$
T, is the temperature $[K]$

x, y, z, are the component of the position vector $[m]$
c, is the heat capacity $[W/kg \cdot K]$
k, is the thermal diffusivity $[W/k \cdot m]$
S_x, S_y, S_z, are the momentum source $[W/m^3]$
Φ, is the dissipation function $[W/m^3]$
S_T, is the energy source $[W/m^3]$

A laminar flux is completely described by Navier-Stokes equations, because, for simple cases, these equations are solvable in an analytic way. More complex fluxes need numerical methods. In the case which are studied the fluid is in turbulent regime. The turbulence manifests itself as random fluctuations of the measured velocity component about a mean value. All the other flow variables i.e. the pressure, temperature, density etc., will also exhibit this additional time-dependent behavior. The Reynolds decomposition defines the flow property φ at this point as the sum of a steady mean component $\mathbf{\Phi}$ and a time varying fluctuating component $\varphi'(t)$ with zero mean value: hence, the generic flow property is defined as: $\varphi(t) = \mathbf{\Phi} + \varphi'(\mathrm{t})$. The turbulent fluctuations always have a tree-dimensional spatial character. Furthermore, visualizations of turbulent flows reveal rotational flow structures, so-called turbulent eddies, with a wide range of length scales. Particles of fluid which are initially separated by a long distance can be brought close together by eddying motions in turbulent flows. As a consequence, heat, mass and momentum are very effectively exchanged. Such effective mixing gives rise to high values of diffusion coefficients for mass, momentum and heat. The largest turbulent eddies interact with and extract energy form the mean flow by a process called vortex stretching. The large eddies are dominated by inertia effects and viscous effects are negligible. Smaller eddies are themselves stretched strongly by somewhat larger eddies and more weakly with the mean flow. In this way the kinetic energy is handed down from large eddies to progressively smaller and smaller eddies in what is termed the energy cascade [34].

In order to solve the Navier-Stokes equations, a substantial amount of research effort is dedicated to the development of numerical methods to capture the important effects due to turbulence. The methods can be grouped into the following three categories, which gives different results of the same problem as it can be seen in the Figure 4.2:

1. Reynolds-averaged Navier-Stokes (RANS) equations: in the RANS method the attention is focused on the mean flow and the effect of turbulence on mean flow properties. Prior to the application of numerical methods the Navier-Stokes equations are time averaged (or ensemble averaged in flows with time-dependent boundary conditions).

Extra terms appear in the time-averaged (or Reynolds-averaged) flow equations due to the interactions between various turbulent fluctuations. These extra terms are modeled with classical turbulence models: among the best known ones are the $\kappa-\varepsilon$ model and the Reynolds stress model.

2. Large Eddy Simulation (LES): this is an intermediate from of turbulence calculations with tracks the behavior of the larger eddies. The method involves space filtering of the unsteady Navier-Stokes equations prior to the computations, which passes the larger eddies and rejects the smaller eddies. Unsteady flow equations must be solved, so the demands on computing resource in therms of storage and volume of calculations are large but this technique is starting to address CFD problems with complex geometry.

3. Direct Numerical Simulation (DNS): these simulations compute the mean flow and all turbulent velocity fluctuations. The unsteady Navier-Stokes equations are solved on spatial grids that are sufficient fine that they can resolve the Kolmogorov length scales at which energy dissipation takes place and with time steps sufficiently small to resolve the period of the fastest fluctuations. These calculations are highly costly in terms of computing resources, therefore the method is not so frequently used for industrial flow computations.

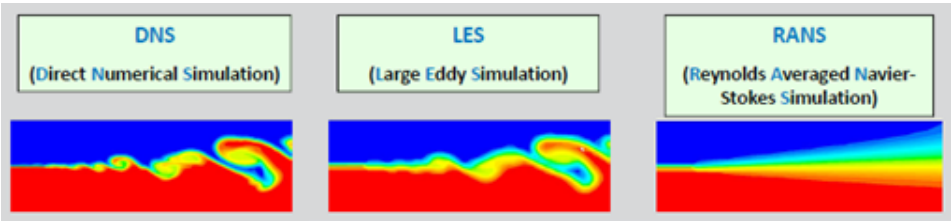

Figure 4.2: Solutions obtained with the different resolved methods [46]

The Figure 4.2 shown the difference between the three methods in solving the equations: from the DNS to the RANS there is the gradual loss of some information about the flow. The vast majority of turbulent flow computations has been carried out with procedures based on the RANS equations, specially of industrial applications. This family of methods is divided in two groups:

– Eddy viscosity models

– Stress transport models

The Eddy viscosity are first order models and they are based on the presumption that there is an analogy between the action of viscous stresses and Reynolds stresses on the mean flow. Both stresses appear on the right hand side of the momentum equation(4.2, 4.3, 4.4), and in the Newton's law of viscosity the viscous stresses are taken to be proportional to the rate of deformation of fluid elements. For an incompressible fluid this gives to:

$$\tau_{ij} = \mu \cdot s_{ij} = \mu \cdot \left(\frac{\partial u_i}{\partial x_j} + \frac{\partial u_j}{\partial x_i} \right) \tag{4.6}$$

Turbulent stresses are found to increase as the mean rate of deformation increases. Boussinesq proposed in 1877 that Reynolds stresses might be proportional to the mean rates of deformation:

$$\tau_{ij} = -\rho \overline{u_i' u_j'} = \mu_t \left(\frac{\partial U_i}{\partial x_j} + \frac{\partial U_j}{\partial x_i} \right) - \frac{2}{3} \rho k \delta_{ij} \tag{4.7}$$

where:
k, is the turbulent kinetic energy per unit mass $[J/kg]$
δ_{ij}, is the Kronecker delta ($\delta_{ij} = 1$ if $i = j$ and $\delta_{ij} = 0$ if $i \neq 0$) [-]
μ_t, is the turbulent or eddy viscosity $[kg/m\ s]$

The methods belonging to this family are divided into other groups:

- Mixing length models (zero-equation): attempt to describe the stress by means of simple algebraic formula for μ_t as a function of position.

- Spalart-Allmaras (one-equation): involves a transport equation for a modified viscosity, the turbulent kinematic viscosity $\tilde{\nu}$ and a definition of a length scale by means of an algebraic formula.

- $\kappa - \varepsilon$ (two-equations): a more sophisticated but also more costly, description of turbulence which allows for the effects of transport of turbulence properties by convection and diffusion and for production and destruction of turbulence. Two transport equations (PDEs), one for the turbulent kinetic energy κ, and further one for the rate of dissipation of turbulent kinetic energy ε, are solved. There are different formulations of this model: $\kappa - \varepsilon$ standard, $\kappa - \varepsilon$ realizable, $\kappa - \varepsilon$ RNG, $\kappa - \varepsilon$ low Reynolds.

- $\kappa - \omega$ (two-equations): it is similar to the previous one ($\kappa - \varepsilon$), but it solves the transport equation for the eddy "turn-over" frequency ω, rather than the turbulent dissipation rate. The frequency ω is related with ε by means of the relation: $\omega = \frac{\varepsilon}{\kappa}$.

This method exists also like SST $\kappa - \omega$, the Shear Stress Transport formulation.

Regarding the Stress transport models, they don't use the Boussinesq hypothesis (eq. 4.7) and the isotropy of the turbulent eddy viscosity but evaluate directly the exact transport equations for Reynolds stresses (R_{ij}, component of the Reynolds stress tensor) with models composed by more equations, algebraic (ASM) or differential. Among the differential models there is the Reynolds Stress Model, which writes the exact equation of Reynolds stress transport.

In the Table 4.1 [34] there is a summary of the main applications of the mentioned methods, with related advantages and limitations.

Table 4.1: Turbulent models and their behavior and usage [34]

Model	Behavior and Usage
Spalart-Almaras	Economical for large meshes. Performs poorly for 3D flows, free shear flows, flows with strong separation. Suitable for mildly complex (quasi-2D) external/internal flows and boundary layer flows under pressure gradient (e.g. airfoils, wings, airplane, fuselage, missiles, ship hulls).
Standard $\kappa - \varepsilon$	Robust. Widely used despite the known limitations of the model. Performs poorly for complex flows involving severe ∇P, separation, strong stream line curvature: Suitable for initial iterations, initial screening of alternative designs and parametric studies
RNG $\kappa - \varepsilon$	Suitable for complex shear flows involving rapid strain, moderate swirl, vortices and locally transitional flows (e.g. boundary layer separation, massive separation and vortex-shedding behind bluff bodies, stall in wide-angle diffusers, room ventilation)
Realizable $\kappa - \varepsilon$	Offer largely the same benefits and has similar applications as RNG. Unable to use with multiple rotating reference frame. Possibly more accurate and easier to converge than RNG.
Standard $\kappa - \omega$	Superior performance for wall-bounded boundary layer, free shear and low Re flows- Suitable for complex boundary layer flows under adverse pressure gradient and separation (external aerodynamics and turbomachinery). Can be used for transitional flows (though tends to predict early transition). Separation is typically predicted to be excessive and early.
SST $\kappa - \omega$	Similar benefits as Standard $\kappa - \omega$. Dependency on wall distance makes this less suitable for free shear flows.
RSM	Physically the most sound RANS model. Avoids isotropic eddy viscosity assumption. More CPU time and memory required. Tougher to converge due to close coupling of equations. Suitable for complex 3D flows with strong streamline curvature, strong swirl/rotation (e.g. curved duct, rotating flow passages, swirl combustors with very large inlet swirl, cyclones).

4.2.2 Near-Wall modeling

Turbulent flows are significantly affected by the presence of wall. Obviously, the mean velocity field is affected through the no-slip condition that has to be satisfied at the wall. However, the turbulence is also changed by the presence of the wall in non-trivial ways. Very close to the wall, viscous damping reduces the tangential velocity fluctuations, while kinematic blocking reduces the normal fluctuations. Toward the outer part of the near-wall region, however, the turbulence is rapidly augmented by the production of turbulence kinetic energy due to the large gradients in mean velocity. So, close to the wall the flow is influenced by viscous effects and does not depend on free stream parameters. The mean flow velocity only depends on the distance y from the wall, fluid density ρ and viscosity μ and the wall shear stress τ_w. According to which has been mentioned before:

$$U = f\left(y, \rho, \mu, \tau_w\right) \tag{4.8}$$

and in a dimensionless analysis,

$$u^+ = \frac{U}{u_\tau} = f\left(\frac{\rho u_\tau y}{\mu}\right) = f(y^+) \tag{4.9}$$

where u_τ,is the friction velocity, defined as:

$$u_\tau = \sqrt{\frac{\tau_w}{\rho}} \tag{4.10}$$

The formula 4.9 is called the *law of the wall* and is different gradually moving away from the wall as shown in the figure 4.3. Now it is necessary to introduce the dimensionless distance from the wall, y^+, defined as:

$$y^+ = \rho u_\tau \frac{y}{\mu} \tag{4.11}$$

The near-wall modeling significantly impacts the fidelity of numerical solutions, inasmuch as walls are the main source of mean vorticity and turbulence. After all, it is in the near-wall region that the solution variables have large gradients, and the momentum and other scalar transports occur most vigorously. Therefore, accurate representation of the flow in the near-wall region determines successful prediction of wall-bounded turbulent flows.

Numerous experiments have shown that the near-wall region can be largely subdivided into three layers. In the innermost layer, called the "viscous sublayer", the flows is almost laminar, and the (molecular) viscosity plays a dominant role in momentum and heat or mass transfer. In the outer layer, called the fully-turbulent layer, turbulence plays a major role. Finally, there

is an interim region between the viscous sublayer and the fully turbulent layer where the effects of molecular viscosity and turbulence are equally important. The figure 4.3 illustrates these subdivisons of the near-wall region, plotted in semi-log coordinates.

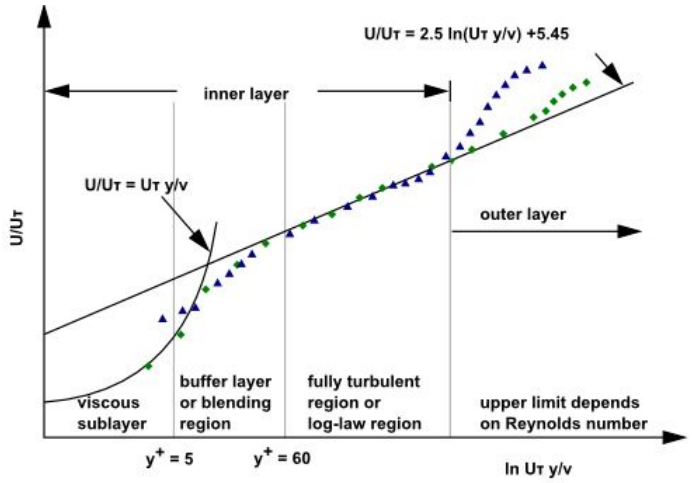

Figure 4.3: Subdivision of the Near-Wall Region [46]

In the *viscous sublayer* ($y^+ < 5$):

$$U = \frac{\tau_w y}{\mu} \tag{4.12}$$

and consequently:

$$u^+ = y^+ \tag{4.13}$$

Outside the viscous sublayer ($30 < y^+ < 500$) in the *buffer layer region,* there is the following log-law:

$$u^+ = \frac{1}{k} \ln\left(y^+\right) + B \tag{4.14}$$

Traditionally, there are two approaches to modeling the near-wall region:

1. Logarithmic-based Wall Functions
2. Near-Wall Model

In the Logarithmic-based Wall Functions, the viscosity-affected inner region, viscous sublayer and buffer layer, is not resolved. Instead, semi-empirical formulas, called "wall functions", are used to bridge the viscosity-affected

region between the wall and the fully-turbulent region. The use of wall functions obviates the need to modify the turbulence models to account for the presence of the wall. To use this approach the position of the first cell center from the wall must be located in the logarithmic region of the boundary layer. In order to do this, it is necessary that the y^+ value is included among 30 and 500. The mesh in proximity of the wall is relatively coarse.

In the Near-Wall Model, the turbulence models are modified to enable the viscosity-affected region to be resolved with a mesh all the way to the wall, including the viscous sublayer. This approach requires a finer near-wall mesh than the other one. Therefore, the y^+ value of the first cell center near the wall must be circa 1. Besides, the number of nodes in the viscous sublayer must be greater than 10. These two approaches are depicted schematically in the Figure 4.4:

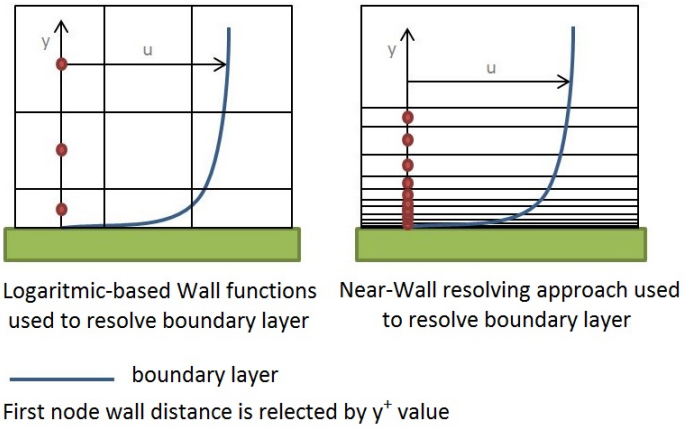

Figure 4.4: Adopted approaches in the study of wall behavior [46]

As stated before, wall functions are set of semi-empirical formulas and functions that in effect "link" the solution variables at the near-wall cells and the corresponding quantities on the wall. For the $\kappa - \varepsilon$ models, $ANSYS^{©}$ Fluent offer these Wall Function approaches:

1. Standard Wall Functions (SWF);
2. Scalable Wall Functions;
3. Non-Equilibrium Wall Functions (NEWF);
4. Enhanced Wall Treatment (EWT).

1. The Standard Wall Function is the default near-wall treatment in ANSYS Fluent. This typology rounds up well the cases with y^+ value

included among 30 and 500, but for small y^+, the numerical results deteriorate. As shown before, switch between those two zones occurs for specific y^+; ANSYS Fluent uses wall unit y^* instead of y^+ and U^* instead of U^+ (in the equilibrium turbulent boundary layer these quantities are approximately equal). In general y^* is defined as [47]:

$$y^* = \frac{\rho C_\mu^{\frac{1}{4}} k^{\frac{1}{2}} y}{\mu} \tag{4.15}$$

where:
k, is the turbulence kinetic energy at considered point $[J/kg]$
C_μ, is an empirical constant $(= 0.09)$
y, is the distance from a generic point P to the wall $[m]$
μ, is the dynamic viscosity of the fluid $[Pa \cdot s]$
ρ, is the fluid molecular density $[kg/m^3]$

ANSYS Fluent,through the SWF, approximates a velocity with a linear function of the velocity the zones with $y^* < 11.225$, and with a logarithmic function above this value. It is less efficient where pressure gradients and significant forces of mass are present. This approach was the industrial standard some yeas ago, but ANSYS Fluent has taken steps to offer more advanced wall formulations which allow a consistent mesh refinement without a deterioration of the results.

2. The scalable wall functions are introduced because they avoid the deterioration of standard wall functions under grid refinement below $y^* < 11.225$. These wall functions produce consistent results for grids of arbitrary refinement. For grids which are coarser than $y^* > 11.225$ the standard wall functions are identical. The purpose of scalable wall functions is to force the usage of the logarithmic law in conjunction with the standard wall functions approach. This is achieved by introducing a limiter in the y^+ calculations such that:

$$\tilde{y}^* = MAX\left(y^+, y^+_{limit}\right) \tag{4.16}$$

With $y^*_{limit} = 11.225$.
The use of the equation 4.16 in the context of the scalable wall functions concept is straightforward, that is, the y^+ formulation used for any standard wall function formula is replaced by $\tilde{y}^*$.

Summarizing, scalable wall functions overcome one of the major drawbacks of the standard wall function approach in that they can be applied on arbitrarily fine meshes. If the boundary layer is not fully resolved, it will be relying on the logarithmic wall function approximation to model the boundary layer without affecting the validity of the scalable wall function approach. If you are not interested in the details of the boundary layer, then it may not be worth fully resolving it.

3. The Non-Equilibrium Wall Functions is a two-layer-based, defined by Clauser (1954). He stated that the equilibrium of the boundary layer (defined as the boundary layer in which locally and instantly the balance between turbulence production and dissipation takes place) depends on the pressure gradient: if it is constant, along the wall there is an equilibrium layer, besides, if there are variable pressure gradients the boundary layer is not in equilibrium. In the NEWF the wall law equation for the velocity is modified (compared with the SWF) paying more attention and accuracy to the pressure gradient. These functions are particularly suitable in case of flux with an adverse pressure gradient because they admit non-equilibrium situations (e.g. separation and reattachment of the fluid vein). The NEWFs account for the effect of pressure gradients on the distortion of the velocity profiles. In such cases the assumption of local equilibrium, when the production of the turbulent kinetic energy is equal to the rate of its destruction, is no longer valid. Therefore, the non-equilibrium wall functions, in effect, partly account for the non-equilibrium effects that are neglected in the standard wall functions.

   The SWFs give reasonable predictions for the majority of high-Reynolds number wall-bounded flows. The NEWFs further extend the applicability of the wall function approach by including the effects of pressure gradient. However, the above wall functions become less reliable when the flow conditions depart too much from the ideal conditions underlying the wall functions. Examples are as follows:

   – Pervasive low-Reynolds-number or near-wall effects (for example, flow through a small gap or highly viscous, low-velocity fluid flow).
   – Massive transpiration through the wall (blowing/suction).
   – Severe pressure gradients leading to boundary layer separations.
   – Strong body forces (for example, flow near rotating disks, buoyancy-driven flows).
   – High three-dimensionality in the near-wall region (for example, Ekman spiral flow, strongly skewed 3D boundary layers).

If any of the above listed features prevail in the flow being modeled, and if it is considered critically important for the success of the simulation, it must employed the near-wall modeling approach combined with the adequate mesh resolution in the near-wall region. ANSYS Fluent provides the enhanced wall treatment for such situations. This approach can be used with the $\kappa - \varepsilon$ and the RSM models.

4. The the Enhanced Wall Treatment is a near-wall modeling that combines a two-layer model with so-called enhanced wall functions. It wants to overcome the limitations regarding to y^+: it is efficient in industrial cases in which it is difficult to maintain the y^+ values of the domain in a prefixed range. If the near-wall mesh is fine enough to be able to resolve the viscous sublayer (typically with the first near-wall node placed at $y^+ \approx 1$), then the enhanced wall treatment will be identical to the traditional two-layer zonal model (see below for details). However, the restriction that the near-wall mesh must be sufficiently fine everywhere might impose a huge computational requirement. Ideally, one would like to have a near-wall formulation that can be used with coarse meshes (usually referred to as wall-function meshes) as well as fine meshes (low-Reynolds number meshes). In addition, excessive error should not be incurred for the intermediate meshes where the first near-wall node is placed neither in the fully turbulent region, where the wall functions are suitable, nor in the direct vicinity of the wall at $y^+ \approx 1$, where the low-Reynolds-number approach is adequate. The goal of this wall treatment is to obtain a model with an high accuracy (also modifying the distribution of the cells on the wall).

   Furthermore, some expedient are introduced in order to avoid excessive errors if the first cell center near the wall stands in the transition sublayer. The achievement of what afore mentioned is obtained by the introduction of a smoother transition profile passing from a zone to the other.

4.2.3 Modeling of multiphase flow

Fluid flow behavior, especially air, and its interaction with airborne particles is one of the main topic of this thesis work. Therefore, it could be appropriate to introduce some concepts on multiphase fluids in order to understand the approach to be used in the simulation stage.

A phase is a region of space (a thermodynamic system), throughout which all physical properties of a material are essentially uniform and with a defined

boundary. The modeling of multiphase flow requires a prior knowledge of:

- the flow regime (e.g. annular, bubbly...)
- the motion regime (i.e. turbulent, laminar)
- the particle diameter (or bubble diameter)
- the type of fluid (dense or diluted)

A dispersed phase flows are flows in which one phase consists of discrete elements not connected. In a separated flow, the two phases are separated by a line of contact. The fluid which will be used inside the room is described like a gas-solid flow. It consist of flows in which solid particles are suspended in a gas.
For convenience, the term discrete or dispersed phase will be used for the particles, droplets or bubbles, while carrier or continuous phase will be used for the carrier fluid [46]. In the following part is presented a brief terminology of the parameters used for the modeling of multiphase flow.

Terminology

Volume fraction of dispersed phase:

$$\alpha_d = \lim_{\delta V \to V^\circ} \frac{\delta V_d}{\delta V} \tag{4.17}$$

where:
δV_d, is the volume of the dispersed phase in volume δV $[m^3]$
V°, is the limiting volume that ensures a stationary average (unlike a continuum, the volume fraction cannot be defined at a point)

Volume fraction of continuous phase:

$$\alpha_c = \lim_{\delta V \to V^\circ} \frac{\delta V_c}{\delta V} \tag{4.18}$$

where:
δV_c, is the volume of the dispersed phase in volume δV $[m^3]$

By definition, the sum of the volume fractions must be unity:

$$\alpha_d + \alpha_c = 1 \tag{4.19}$$

Bulk density (or apparent density) of the dispersed phase: is the mass of the dispersed phase per unit volume of mixture:

$$\overline{\rho_d} = \lim_{\delta V \to V^\circ} \frac{\delta M_d}{\delta V} \tag{4.20}$$

where:
δM_d, is the mass of the dispersed phase $[kg]$

The bulk density is related to the material density ρ_d by:

$$\overline{\rho_d} = \alpha_d \rho_d \tag{4.21}$$

The sum of the bulk densities for the dispersed and continuous phases is the *mixture density*:

$$\rho_m = \overline{\rho_d} + \overline{\rho_c} \tag{4.22}$$

An important parameter to the definition of dispersed-phase flows is the *dispersed-phase mass concentration*:

$$C = \frac{\overline{\rho_d}}{\overline{\rho_c}} \tag{4.23}$$

Our application concerns a particle count because the particulate diameter which it is treated is in around 0.5 μm. The concentration it will be calculated in number of particles per meter cube of air.

Stokes Number: is a very important parameter in fluid-particle flows. It is related to the particle velocity and is defined as:

$$Stk = \frac{\tau_v}{\tau_F} \tag{4.24}$$

where:
τ_F, is the characteristic time of the flow field $[s]$ τ_v, is the relaxation time of the particle $[s]$

If
$Stk \ll 1$, the response time of the particles is much less than the characteristic time associated with the flow field. In this case the particles will have ample time to respond to the changes in flow velocity and, the particle and fluid velocities will be nearly equal (velocity equilibrium) to the fluid flow velocities.

$Stk \gg 1$, the particle will have essentially no time to respond to the fluid velocity changes and the particle velocity will be little (or through

and through not) affected by fluid velocity change. Hence, the particle will proceed independently by the fluid and will leave the fluid stream in which it was carried. The same idea extends to Stokes number based on thermal response time [46].

Multiphase modeling coupled with turbulence

Turbulence modeling with multiphase flow is challenging task. Presently, single-phase turbulence models (such as $\kappa - \varepsilon$ or RSM) are used to model turbulence in the primary phase only. The turbulence equations may contain additional terms to account for turbulence modification by secondary phases. If phases are separated and the density ratio is of order 1 or if the particle volume fraction is low (less than 10%), then a single-phase model can be used to represent the mixture. In other case modified models may be used which take in account the particle presence.

An important concept in the analysis of multiphase flows is the coupling process between carrier fluid and dispersed phase (i.e. particles): if the flow of one phase affects the other while there is no reverse effect, the flow is said to be *one-way-coupled*; instead, if there is a mutual effect between the flows of both phases, then the flow is *two-way-coupled*.

The mass coupling is the addition of mass through evaporation or the removal of mass from the carrier stream by condensation.

The momentum coupling is the result of an interaction force, such as a drag force, between the dispersed and continuous phase, and turbulence. Momentum coupling can also occur with momentum addition or depletion due to mass transfer.

Energy coupling occurs through heat transfer between phases. Thermal and kinetic energy can also be transferred between phases owing to mass transfer [34].

The Figure 4.5 shows the coupling between the equation of the fluid and of the particles.

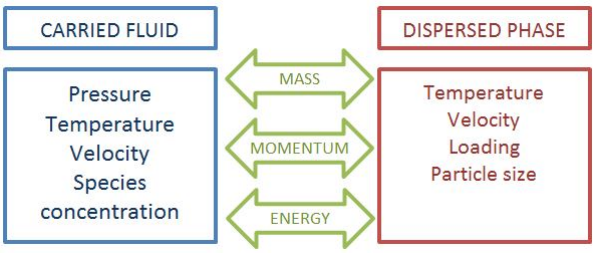

Figure 4.5: Coupling between the equations of different phases [46]

In order to model the multiphase flows, it is possible to follow two type of formulations which are implemented with different models. The different approaches are:

1. *Langrangian formulation* of one or more phases, or the interfaces:
   - Discrete Phase Model (DPM)
   - Front Tracking method (FT)
2. *Eulerian formulation of the phases or of the interfaces:*
   - Algebraic Slip Mixture Model (ASMM)
   - Two-Fluid Eulerian-Eulerian (E-E)
   - Volume-of-Fluid method (VOF)
   - Level Set method (LS)

Not all the models cited are available in all CFD codes; particularly there are: DPM, ASMM, E-E and VOF.

The Lagrangian method is the easier and cheaper in term of computational costs; the Eulerian method implements better the physical description of phenomenon increasing the computational cost per iteration.

For a proper choice of the method, it is necessary to know in advance:

- The volume fraction
- The particle load
- The Stokes number

The most used multiphase models are described below:

- Eulerian-Lagrangian model (so called DPM)

  Its name derives from the fact that the gas continuous phase is modeled with an Eulerian approach, while the solid dispersed phase is modeled with a Lagrangian approach. In fact, the fluid phase is treated as a continuum by solving the Navier-Stokes equations, while the dispersed phase is solved by tracking a large number of particles, bubbles, or droplets through the calculated flow field. The dispersed phase can exchange momentum, mass and energy with the fluid phase. A fundamental assumption made in this model is that the dispersed secondary phase n occupies a low volume fraction (less than $10 \div 12\%$),

even though high mass loading is acceptable. Indeed, the average particle spacing, L, is related to the dispersed volume fraction by [48]:

$$\frac{L}{d_p} = \left(\frac{\pi}{6\alpha_d}\right)^{\frac{1}{3}} \tag{4.25}$$

where

L, is the average particle spacing $[m]$

d_P, is the average particle diameter $[m]$

When the ratio of the equation 4.25 is greater than 5, the continuous gas phase can be regarded as a single phase, neglecting the influence of the small volume fraction occupied by the dispersed solid phase.

The particle or droplet trajectories are computed individually at specified intervals during the fluid phase calculation.

Jump conditions are averaged in time and space and introduced in:

- the dispersed phase balance equations (1 way coupling)
- the continuous phase balance equations (2 way coupling)

Problems arise when the dispersed volume fraction is high. This model is applicable to steady and unsteady flows.
The Figure 4.6 resumes the concepts at the base of the Eulerian-Lagrangian model: the dispersed phase is solved tracking a large number of particles and the continuous phase is treated as a continuum by solving Navier-Stokes equations; it is underlined the possible coupling between the continuous and dispersed phases.

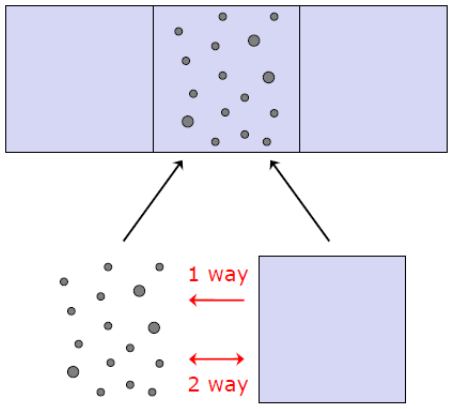

Figure 4.6: Eulerian-Lagrangian model (or DPM) [46]

The equation of the Eulerian-Lagrangian model are:

Continuous phase:

$$\frac{\partial \rho}{\partial t} + \nabla(\rho \mathbf{v}) = \mathrm{S_m} \tag{4.26}$$

$$\frac{\partial(\rho \mathbf{v})}{\partial t} + \nabla(\rho \mathbf{v}\mathrm{v}) = \rho \mathrm{g} - \nabla \mathrm{P} + \nabla \cdot \mu \nabla \mathbf{v} + \mathbf{F} \tag{4.27}$$

$$\frac{\partial(\rho T c_p)}{\partial t} + \nabla(\rho \mathbf{v} \mathrm{c_p T}) = \nabla(\mathrm{k} \nabla \mathrm{T}) + \mathrm{S} \tag{4.28}$$

Dispersed phase:

$$\frac{\partial U_P}{\partial t} = F_D(U - U_P) + \frac{(\rho_P - \rho)}{\rho_P} g + F_P \tag{4.29}$$

$$\frac{\partial(m_P c_P T_P)}{\partial t} = hA_P(T - T_P) + \frac{dm_P}{dt} h_{fg} + \varepsilon_P A_P \sigma_o(\theta_R^4 - T_P^4) + S_P \tag{4.30}$$

In case of N dispersed phases, the set of equations will be composed by:

- 1 equation of mass conservation;
- 3 equations of momentum conservation;
- 1 equation of energy conservation;
- N-particles/clouds equations of particle trajectory;
- N-particles/clouds equations of particle energy;

The computational costs and time depend mainly on the number of particles.

It can be done another consideration on the type of way of coupling. The flow can be considered dilute, thus neglecting particle–particle interaction, if the ratio between the momentum response time of a particle and the average time between particle– particle collisions is less than one or if the following condition is verified [48]:

$$d_P < A = \frac{1.33\mu}{Z\rho\sigma} \tag{4.31}$$

where:

Z, ratio between particulate mass flow rate and gas mass flow rate $[-]$

ρ, gas density$[kg/m^3]$

σ, standard deviation of particle fluctuation velocity $[m/s]$

μ, gas dynamic viscosity $[Pa \cdot s]$

σ is the standard deviation of the particle fluctuation velocity and it is of the order of the RMS of the turbulence fluctuations of the gas phase.
If this inequality is verified the particle-particle interaction could be neglected [48] and the one-way coupling can be used.

– Eulerian-Eulerian model (E-E)

The volume fractions of discrete and continuous phases are considered as continuous functions of space and time and their sum is the unit.

The Eulerian-Eulerian model solves a set of momentum and continuity equation for each phase. The system is closed using constitutive relations obtained from empirical information or, in the case of granular flows, from the application of kinetic theories. The coupling is achieved through the pressure and inter-phase exchange coefficient and it is managed differently according to the type of phase involved: granular (fluid-solid) or non-granular (fluid-fluid) flows.

The momentum exchange between the phases is also dependent upon the type of mixture being modeled.

Balance equations and jump conditions are averaged in time and space. The inter-facial sources for the k^{th}-phase are given empirically. Transport equations for the modeling of the interface may be added. Due to the complexity of the model, calibration may be difficult in some cases. The Figure 4.7 resumes the concepts at the base of the Eulerian-Eulerian model: the dispersed and the continuous phase are treated as a continuum by solving Navier-Stokes equations; the coupling is achieved through the pressure and inter-phase exchange coefficient and the inter-facial sources for the phases are given empirically.

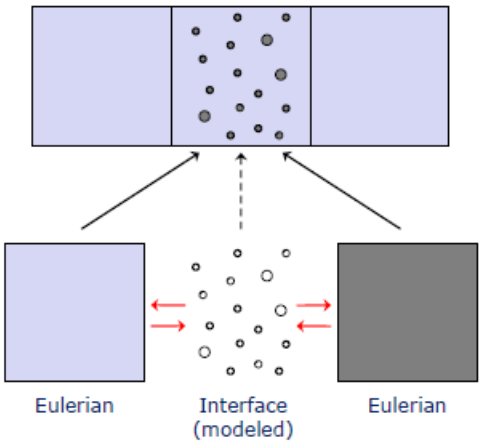

Figure 4.7: Eulerian-Eulerian model (E-E) [46]

For the q-phase:

$$\frac{\partial(\alpha_q \rho_q)}{\partial t} + \nabla(\alpha_q \rho_q \mathbf{U_q}) = \sum_{p=1}^{n}(\dot{m}_{pq} - \dot{m}_{qp}) + S_q \tag{4.32}$$

$$\frac{\partial(\alpha_q \rho_q \mathbf{U_q})}{\partial t} + \nabla(\alpha_q \rho_q \mathbf{U_q U_q}) = -\alpha_q \nabla P + \nabla \Im_q + \alpha_q \rho_q \mathbf{g} +$$

$$+ \sum_{p=1}^{n}(\mathbf{R_{pq}} + \dot{m}_{pq}\mathbf{U_{pq}} - \dot{m}_{qp}\mathbf{U_{qp}}) + \mathbf{F_q} + \mathbf{F_{lift,q}} + \mathbf{F_{vm,q}} \tag{4.33}$$

$$\frac{\partial(\alpha_q \rho_q h_q)}{\partial t} + \nabla(\alpha_q \rho_q \mathbf{U_q} h_q) = \alpha_q \frac{\partial P_q}{\partial t} + \Im_{\mathbf{q}} \nabla \mathbf{U_q} - \nabla \mathbf{q_q} +$$

$$+ S_q + \sum_{p=1}^{n}(Q_{pq} + \dot{m}_{pq} h_{pq} - \dot{m}_{qp} h_{qp}) \tag{4.34}$$

In case of N phases, the set of equations will be composed by:

- N-1 equation of mass conservation;
- 3N equations of momentum conservation;
- N equation of energy conservation;

– Q interface modeling

Computational time depends on the number of phases, complexity of the problem (convergence rate) and interface modeling.

The two-fluid or multi-fluid Eulerian model is the most complete mathematical formulation of multiphase flows and can be applied in a wide range of scales and applications. The accuracy of the model depends mainly on the quality of the inter-phase exchange coefficient models (jump conditions) and their calibration (main drawbacks). Another drawback is the lack of stability and the low convergence rate.

The Eulerian-Lagrangian approach is appropriate to model particles which occupy a volume fraction less than 10%. For this reason this model is chosen in several simulations in the ventilation field.

4.3 Case Study: geometry, mesh generation and operating theater modeling

In order to built the 3D model of the operating theater of the case of study, it has been used the Design Modeler by ANSYS. Following the real dimensions of the studied operating theater, it was possible to create the 3D model of it. In accordance with the German regulation the dummies, representing the surgical staff, the surgical table and the aerosol diffusers were located in the right position prescribed for the tests. The dummies and the aerosol diffusers have the dimensions prescribed by the regulation (shown in Figure 2.3 and Figure 2.4), while the surgical table was modeled with an height prescribed by the German regulation and a real length of 2.07 m. Besides, it was considered as not secondary, to add the two surgical lamps because their position is relevant relating to the supply air flux. To their representation it was followed the shape of the real ones with an obvious addition of some simplifications.

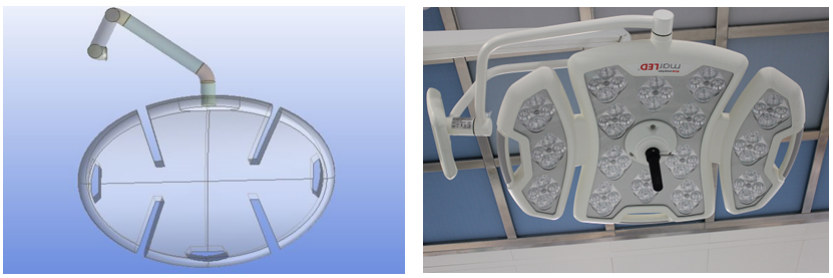

Figure 4.8: Real and modeled surgical lamp

On the ceiling diffuser are positioned the filters composing the ceiling filter system. In the same way the exhaust grille positions have been reproduced faithfully in the four corners of the room, how it can be seen in Figure 4.9.

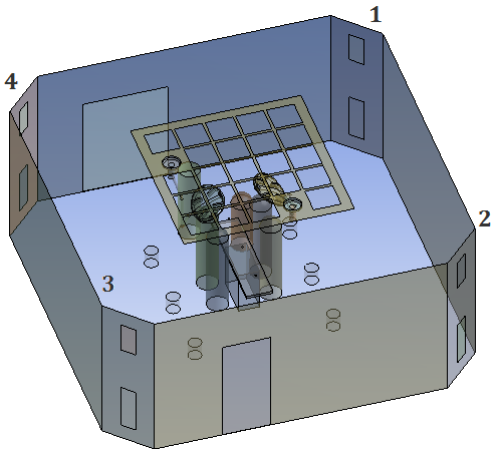

Figure 4.9: Isometric 3D rendering of the OT B2 under evaluation with the configuration for the test according to DIN 1964-4 [32]

Two doors with their open narrow slits between the floor and the door have been included in the modeling. The narrow slit are: 0.5 cm for the service door and 1 cm for the main sliding door. It is necessary to add a note: the reference point chosen as axis origin is the center of the room at the level of the floor, as shown in Figure 4.10.

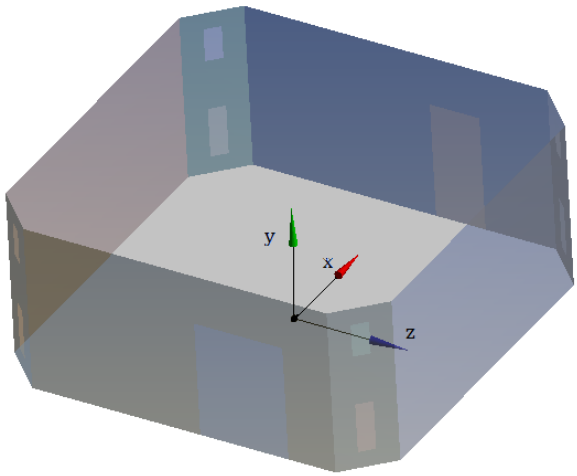

Figure 4.10: Spatial reference system of the operating theater

Once the CFD modeling was finished the project was imported in the ANSYS Mesher. With the 'standard' configuration of the room, it is modeled another scenario with a different disposition of the surgical lamp frames. It is used to understand what may happen if there is only one central lamp frame in spite of two lateral ones. The isometric view and a particular of the model are reported in the Figure 4.11.

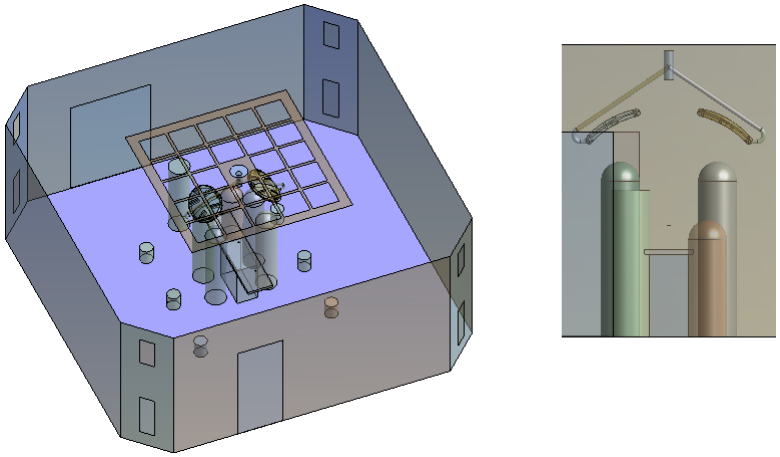

Figure 4.11: CAD rendering of isometric view and a particular of the room in configuration called D

In all scenarios simulated, the elements of the mesh are tetrahedral because the internal geometry present different forms that are hardly compatible with hexahedral grids (especially in the proximity of the lamps and dummies). To obtain cells slightly deformed, in order to have a maximum skewness value under 0.94, tetrahedral cells are the best choice. For each mesh, the domain is divided into three concentric volumes:

- the inner volume is in the critical zone, and comprehends all the footprint of the diffuser ceiling. It is characterized by the smallest cell size (approximately 3.5 cm);
- the median volume is around the critical zone volume, and it is characterized by an intermediate size of the cells (approximately 5 cm);
- the outer volume has a coarse mesh with mesh refinements in proximity of the narrow slits of the two doors and close to the exhaust grilles (approximately 8 cm).

A visual description of the partition of the entire OT volume into three different interior volumes and therefore into three different mesh size and number of cells, can be seen in Figure 4.12 and Figure 4.13.

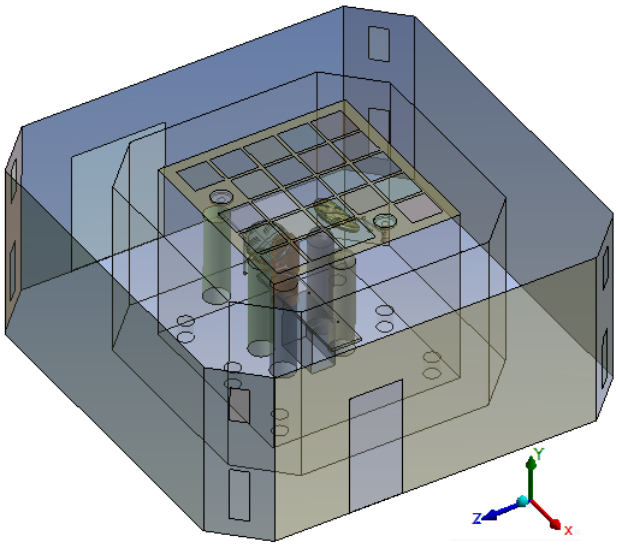

Figure 4.12: Isometric 3D-view of the modeled OT with the three different volumes adopted for the mesh generation

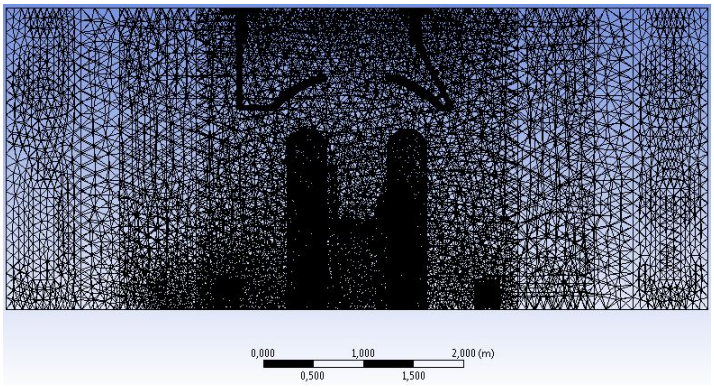

Figure 4.13: Tetrahedral mesh of the OT, with three different cell sizes from the center to the periphery

4.4 Case Study: the Simulation Settings

The studied cases are different, besides for the internal arrangement, also for the boundary condition settings. These settings will be put in evidence for each simulation in the next sections. Now we want to introduce the common settings and assumptions which we have adopted.

Geometric semplifications

First, we introduce the geometric simplifications adopted for all the simulations carried out:

- modeling of the operating table with two boxes, one for the base and the other to the table;
- modeling of the medical team using cylinders with hemispherical ends;
- modeling of medical equipment through cylinder with hemispherical head;
- modeling of the artificial aerosol diffusers as cylinders.

Physical assumptions

Other assumptions made during the pre-processing are:

- The working fluid is dry air;
- The physical-chemical air properties are constant, such as:

$$\rho = 1.225 \frac{kg}{m^3}$$

$$\mu = 1.7894 \cdot 10^{-5} \frac{kg}{m \cdot s}$$

- particles is DEHS in accordance with the UNI EN 1822-2 [16]. The characteristics of the synthetic oil used are described in Table 4.2.

Table 4.2: Extract of specifications for DEHS and other aerosol substances at 20°C by UNI EN 1822-2 [16]

	DEHS	PAO [a]	Paraffin oil (low visc.)
Chemical designation	Sebacic acid-bis(2-ethylhexyl) ester	Poly-Alpha-Olephin (e.g. CAS [b] No. 68649-12-7)	Mixture (e.g. CAS # 64742-46-7)
Trivial name	Diethylhexylsebacyte	Polyalphaolefin	Paraffinoil
Density (kg/m^3)	912	800 – 820 (820 [c])	843
Melting point (K)	225	~ 280	259
Boiling point (K)	529	650 – 780 (674 [c])	
Flash point (K)	> 473	445 – 500	453
Vapour pressure at 293 K (µPa)	1,9	100 – 130	
Dynamic viscosity (kg/m s)	0,022 to 0,024	0,003 1 – 0,004 at 373 K (0,013 at 313 K [c]) (Kinematic viscosity at 373 K: 3,8 – 4,1 mm^2/s)	0,026

[a] US Patents 5,059,349 [3] and 5,059,352 [4] describe and restrict the use of PAO for filter testing. Material properties of PAO as per Japan JACA Standard No. 37-2001: "The guideline of substitute materials to DOP" [5], Japan JISZ Standard No. 8901-206 [6] and ISO Standard No. 14644-3 [7].

[b] CAS #, Chemical Abstracts Service Registry Number, substances have been registered in Chemical Abstracts, issued by American Chemical Society [8].

[c] Data for "Emery 3004" as a specific example of a PAO.

Source: Crosby, David W., Concentration produced by a Laskin nozzle generator, a comparison of substitute materials and DOP, 21st DOE/NRC Nuclear Air Cleaning Conference [9].

Turbulence model adopted

The majority of numerical predictions of the air flux are obtained by applying the Standard $\kappa-\varepsilon$ model which uses the hypothesis of eddy viscosity models. This approach is considered more efficient than a low-Reynolds models which requires a finer mesh near the solid surfaces to strengthen the stability of the simulation.

Based on empirical parameters, the Standard $\kappa - \varepsilon$ model is easy to program, reasonably accurate and numerically robust in producing converged solutions even for flows with low turbulence level and unstable temperature stratification.

All model coefficients are constant and determined from experimental campaigns. Despite these empirical coefficients have wide fields of application, they are not universal. It is common practice to modify the $\kappa - \varepsilon$ model in order to improve the computational results. Some modification are related with extending the turbulence models for low Reynolds numbers, and to solve the flow also close to the solid surfaces.

To study the flow and the contamination levels in the critical area close to the operating table, typically invested by unidirectional flow, it was observed that the model RNG has no special advantages until the buoyancy forces are not dominant [49].

The Standard $\kappa - \varepsilon$ model is weakly adaptable to complex flows which involve severe pressure gradient, separations, strong streamline curvature, strong swirl/rotation and is recommended for the first iterations.

In addition to the Standard $\kappa - \varepsilon$ model there is also the Realizable $\kappa - \varepsilon$. The term "Realizable" was introduced by Schumann in 1977 and it means that the model satisfies certain mathematical constraints about the normal stresses, consistent with the physics of turbulent motions. Combining the Boussinesq relation (4.7) and the definition of turbulent viscosity the following expression, of the normal stress in a Reynolds incompressible flow, is obtained:

$$\overline{u^2} = \frac{2}{3}k - 2\nu_t \frac{\partial U}{\partial x} \tag{4.35}$$

Being:

$$\nu_t = \frac{\mu_t}{\rho} \tag{4.36}$$

with:

$$\mu_t = \rho C_\mu \frac{k^2}{\varepsilon} \tag{4.37}$$

It is obtained:

$$\overline{u^2} = \frac{2}{3}k - 2C_\mu \frac{k^2}{\varepsilon}\frac{\partial U}{\partial x} \tag{4.38}$$

And being $\overline{u^2}$ positive by definition, we can state that a method is "realizable" if it is verified the following inequality:

$$\overline{u^2} = \frac{2}{3}k - 2C_\mu \frac{k^2}{\varepsilon}\frac{\partial U}{\partial x} > 0 \tag{4.39}$$

Hence if:

$$\frac{k}{\varepsilon}\frac{\partial U}{\partial x} > \frac{1}{3C_\mu} \approx 3.7 \tag{4.40}$$

In addition, another condition of realizability is the positivity of the Schwarz inequality for shear stresses:

$$\frac{\overline{u_\alpha u_\beta}^2}{\overline{u_\alpha^2 u_\beta^2}} \leq 1 \tag{4.41}$$

with $\alpha = 1, 2, 3$; $\beta = 1, 2, 3$

Based on these realizability constraints W. Reynolds as well as Shih, Zhu and Lumley [50] proposed following form of an equation for C_μ:

$$C_\mu = \frac{1}{A_0 + A_s U^{(0)} \frac{k}{\varepsilon}} \tag{4.42}$$

Shih, Zhu, Lumley gave this formulation to the terms of the previous equation:

$$U^{(0)} = \sqrt{S_{ij}S_{ij} + \tilde{\Omega}_{ij}\tilde{\Omega}_{ij}} \tag{4.43}$$

where:

$$\tilde{\Omega}_{ij} = \Omega_{ij} - 2\varepsilon_{ijk}\omega_k \tag{4.44}$$

$$\Omega_{ij} = \overline{\Omega}_{ij} - \varepsilon_{ijk}\omega_k \tag{4.45}$$

Where $\overline{\Omega}_{ij}$, is the mean rate-of-rotation tensor viewed in a rotating reference frame with the angular velocity ω_k. Only the model constants A_0 is unknown. In Fluent A_0 is equal to 4.04.

Therefore, the easiest way to ensure the realizability (i.e. the positivity of the normal stresses and the Schwarz inequality to the shear of the Reynolds tensor) is to make variable C_μ making it susceptible to the average flow (to average deformation) and the turbulence. This idea is well supported by experimental evidence. For example it was found that C_μ is equal to 0.09 in the inertial sublayer of the boundary layers of equilibrium, while it is 0.05 in the case of flows with strong homogeneous shear. The Realizable $\kappa-\varepsilon$ model proposed by Shih et al. [50] has been introduced to face obvious traditional lacks. This was done by taking the following precautions:

- New formula of turbulent viscosity which includes the C_μ variable;
- New equation model for the dissipation rate of turbulent energy (ε) based on the equation of the dynamics of mean-square vorticity fluctuation [50].

Based on the above mentioned discussions on the various turbulence model adopted in the literature, it was decided to adopt the Realizable $\kappa-\varepsilon$ model for the numerical prediction on the work of this Master Thesis.

Other common settings required by Fluent

In order to achieve a good convergence of the equations solved by the program, each simulation was carried out in transient regime. This is just an expedient because any forcer isn't present into the operating theater. Other common settings for each simulation regard the pressure-velocity coupling (this problem is connected with the fact that the momentum equation contains the pressure term and for each iteration the pressure term is calculated by the velocity field) and the method of spatial discretisation. Furthermore,

between the wall functions shown before, the scalable wall functions were chosen for each simulation, because they overcome easily the restriction of the Standard Wall Functions. In the following list the settings which each simulation has in common are resumed:

- Transient simulation
- SIMPLE scheme for the pressure-velocity coupling;
- Initially first order methods for the spatial discretisation of all quantities and than second order methods;
- Initially low under-relaxation factors and than the default values;
- Scalable Wall Functions for the wall conditions.

The simulated scenarios in this work are summarized in the following table:

Table 4.3: List of the simulated scenarios with a brief description

Name	**lay − out type**	**Lamp frame**	**Boundary conditions**
A2 − SG	Internal contamination	2	2 closed doors with slits all exhaust grilles available experimental boundary conditions
A1	External contamination	2	2 closed doors with slits all exhaust grilles available theoretical boundary conditions
A2	Internal contamination	2	2 closed doors with slits all exhaust grilles available theoretical boundary conditions
B2	Internal contamination	2	2 closed doors with slits 2 exhaust grilles closed on 1 corner theoretical boundary conditions
C2	Internal contamination	2	sliding door opened all exhaust grilles available theoretical boundary conditions
D1	External contamination	1	2 closed doors with slits all exhaust grilles available theoretical boundary conditions
D2	Internal contamination	1	2 closed doors with slits all exhaust grilles available theoretical boundary conditions

The first scenario (A2-SG) is useful to the validation stage. In fact, it adopts the experimental values as boundary conditions with the operating theater lay-out prescribed by the German standard to evaluate the protection class of the ventilation system against the contamination coming from inside the critical zone. This lay-out is the one studied for the validation of the CFD model. The second (A1) and the third (A2) scenarios use the theoretical values for the boundary conditions and are arranged respectively withe the lay-out described in the Figure 2.3 and Figure 2.4. This models are useful for a comparison between this 'standard' configuration and other with some different aspects, to underline what may happens if the main sliding door is opened (Scenario B2), if each exhaust grille of the corner 4 (see Figure 4.9) is obstucted (Scenario C2) and if another configuration of the lamp frames is adopted (Scenario D1 and D2). The scenarios D1 and D2 adopt a solution with only one lamp frame positioned in substitution of the central high speed filter. In this way the other two filters, which in the other scenarios house the two lamp frames, are now occupied with two filters. The geometry of these two non-standard scenarios is designed with the standard ones and it is shown in the Figure 4.11.

4.4.1 A2-SG configuration: models for the validation stage

This simulation scenario is necessary to conduct the validation, in fact, the boundary conditions of it are those measured during the experimental stage, in order to compare the results of this with the ones found out in the experimental campaign. It adopts the configuration of the room for the verification of the removal of the particles generated inside of the critical zone in the real arrangement of the room: the surgical lamps are very similar to the real ones and every exhaust grille is open. The two central aerosol diffusers are inside the critical zone, according to the DIN 1964-4 [32]. The filter ceiling is composed by 23 filters, disposed faithfully, like in the reality. For these simulations the following additional assumptions are done:

- closed doors
- narrow slit between floor and lower extremity of the main sliding door
- only convective heat flux within the room

Information about the mesh

The mesh is composed by tetrahedral cells. Like in the other cases, there are three regions with different reference cell size:

– the inner one (cell size circa 0.035 m);

– the middle one (cell size circa 0.05 m;

– the outer one (cell size circa 0.08 m).

There are overall 9'957'445 cells.

Boundary Condition

– Condition: *Velocity Inlet, T=293 K*

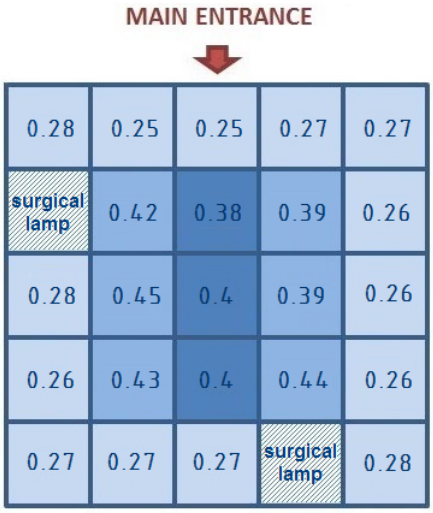

Figure 4.14: Average velocities at each filter of the ceiling filter system in m/s

This condition is imposed on the supply air filters which exhibit different velocities. The velocities are those find out in the experimental campaign. In particular, for each filter, five samples lasting 100 seconds, four at the corners and one in the center of the filter, were carried out. The velocity average for each filter is reported in the Figure 4.14.

If it is verified the hypothesis for which the particulate volumetric fraction is less than 10÷12 % it is possible use the Eulerian-Lagrangian approach. It is implemented in Fluent with the Discrete Phase Model (DPM). In addition, if it is verified also that the particle-particle interaction is negligible, conform with the relation 4.31, it is possible to develop a motion field emitting air (108 m^3/h) from the aerosol diffusers and than to release the particulate (with a diameter of 0.5 μm),

in the right concentration ($44.2 \cdot 10^6$ pp/m^3), from them, in the post-processing stage. These two hypotheses are verified a posteriori, in the post-processing stage. This concentration was found during the experimental campaign in the operating theater and it is the one produced by the aerosol generator. Hence, the velocity inlet condition is applied to 6 aerosol diffusers. The velocity of particle injection is around 0.28 m/s and to impose this condition on the surface of the aerosol diffusers it was create a proper user define function (udf). The section 4.4.7 explains in the details the generation of the particles and shows the effect of the user define function of the aerosol diffuser.

- Condition: *Pressure Outlet, T=293 K*
  - This condition is imposed in narrow slit between each door and the floor; it is imposed a *gauge pressure* of -8 Pa with outside, like the value reported by the monitoring system of the OT;
  - This condition is imposed on the exhaust grilles; it is imposed a *gauge pressure* of 0 Pa. The pressure outlet conditions are summarized in the Figure 4.15.

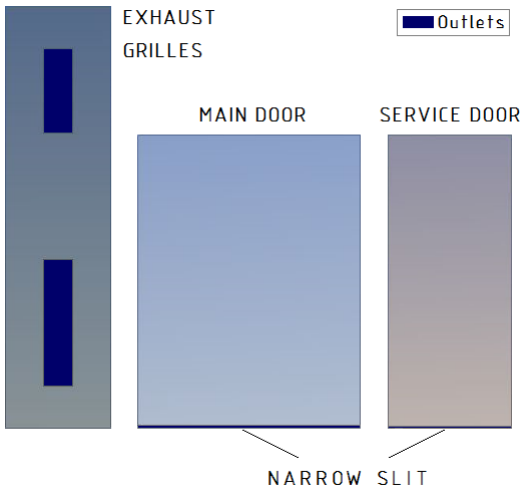

Figure 4.15: CAD depiction of two exhaust grilles, main door and the service door

- Condition: *Wall, no slip, adiabatic* This condition is imposed on the wall, ceiling (excluding the filter system), floor and on the surfaces of the doors, table, surgical light arms. This condition is imposed also in the three particles counter probes (with the 'trap' condition for the

DPM, as shown in Figure 4.16). They are simulated like little circles with a diameter of 34 mm and are located 24 cm above the table as shown in Figure 4.16.

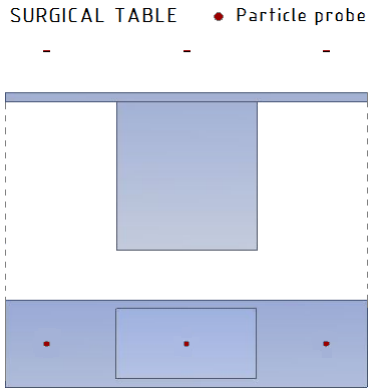

Figure 4.16: CAD depiction of the surgical table with positions of the particle counter probe (red circles) over it

– Condition: *Wall, no slip, heat flux*

  This condition is imposed on the dummy surfaces which represent the surgical staff and the medical equipment. In particular according to the DIN 1964-4 [32] the different dummies release different heat rate as shown in the Table 4.7.

Table 4.4: Different heat flux from the dummy surface according to DIN 1964-4 [32] for the simulations A2-SG

Anesthetist	$Q = 100\ W$
Surgical staff member	$Q = 100\ W$
Equipment	$Q = 300\ W$

In Fluent it is necessary to set the heat flux per square meter of emitting surface, the values are found out dividing the heat flux, prescribe by the German standard for each dummy, with the surface and the results are shown in the table 4.17:

Table 4.5: Heat flux per square meter to set in the boundary conditions in Fluent for the simulations A2-SG

Anesthetist	$q = 53.05\ W/m^2$
Surgical staff member	$q = 44.21\ W/m^2$
Equipment	$q = 159.15\ W/m^2$

– Condition: *Interior*

  All the monitoring surfaces are considered as interior with exception of the sampling probes at 24 cm above the table which occupy a physical location. In this way, they aren't considered in the simulation stage but only in the post-processing.

4.4.2 A1 and A2 configurations: project conditions

This two scenarios adopt the configuration of the OT for the verification of the removal of the particles generated outside and inside of the critical zone in the real arrangement of the OT: the surgical lamps are very similar to the real ones and every exhaust grille is working. In the scenario called A1, the two central aerosol diffusers are outside the critical zone; while, in the scenario called A2, the two central aerosol diffusers are inside the critical zone. As explained by the Figure 2.3 and Figure 2.4 in Chapter 2. The filter ceiling diffuser is composed by 23 filters, disposed faithfully, like in the reality. For these scenarios the following additional assumptions have been done:

– closed doors

– narrow slit between floor and lower extremity of the main sliding door and the service door

– only convective heat flux within the room

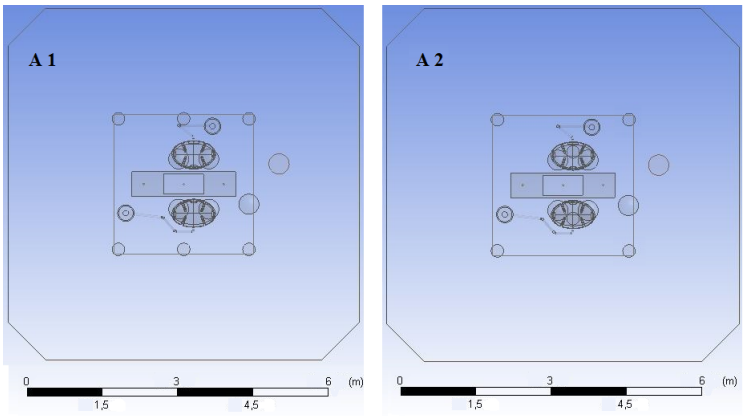

Figure 4.17: y-view of the modeled room in A1 and A2 scenarios, conforming to the DIN 1964-4 [32]

How it can be seen the difference in the previous figure is the disposition of the two central aerosol diffusers, according to the DIN 1964-4 [32].

Information about the mesh

The mesh is composed by tetrahedral cells. There are three main regions with different reference cell size:

- the inner one (cell size circa 0.035 m);
- the middle one (cell size circa 0.05 m);
- the outer one (cell size circa 0.08 m).

There are overall 9'957'445 cells in the A1 configuration and 10'122'109 in the A2 one.

Boundary Conditions

- Condition: *Velocity Inlet, T=293 K*

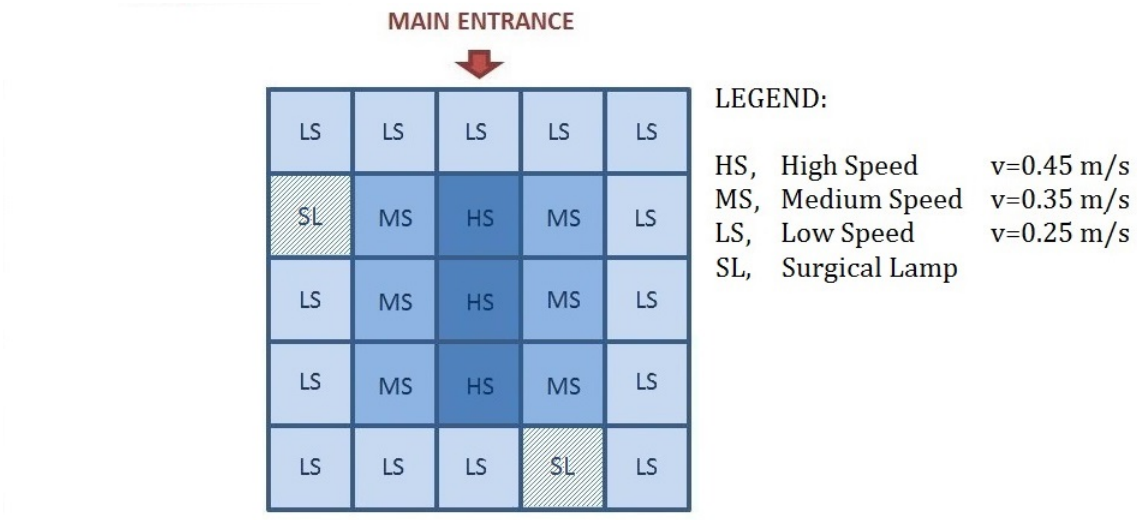

Figure 4.18: Filters of the ceiling diffuser system, different type with different air supply velocities for the scenarios A1 and A2

This condition is imposed for each of the 23 supply air HEPA filters H14. The velocities of each inlet filter vary depending on the type of filter installed in the ceiling diffuser: Low Speed (LS), Medium Speed (MS) and High Speed (HS), as shown in Table 4.15.

Table 4.6: Different inlet supply velocity of the H14 HEPA filers of the OT ceiling diffuser

v_{LS}	0.25 m/s
v_{MS}	0.35 m/s
v_{HS}	0.45 m/s

If it is verified the hypothesis for which the particulate volumetric fraction is less than $10 \div 12$ % it is possible use the Eulerian-Lagrangian approach. It is implemented in Fluent with the Discrete Phase Model (DPM). In addition, if it is verified also that the particle-particle interaction is negligible, conform with the equation 4.31, it is possible to develop a motion field emitting air (108 m^3/h) from the aerosol diffusers and than to release the particulate (with a diameter of 0.5 μm), in the challenge concentration ($44.2 \cdot 10^6$ pp/m^3), from them, in the post-processing stage. These two hypotheses are verified a posteriori, in the post-processing stage. The challenge concentration was found during the experimental campaign in the operating theater and is the worst concentration of particle obtained in the room. Hence, the velocity inlet condition is applied to 6 aerosol diffusers. The velocity of particle injection is around 0.28 m/s and to impose this condition on the surface of the aerosol diffusers it was create a proper user define function (udf). The section 4.4.7 explains in the details the generation of the particles and shows the effect of the user define function of the aerosol diffuser.

- Condition: *Pressure Outlet, T=293 K*
  - This condition is imposed in the free space between the floor and the doors; it is imposed a *gauge pressure* of -15 Pa with respect to the external and adjacent environments (as shown in Figure 4.15).
  - This condition is imposed on all the exhaust grilles; it is imposed a *gauge pressure* of 0 Pa
- Condition: *Wall, no slip, adiabatic* This condition is imposed on the wall, ceiling (excluding the filter system), floor and on the surfaces of the doors, table, surgical light arms. This condition is imposed also in the three particles counter probes (with the 'trap' condition for the DPM, as shown in Figure 4.16). They are simulated like little circles with a diameter of 34 mm and are located 10 cm above the table.

– Condition: *Wall, no slip, heat flux* This condition is imposed on the dummy surfaces which represent the surgical staff and the medical equipment. In particular according to the DIN 1964-4 [32] the different dummies release different heat rate as shown in the Table 4.7.

Table 4.7: Different heat flux released from the dummy surface according to DIN 1964-4 [32] for the simulations A1 and A2

Anesthetist	$Q = 100\ W$
Surgical staff member	$Q = 100\ W$
Equipment	$Q = 300\ W$

In Fluent it is necessary to set the heat flux per square meter of emitting surface, the values are found out dividing the heat flux, prescribe by the German standard for each dummy, with the surface and the results are shown in the table 4.17:

Table 4.8: Heat flux per square meter to set in the boundary conditions in Fluent for the simulations A1 and A2 for the different type of dummies

Anesthetist	$q = 53.05\ W/m^2$
Surgical staff member	$q = 44.21\ W/m^2$
Equipment	$q = 159.15\ W/m^2$

– Condition: *Interior*

All the monitoring surfaces are considered as interior with exception of the sampling probes at 24 cm above the table which occupy a physical location.. In this way, they aren't considered in the simulation stage but only in the post-processing.

4.4.3 B2 configuration: two exhaust grilles occluded

This simulation adopts the configuration of the room for the test of the removal of the particles generated inside of the critical zone in the real arrangement of the room. In this configuration, which it is called B2, the two exhaust grilles, located in the opposite corner relative to the main entrance, are occluded. The filter ceiling diffuser is composed by 23 filters, disposed faithfully, like in the reality. For these scenario the following additional assumptions were assumed:

– two grilles occluded (at the opposite corner of the main entrance, the sliding door)

- closed doors
- narrow slit between floor and the lower extremity of the main sliding door and the service door
- only convective heat flux within the room

Information about the mesh

The mesh is composed by tetrahedral cells. Like in the other cases, we have three main regions with different reference cell size:

- the inner one (cell size circa 0.035 m);
- the middle one (cell size circa 0.05 m);
- the outer one (cell size circa 0.08 m).

There are overall 10'122'109 cells (the same of the configurations: A2 and C2).

Boundary Condition

- Condition: *Velocity Inlet, T=293 K*

  This condition is imposed on the supply air equipped with HEPA filters which exhibit different velocities. We have:

Table 4.9: Different velocity magnitude at operating room inlets for the simulation B2

v_{LS}	0.25 m/s
v_{MS}	0.35 m/s
v_{HS}	0.45 m/s

For the H14 HEPA filter layout in the ceiling diffuser see the Figure 4.18 in the other two scenarios introduced before. From the aerosol diffusers is injected at fixed airflow rate(total airflow: 108 m^3/h) and than, in post processing (thanks to the hypothesis done previously), is injected through them an aerosol challenge (with a fixed diameter of 0.5 μm), in a fixed concentration ($44.2 \cdot 10^6$ pp/m^3), produced by the aerosol generators during the experimental campaign in the operating theater. Hence, the velocity inlet condition is applied also to 6 aerosol diffusers. The velocity of particle injection is around 0.28 m/s and

to impose this condition on the surface of the aerosol diffusers it was create a proper user define function (udf). The section 4.4.7 explains in the details the generation of the particles and shows the effect of the user define function of the aerosol diffuser.

- Condition: *Pressure Outlet, T=293 K*
  - This condition is imposed at the narrow slit between the floor and each door; it is imposed a *gauge pressure* of -15 Pa with outside
  - This condition is imposed on the exhaust grilles at the corner called 1,3,4; it is imposed a *gauge pressure* of 0 Pa

  The pressure outlet conditions are summarized in the Figure 4.15.

- Condition: *Wall, no slip, adiabatic*

  This condition is imposed on the wall, ceiling (excluding the filter system), floor and on the surfaces of the doors, table, surgical light arms. It is also imposed on the exhaust grilles on the corner called 2 (according to the Figure 4.9). This condition is imposed also in the three particle counter probes (with the 'trap' condition for the DPM). They are simulated like little circles with a diameter of 34 mm and are located 10 cm above the table (see Figure 4.16).

- Condition: *Wall, no slip, heat flux*

  This condition is imposed on the dummy surfaces which represent the surgical staff and the medical equipment. In particular according to the DIN 1964-4 [32] the different dummies release different heat rate as shown in the Table 4.7.

Table 4.10: Different heat flux from the dummy surface according to DIN 1964-4 [32] for the simulations B2

Anesthetist	$Q = 100\ W$
Surgical staff member	$Q = 100\ W$
Equipment	$Q = 300\ W$

In Fluent it is necessary to set the heat flux per square meter of emitting surface, the values are found out dividing the heat flux, prescribe by the German standard for each dummy, with the surface and the results are shown in the table 4.17:

Table 4.11: Heat flux per square meter to set in the boundary conditions in Fluent for the simulation B2 for the different type of dummies

Anesthetist	$q = 53.05\ W/m^2$
Surgical staff member	$q = 44.21\ W/m^2$
Equipment	$q = 159.15\ W/m^2$

– Condition: *Interior*

  All the monitoring surfaces are considered as interior with exception of the sampling probes at 24 cm above the table which occupy a physical location. In this way, they aren't considered in the simulation stage but only in the post-processing.

4.4.4 C2 configuration: the main entrance not closed

This simulation scenario adopts the configuration of the room for the test of the removal of the particulate generated inside of the critical zone in the real arrangement of the room. In this configuration, which we called C2, the main entrance is not closed. The filter ceiling diffuser is composed by 23 H14 HEPA filters, disposed faithfully, like in the reality. For these simulations we make the following additional assumptions:

– open main sliding door

– service door closed

– narrow slit between floor and lower extremity of the service door

– only convective heat flux within the room

Information about the mesh

The mesh is composed by tetrahedral cells. Like in the other cases, we have three main regions with different reference cell size:

– the inner one (cell size circa 0.035 m);

– the middle one (cell size circa 0.05 m);

– the outer one (cell size circa 0.08 m).

Boundary Condition

– Condition: *Velocity Inlet, T=293 K*

This condition is imposed on the supply air filters which exhibit different velocities. We have:

Table 4.12: Different velocity magnitude at operating room inlets for the simulation C2

v_{LS}	0.25 m/s
v_{MS}	0.35 m/s
v_{HS}	0.45 m/s

For the velocity distribution see the figure 4.18. From the aerosol diffusers is injected at fixed airflow rate(total airflow: 108 m^3/h) and than, in post processing (thanks to the hypothesis done previously), is injected through them an aerosol challenge (with a fixed diameter of 0.5 μm), in a fixed concentration ($44.2 \cdot 10^6$ pp/m^3), produced by the aerosol generators during the experimental campaign in the operating theater. Hence, the velocity inlet condition is applied also to 6 aerosol diffusers. The velocity of particle injection is around 0.28 m/s and to impose this condition on the surface of the aerosol diffusers it was create a proper user define function (udf). The section 4.4.7 explains in the details the generation of the particles and shows the effect of the user define function of the aerosol diffuser.

– Condition: *Pressure Outlet, T=293 K*

  – This condition is imposed at the narrow slit between the floor and the service door and on all the surface of the main door; it is imposed a *gauge pressure* of 0 Pa with outside
  – This condition is imposed on the exhaust grilles; it is imposed a *gauge pressure* of 0 Pa

The pressure outlet conditions are summarized in Figure 4.15.

– Condition: *Wall, no slip, adiabatic*

This condition is imposed on the wall, ceiling (excluding the filter system), floor and on the surfaces of the service door, table, surgical light arms. This condition is imposed also in the three particle counter probes (with the 'trap' condition for the DPM). They are simulated

like little circles with a diameter of 34 mm and are located 10 cm above the table (see Figure 4.16).

– Condition: *Wall, no slip, heat flux*

This condition is imposed on the dummy surfaces which represent the surgical staff and the medical equipment. In particular according to the DIN 1964-4 [32] the different dummies release different heat rate as shown in the Table 4.7.

Table 4.13: Different heat flux from the dummy surface according to DIN 1964-4 [32] for the simulations C2

Anesthetist	$Q = 100\ W$
Surgical staff member	$Q = 100\ W$
Equipment	$Q = 300\ W$

In Fluent it is necessary to set the heat flux per square meter of emitting surface, the values are found out dividing the heat flux, prescribe by the German standard for each dummy, with the surface and the results are shown in the table 4.17:

Table 4.14: Heat flux per square meter to set in the boundary conditions in Fluent for the simulations C2

Anesthetist	$q = 53.05\ W/m^2$
Surgical staff member	$q = 44.21\ W/m^2$
Equipment	$q = 159.15\ W/m^2$

– Condition: *Interior*

All the monitoring surfaces are considered as interior with exception of the sampling probes at 24 cm above the table which occupy a physical location. In this way, they aren't considered in the simulation stage but only in the post-processing.

4.4.5 D1 and D2 configurations: one central lamp base

In these configurations the ceiling diffuser is modified. There are now 24 H14 HEPA filters: the central high-speed filter is replaced by the unique surgical lamp base. The place which got the lamp bases in the previous simulations are replaced by two low-speed filters.These simulations adopt the configuration of the room for the verification of the removal of the particulate

generated outside and inside of the critical zone in the real arrangement of the room. In the configuration called D1, the two central aerosol diffusers are outside the critical zone; in the configuration called D2, the two central aerosol diffusers are inside the critical zone.

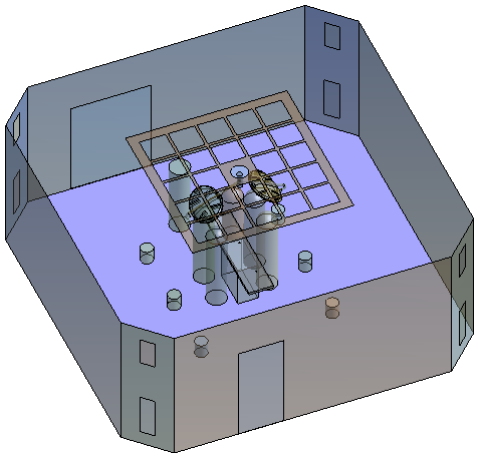

Figure 4.19: Isometric view of the modeled operating theater in configuration D1

The following assumptions were done:

- closed doors
- narrow slit between floor and lower extremity of the door
- only convective heat flux within the room

Information about the mesh

The mesh is composed by tetrahedral cells. Like in the other cases, we have three regions with different reference cell size:

- the inner region (cell size circa 0.035 m);
- the middle region (cell size circa 0.05 m);
- the outer region (cell size circa 0.08 m).

There are overall 9'550'319 cells in the D1 configuration and 9'651'272 in the D2 one.

Boundary Condition

– Condition: *Velocity Inlet, T=293 K* This condition is imposed on the supply air filters which exhibit different velocities, as shown in Table 4.15 and in Figure 4.20.

Table 4.15: Different velocity magnitude at operating room inlets for the simulations D1 and D2

v_{LS}	0.25 m/s
v_{MS}	0.35 m/s
v_{HS}	0.45 m/s

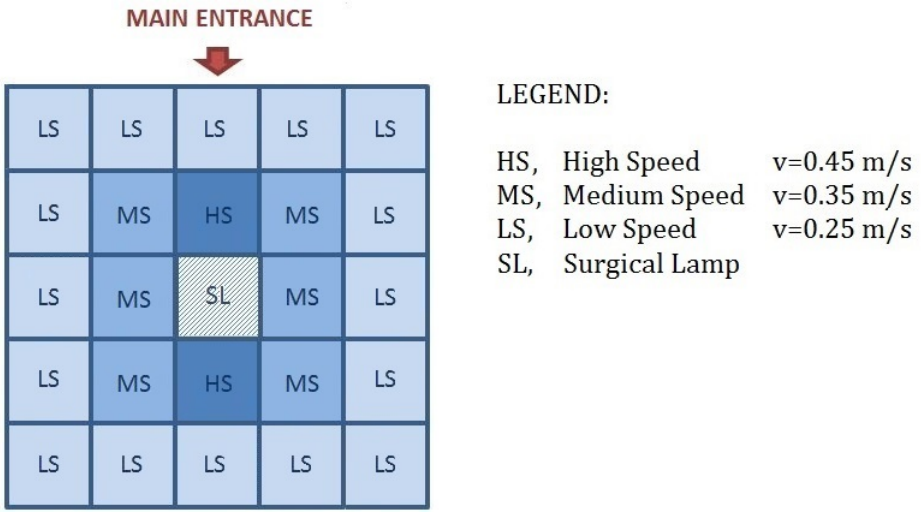

Figure 4.20: Filters of ceiling filter system in configuration called D, different type with different air supply velocities

For the velocity distribution see the figure 4.18. For the velocity distribution see the figure 4.18. From the aerosol diffusers is injected at fixed airflow rate(total airflow: 108 m^3/h) and than, in post processing (thanks to the hypothesis done previously), is injected through them an aerosol challenge (with a fixed diameter of 0.5 μm), in a fixed concentration ($44.2 \cdot 10^6$ pp/m^3), produced by the aerosol generators during the experimental campaign in the operating theater. Hence, the velocity inlet condition is applied also to 6 aerosol diffusers. The velocity of particle injection is around 0.28 m/s and to impose this condition on the surface of the aerosol diffusers it was create a proper user define function (udf). The section 4.4.7 explains in the details the generation

of the particles and shows the effect of the user define function of the aerosol diffuser.

- Condition: *Pressure Outlet, T=293 K*

  - This condition is imposed at the narrow slit between the floor and each door; it is imposed a *gauge pressure* of -15 Pa with outside
  - This condition is imposed on the exhaust grilles; it is imposed a *gauge pressure* of 0 Pa

  The pressure outlet conditions are summarized in the Figure 4.15.

- Condition: *Wall, no slip, adiabatic*

  This condition is imposed on the wall, ceiling (excluding the filter system), floor and on the surfaces of the doors, table, surgical light arms. This condition is imposed also in the three particulate counters (with the 'trap' condition for the DPM). They are simulated like little circles with a diameter of 34 mm and are located 10 cm above the surgical table, as shown in Figure 4.16.

- Condition: *Wall, no slip, heat flux*

  This condition is imposed on the dummy surfaces which represent the surgical staff and the medical equipment. In particular according to the DIN 1964-4 [32] the different dummies release different heat rate as shown in the Table 4.7.

Table 4.16: Different heat flux from the dummy surface according to DIN 1964-4 [32] for the simulations D1 and D2

Anesthetist	$Q = 100\ W$
Surgical staff member	$Q = 100\ W$
Equipment	$Q = 300\ W$

In Fluent it is necessary to set the heat flux per square meter of emitting surface, the values are found out dividing the heat flux, prescribe by the German standard for each dummy, with the surface and the results are shown in the table 4.17:

Table 4.17: Heat flux per square meter to set in the boundary conditions in Fluent for the simulations D1 and D2

Anesthetist	$q = 53.05\ W/m^2$
Surgical staff member	$q = 44.21\ W/m^2$
Equipment	$q = 159.15\ W/m^2$

– Condition: *Interior*

  All the monitoring surfaces are considered as interior with exception of the sampling probes at 24 cm above the table which occupy a physical location. In this way, they aren't considered in the simulation stage but only in the post-processing.

4.4.6 Evaluation of the solution independence by the mesh size

To conduct simultaneously to the validation, also a sensitivity analysis on the mesh, it was decided to distinguish three different types of mesh in the standard configuration which we call A1:

– Fine, with 9'957'445 cells:
  in this mesh we have created three volumes: the inner one has a reference size equal to 0.035 m, the middle one has a reference size equal to 0.05 m and the outer one has a reference size equal to 0.08 m;

– Medium, with 8'700'175 cells:
  in this mesh we have created three volumes: the inner one has a reference size equal to 0.05 m, the middle one has a reference size equal to 0.12 m and the outer one has a reference size equal to 0.20 m;

– Coarse, with 5'429'056 cells:
  in this mesh we have created three volumes: the inner one has a reference size equal to 0.15 m, the middle one has a reference size equal to 0.30 m and the outer one has a reference size equal to 0.50 m;

In all cases the elements of the mesh are tetrahedral. Obviously, in the curvature and proximity the mesh elements are more refined than the reference size reported in the previous list. The simulations carried on with these meshes have the same setting of the simulation A1. In the next chapter the results of the sensitivity analysis about the mesh size are shown in details.

4.4.7 Calculation of particle injections

It is important to put the attention on the way in which it was calculate the particle injection. We used the mean concentration generated during the experimental campaign in the OT. Comparing with the reference concentration indicated in the German standard ($35.5 \cdot 10^6$ pp/m^3), the used one is greater and so the condition is pejorative. With the available data it was possible to calculate the particle mass flow required by Fluent.

Table 4.18: Data for the calculation of particulate mass flow rate from each aerosol diffuser to set like boundary condition

Mean measured concentration	$27.8 \cdot 10^9$	pp/m^3
Air mass-flow	108	m^3/h
Reference concentration (according to DIN 1964-4:2008 [18])	$44.2 \cdot 10^6$	pp/m^3
Particulate flow	$3.002 \cdot 10^{11}$	pp/h
Particle diameter	$0.5 \cdot 10^{-6}$	μm
Particle volume	$6.545 \cdot 10^{-20}$	m^3
Particle density (DEHS)	912	kg/m^3
Total particulate mass flow	$4.978 \cdot 10^{-9}$	kg/s
Particulate mass flow for each aerosol diffuser	$8.297 \cdot 10^{-10}$	kg/s

In order to have a controlled velocity at the inlet of aerosol diffuser it was created an user define function in Fluent (udf). It imposes an air flux limited on a portion of the cylinder. In this way, with the right air mass flow, it is assured a velocity of 0.28 m/s at the inlet of aerosol diffuser. Some pictures of the particles injected from the diffuser are shown below.

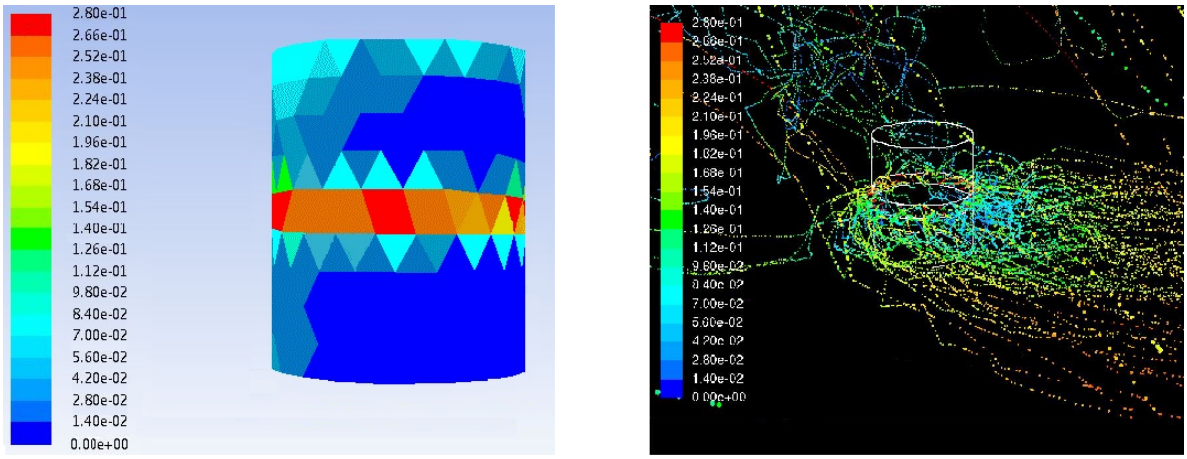

Figure 4.21: Contour of velocity magnitude and particle traces colored by velocity magnitude

Chapter 5

Result analysis

In these chapter it is possible to retrace the path followed to make a proper study. The work carried out is divided in four main parts which will be amply described in the next sections and are listed below:

1. Evaluation of the convergence of each simulation and confirmation of initial hypothesis about the behavior of the fluid and the particles;
2. Evaluation of the solution independence by the mesh size;
3. Validation of the 3-D model by means of experimental data collected in the real operating room in the configurations prescribed by the standards;
4. Analysis of all the simulated configurations which are not conformed with the standard utilization of the room.

5.1 Evaluation of the convergence and confirmation of initial hypothesis

The first part takes into account the achievement of convergence criteria. During the iterations it is useful, initially, to monitor the convergence watching the plot of residuals of the implemented equations and monitoring some properties or physical quantities (for example: mass-flow at the outlets, pressure at the inlet, velocity, etc.) and the balance of all fluxes (in the post-processing).
In the following page it is possible to view some example of convergence control.
The Figure 5.1 reports the residual trend in the last two-hundred-fifty iterations of the simulation called A2. It is important to underline that, because

of the simulation is carried out in transient mode, the residuals exhibit a periodic trend. It is possible to view that, as it is correct, each equation residual is under the value of 10^{-3} and that the energy equation residuals are under the value of 10^{-6} for each iteration.

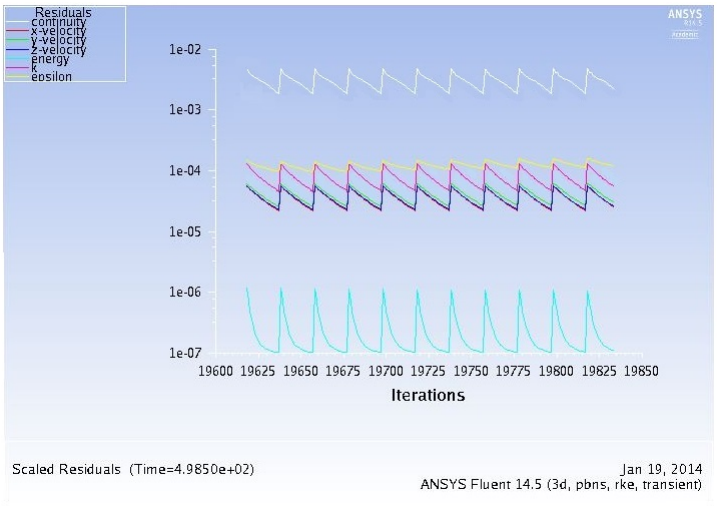

Figure 5.1: Residuals of the simulation number A1

In the Figure 5.2, there is the trend value of static pressure monitored on one of the filters composing the ceiling filtering system. As it can be seen its value is almost constant with the iterations, or, in any case, its variation is in a very narrow range.

Figure 5.2: Convergence history of velocity static pressure on a filter

The same consideration made for the pressure value is possible to repeat for the velocity magnitude on on of the eight return grilles. The result it can

be seen in the Figure 5.3.

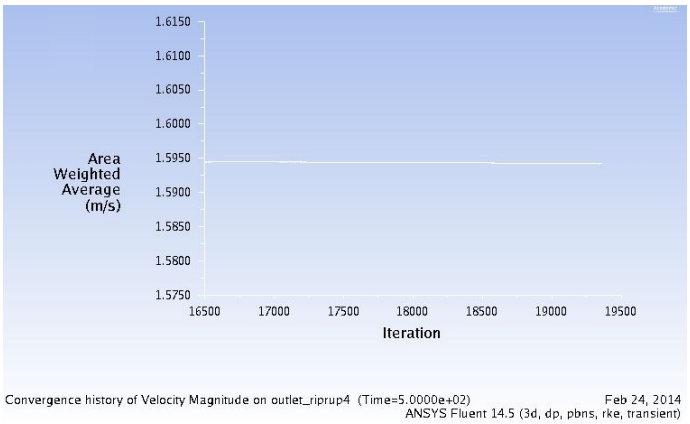

Figure 5.3: Convergence history of velocity magnitude on an exhaust grille

In the Figure 5.4 there is the result of the balance of the all air max fluxes entering and coming out from the operating theater. The result is very close to zero.

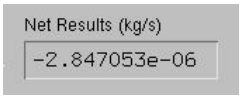

Figure 5.4: Net result of fluxes

The residual values and the balance of all mass fluxes show that the convergence of this simulation is reached. For a reason of brevity the results of other simulations are omitted, but the same results are reached in all the simulations carried out.
Other important data, which are observed in the post-processing stage, regard the hypothesis about the discrete phase volume fraction and the interaction between particle-particle done in Chapter 4.
The fundamental assumption made in this model is that the dispersed secondary phase occupies a low volume fraction (less than $10 \div 12\%$). In effect by the post-processing it has been found a maximum value of dispersed phase volume fraction equal to:

$$7.77 \cdot 10^{-7}\% \tag{5.1}$$

This hypothesis is verifiable only in the post processing.
Furthermore, it was done another consideration. How it is well explaned in the article of Marocco [48], the flow can be considered diluted, thus neglecting particle-particle interaction, if the ratio between the momentum response

time of a particle and the average time between particle-particle collisions is less than one or if the condition in the equation 4.31 is verified. In the studied case the data are:

$\dot{m}_{air} = 2.311\ kg/s$

$\dot{m}_{part} = 4.978 \cdot 10^{-9}\ kg/s$

from which: $Z = \dot{m}_{part}/\dot{m}_{air} = 2.12042 \cdot 10^{-9}$

$\rho_{air} = 1.225\ kg/m^3$

$\mu_{air} = 1.789 \cdot 10^{-5} Pa \cdot s$

$\sigma = 1.556\ m/s$

$$0.5 \cdot 10^{-6} = d_p < A = \frac{1.33\mu}{Z\rho\sigma} \approx 5'900 \tag{5.2}$$

It is abundantly verified the hypothesis afore mentioned according to the equation 4.31.
Therefore, it is possible to conclude that the dispersed phase does not exchange momentum, mass and energy with the fluid phase: the dispersed secondary phase (particulate) occupies a low volume fraction (considerably less than 10-12%),as shown by data 5.1. Furthermore, the flow can be considered dilute, thus neglecting particle-particle interaction, because of the equation 5.2. Thanks to this facts, it is possible to confirm the initial hypothesis and accept the solutions found out, developing the flow field and the subsequently injecting the particles via the DPM interaction tool in post-processing.

5.2 Evaluation of the solution independence by the mesh size

Now, as mentioned before, it is necessary to confirm the hypothesis that the found solutions are independent by the mesh size. Usually, it is a good practice use the Grid Convergence Index (GCI) method formulated by Roache in the 1994 [47]. Unfortunately, this procedure has some limitations linked with the type of the meshes used. In fact the meshes used are unstructured and present local adaptions in particular near the curvatures and in proximity of the narrow slit between floor and the two doors and between one filter and the adjoined one. In his paper, Roache [47], states that if the base grid is unstructured, the GCI procedure would still apply if one used a systematic

method of grid refinement or coarsening, e.g. refining each base grid triangle into four new triangles. However, if the coarsening or refinement is also unstructured, there is no systematic and quantifiable grid refinement index, like the one indicated in his method, to use in the procedure. Roache suggests a trial method to determine this index also for unstructured meshes but he adds that it does not have the firm basis of a structured grid refinement, and may significantly underestimate or overestimate the accuracy.
To overpass this problem and to give and idea about the solution independence by the mesh size, it was carried out a comparison between three solutions found out with three meshes characterized by different sizes.

Table 5.1: Different mesh sizes used to evaluate the mesh independence of the solution

Mesh coarse	5′429′056 number of cells
Mesh medium	8′700′175 number of cells
Mesh fine	9′957′445 number of cells

In order to verify this hypothesis, the velocity values along some relevant lines, were plotted, in particular, where the meshes exhibit the major difference in term of cell size. Comparing on the same graph the results obtained in the three different cases it is simple and immediate to verify the hypothesis about the independence of the solution by the mesh size. In the graphs reported in the Figure 5.5, Figure 5.6, Figure 5.7, it is shown the comparison between the solution found out in the three different simulations using the same arrangement of the room but different number of cells.

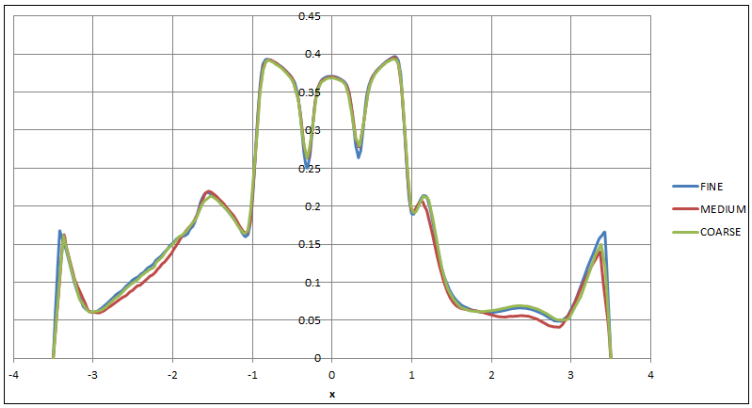

Figure 5.5: Velocity comparison on axis y=1.5 m and z=0 in x-axis-direction for the different mesh size

The Figure 5.5 reports the velocity trend along a line at an height of 1.5 m which continues along the middle of the surgical table. The Figure 5.6 reports the velocity trend along a line at an height of 1.5 m which extends along a diagonal of the room, from a corner to the opposite one, in order to include every zone with different mesh sizes.

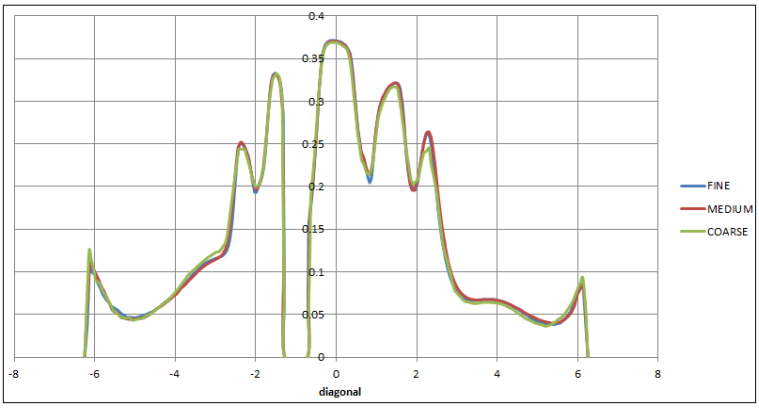

Figure 5.6: Velocity comparison on axis y=1.5 m in diagonal-direction

The last point of interest is the result near a return grille. The solution is shown in the Figure 5.7

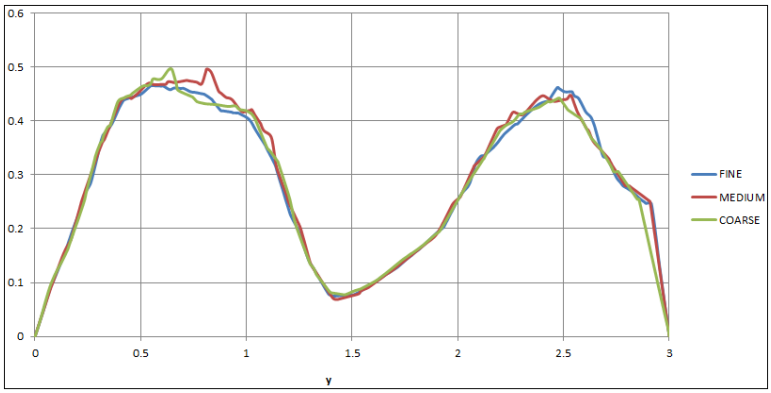

Figure 5.7: Velocity comparison near the return grille number 4 in y-direction

Other functional parameters relative to the simulations have been taken into account in the study of independence grid, giving the same results as for the velocity whose results are exposed. Based on the results afore mentioned, it is possible to conclude that the solution is, with a good approximation, independent by the mesh size. This fact can permit to proceed with the study toward the core of the work.

5.3 Experimental validation of the OT 3-D model

This section considers the validation of the conceived OT 3-D model studied in this work. It is a central part of the work, in fact, it is only thanks to the verification of the correspondence between experimental data and model results, that the model becomes valuable. The experimental campaign has taken place in the operating theater B2 in the hospital San Gerardo in Monza.

5.3.1 Instrumentation used

The internal conditions are the same of the ones simulated in the configurations A1 and A2. In fact there are:

- 4 dummies representing the surgical staff which release 100 W each by means of a lamp;
- 1 dummy representing the anesthetist which release 100 W by means of a lamp;
- 1 dummy representing the medical equipment which release 300 W by means of an electrical resistance;
- 6 small cylinders which release air and particles in the desired concentration;
- 2 real surgical lamps with the joints attached at the peripheral frame of the ceiling diffuser;
- 1 real surgical table;
- 23 absolute HEPA filters composing the ceiling diffuser system

The dummies are made of nonwoven synthetic material which should not release particles and fibers and they could assume the desired shape thanks to a small fan located in their bases. In the Figure 5.8 and Figure 5.10, there are some picture taken during the experimental campaign to show the components used during the tests.

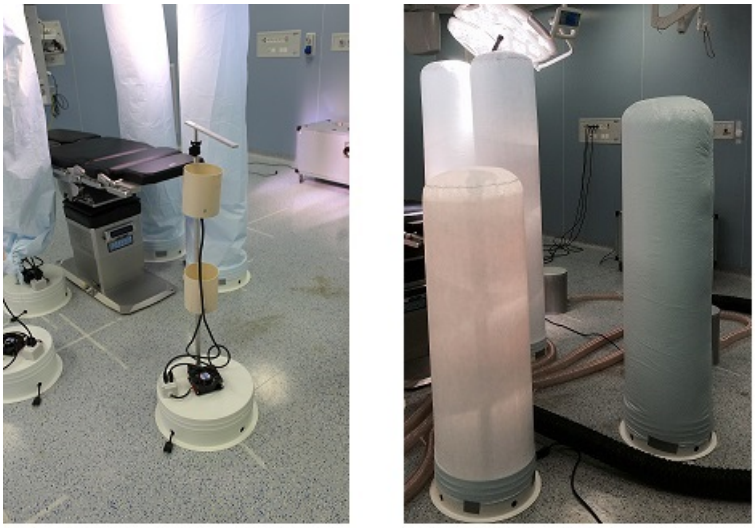

Figure 5.8: On the left: the dummies at the end of the test; on the right: the dummies during the test

The aerosol generation is realized by an ultrasonic aerosol generator which creates an injection of DEHS (Di-Ethyl-Hexyl-Sebacat), a oil often used to test the filter efficiency. The particles, by means of an airflow blown by a fan, are conveyed in a six-ways aerosol distributor. From it, the particle stream is carried homogeneously to the six aerosol diffusers. To measure the reference concentration it is necessary to dispose of dilution systems in order to dilute the aerosols for measurement with particle counters which may be damaged by an high amount of particles. The dilution system was set up to dilute 1'000 times the challenge aerosol generated.

Figure 5.9: Fan and aerosol generator used in during the experimental campaign

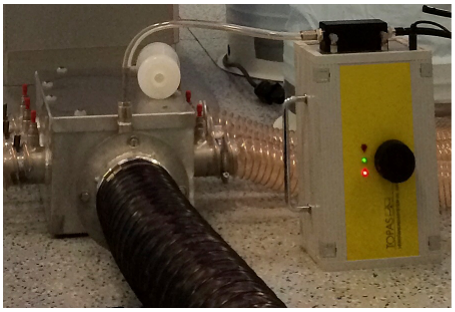

Figure 5.10: On the left: the six-way aerosol distributor and the OPC dilution system; on the right: one of the six real aerosol diffusers

5.3.2 Measurement instruments

In order to measure the quantities to compare with the simulation results, three main measurement instruments have been used:

1. *Optical Particle Counter (OPC)*: The instrument uses a laser-diode light source and collection optics for particle detection. Particles scatter light from the laser diode. The collection optics collect and focus the light onto a photo diode that converts the bursts of light into electrical pulses. The pulse height is a measure of particle size. Pulses are counted and their amplitude is measured for particle sizing. Results are displayed as particle counts in the specified size channel and are also printed at the end of each count. The probe can be located on the instrument or on a support for remote measurements. The particle sizes of interest for this study are larger or equal to 0.5 μm. The technical specification and a photo of the Optical Particle Counter used is reported in Figure 5.11 and Figure5.12.

Model: Solar 3100+, Lighthouse

Size range:	0.3-25 μm
Standard channel size:	0.3, 0.5, 1, 5, 10, 25 μm
Flow Rate:	28.3 l/m
Counting efficiency:	50% @ 0.3 μm; 100% @ ≥ 0.45 μm
Concentration limit:	35.5x10 pp/m @ 10%
Sampling tube:	Bev-e-line ∅ 5 mm
Sampling probe size:	∅ 34 mm; stainless steel

Figure 5.11: Technical specification of the OPC, conforming to the requirements of ISO 21504-4 [26]

Figure 5.12: The OPC Solair 3100+ (on the floor) and the isokinetic particle sampling probe with its tripod (on the table) used during experimental tests

2. *Hot-wire thermo-anemometer with RH probe*: This is a punctual velocity, temperature and Relative Humidity, indicator and it is a data-logger.

Velocity:	
Range:	0 to 50 m/s
Accuracy:	±0.015 m/s, whichever is greater
Resolution:	0.01 m/s
Temperature:	
Range:	-10 to 60°C
Accuracy:	±0.3°C
Resolution:	0.1°C

Figure 5.13: Multi-purpose instrument for measuring the speed with hot-wire anemometer and its technical specification (Source TSI Inc.)

The hot-wire anemometer measures a fluid velocity by noting the heat convected away by the fluid. The core of the anemometer is an exposed hot wire either heated up by a constant current or maintained at a constant temperature. The heat lost to fluid convection is a function of the fluid velocity. By measuring the change in wire temperature under constant current or the current required to maintain a constant wire temperature, the heat lost can be obtained. The heat lost can

then be converted into a fluid velocity in accordance with convective theory. This measurement instrument has been used to measure the velocity, the temperature and the humidity in some points of interest in order to compare them with the values obtained in the simulation. This measure is directional.

3. *Vane anemometer*:It is a good measurement instrument to calculate the air velocity on a return grille or a supply air diffuser. It is composed by a fan exposed to the air flow, which induces the rotation of the fan. It small fan provide electrical impulses by means a magnet located on a blade and a sensor on the support. In this way it is generated a wave which mathematically processed gives the velocity value. This measure is directional and it is data-logger.

Velocity:

Range:	0.25 to 30 m/s
Accuracy:	±1.0% of reading ±0.02 m/s

Temperature:

Range:	0 to 60°C
Accuracy:	±0.5°C
Resolution:	0.1°C

Figure 5.14: Technical specification of the vane anemometer (Source TSI Inc.)

Figure 5.15: Vane anemometer and its utilization during the test

5.3.3 Experimental campaign and simulation A1 and A2

The experimental campaign has started with the preparation of the components described in the previous sections. Initially it was carried out a particle sampling on the three points of interest on the surgical table (head, thorax and feet) in absence of generated contamination and with the dummies switched on, in order to verify if there is contamination coming from the dummies.

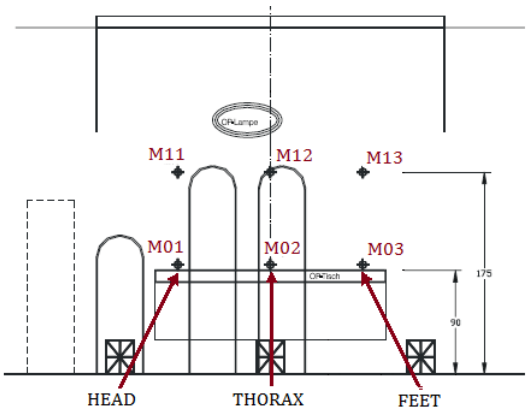

Figure 5.16: Experimental measurement points layout according to DIN 1964-4 [32]

For the three points (see Figure 5.16), five samples have been done, lasting two minutes each. The particle counts detected on each of the three points are approximately zero. After this, it was carried out a particle sampling on the same three points on the surgical table in absence of generated contamination and with the dummies switched on. The results shows a very low amount of particles with a diameter $\geq$0.5 μm in the region of the thorax. During the other tests, in effect, in this region, it was found a certain amount of particles. It is possible to conclude that, in spite of the dummy material is synthetic nonwoven fabric, they could be deteriorated or dirty. Furthermore, the dummies are maintained in their shape thanks to a fan on the base which draws air from the floor. This mechanism, united with the deterioration of the fabric, tends to provoke a particles release from the dummies which are very close to the surgical table and therefore to the OPC probe.
After this verification, it was produced the reference challenge contamination in the airflow coming out from the six aerosol diffusers, at least equal or greater than the reference concentration indicated in the German standard DIN 1964-4 [32]. The DIN 1964-4 [32] indicates an aerosol diffuser total

airflow equal to 108 m^3/h and a reference particle concentration equal to $35.3 \cdot 10^6$ pp/m^3 at 0.5 μm. During the test, with the same airflow, a reference concentration of $44.2 \cdot 10^6$ pp/m^3 at a value $\geq$0.5 μm, has been measured. Measurements to verify the maintenance of the right particle generation have been carried out during each test. For boh configuration A1 and A2 has been carried out the test for the determination of the protection class SG, according to the DIN 1964-4 [32]. In order to validate the CFD model, some points of interest, in the operating theater, have been considered only for the configuration called A2. This choice was obliged by the exigence to make the operating theater aviable for the operations as soon as possible. The core of the validation consists in the comparison between the values found out in these points, during the experimental tests, and the values obtained, at the same points, in the simulations. In this regard, measurements of air velocity, temperature and particle concentration have been sampled. Figure 5.17 shows the locations of the experimental measurement points within the OT.

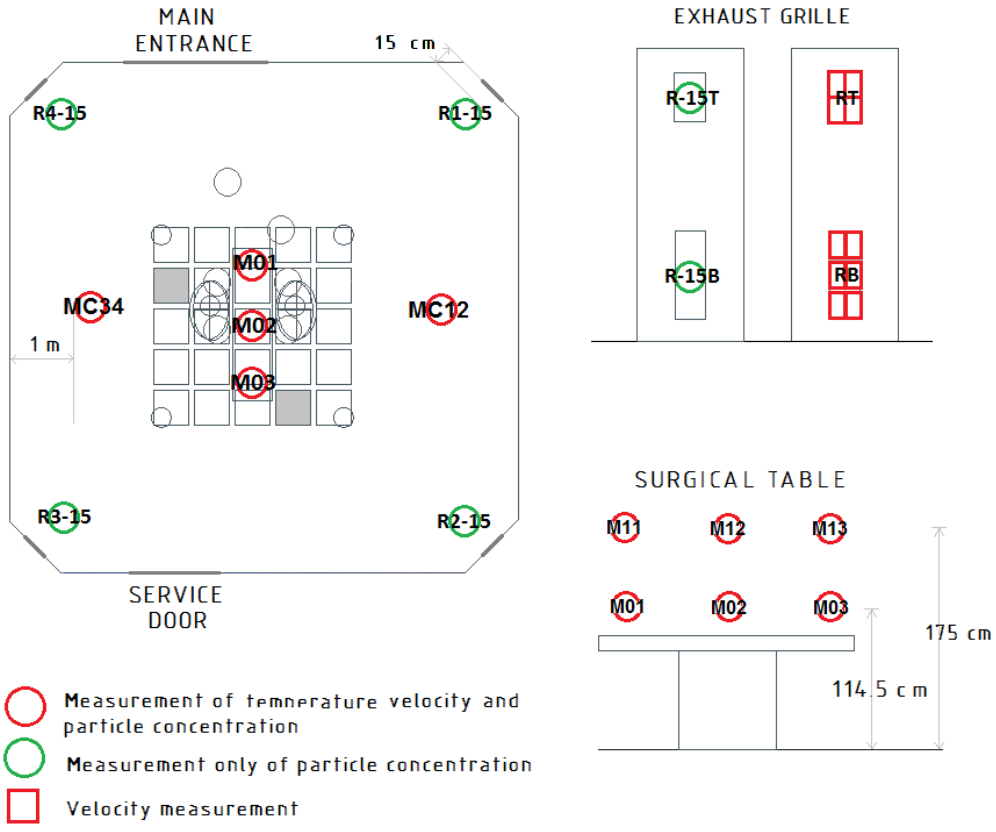

Figure 5.17: Experimental measurement points layout

Velocity and temperature measurements have been taken with the the hot-wire thermo-anemometer and its temperature probe.
The measurement points are:

- for each inferior exhaust grille: six points on the exhaust grille surface
- for each superior exhaust grille: four points on the exhaust grille surface
- on the surgical table: three points in correspondence of the head, thorax and feet of the patient at an height of 1.145 m from the floor
- on the surgical table: three points in correspondence of the head, thorax and feet of the patient at an height of 1.75 m from the floor

Particle concentration measurement points have been taken in the following way:

- for each exhaust grille: one point in the center of the exhaust grille, 15 cm far from it;
- on the surgical table: three points in correspondence of the head, thorax and feet of the patient at an height of 1.145 m from the floor
- on the surgical table: three points in correspondence of the head, thorax and feet of the patient at an height of 1.75 m from the floor
- in the middle of two the lateral wall without the doors: one point for each wall at an height of 1.7 m, 1 m far from the wall

Determination of the cleanliness class and the SG index

It is necessary to recall some concepts useful in this stage of the work. In fact, with the particle data sampled, it is possible to calculate the cleanliness class in the critical area. This test was carried out for both configurations prescribed by the German regulation DIN 1964-4 [32]. In each arrangement of the aerosol diffusers the ceiling filtering system assures the desired level of cleanliness: ISO 5. It means that the particles with a diameter equal and above 0.5 μm are in the right concentration, according to the standard DIN 1964-4 [32]:

ISO classification number (*N*)	Maximum concentration limits (particles/m³ of air) for particles equal to and larger than the considered sizes shown below (concentration limits are calculated in accordance with equation (1) in 3.2)					
	0,1 µm	0,2 µm	0,3 µm	0,5 µm	1 µm	5 µm
ISO Class 5	100 000	23 700	10 200	3 520	832	29

Figure 5.18: Concentration required for an ISO 5 class of cleanliness according to the UNI EN ISO 14644-1 [20]

In addition to the determination of the cleanliness level, the German regulation fixes another parameter to qualify the ventilation system in an operating theater. It is necessary to recall the formula to obtain the index SG (Schutzgrades) indicated by the DIN 1964-4 [32] as a parameter to describe protection class of the critical zone:

$$SG_x = -\log\left(\frac{C_x}{C_{ref}}\right) \tag{5.3}$$

where:
C_X, particle concentration measured in the x-location of the room $[pp/m^3]$
C_{ref}, particle reference concentration $[pp/m^3]$

The parameter SG can assume the values between 0 and 5 as explained in Table 5.2.

Table 5.2: The range of values of the protective effect, SG

Excellent	5.0
Very moderate	1.0
No protective	0

The following part of this chapter deals with the discussions of the numerical simulation and experimental measurements done on the different case scenarios of OT.

Case A1

Case A1 deals with the standard lay-out of the OT with the external contamination setting, according to DIN 1964-4 [32]. Figure 5.20 shows the velocity vectors of the section plane called T obtained from the CFD simulation of this case, according to the setting parameters introduced in Chapter 4.

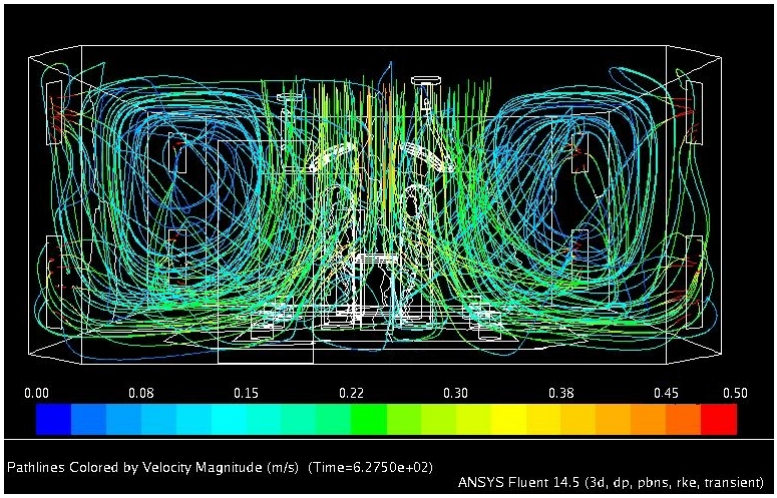

Figure 5.19: Pathlines Colored by velocity magnitude, within all the space of the OT, for the case A1

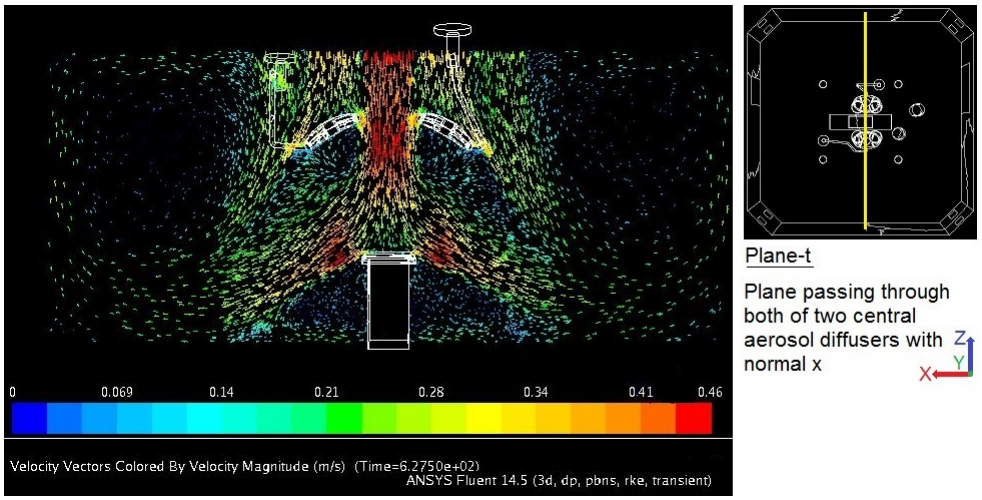

Figure 5.20: Velocity vectors on the plane called t, according to the figure on the right, for the case A1

It is important to notice how the main airflow path coming from the ceil-

ing diffuser is influenced by the two surgical lamps. In fact, small vortexes can be seen just beneath the surgical lamps, just downstream the main airflow, as shown in Figure 5.21, in whicth the section-r better explains how, the surgical lamps and theirs arms influence the airflow path and generate vortexes over the operating table and dummies. Even though, some small vortexes are present near the connections between the lamp arms and the ceiling diffurser. These disturbances do not influence so much the main airflow path over the operating table and therefore the contamination, because the differential velocities of the HEPA filters increase the washing effect towards the periphery of the diffuser.

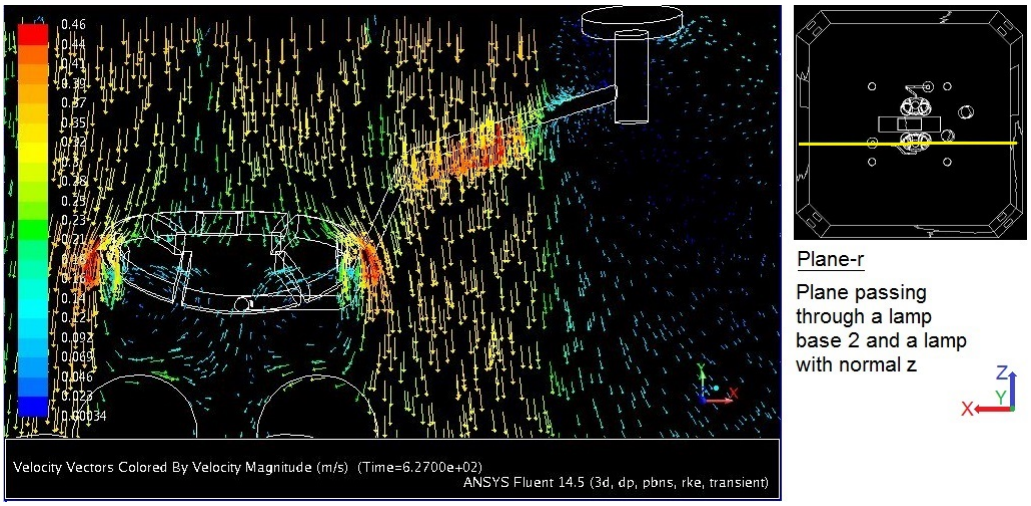

Figure 5.21: Detail of velocity vectors on the plane called t, according to the figure on the right, for the case A1

The two recirculation vortex present in the upper part of the room (see Figure 5.20) clearly shows how the return grilles influence the air diffusion within the OT. As well as, the presence of dummies close to the operating table influences the air-path between the two dummies, increasing the air velocity and turbulence. Small recirculations are also present beneath the operating table, which can be elected as the lowest air velocity zone within the OT and also one of the dirtiest. As in Figure 5.20, even better in Figure 5.21, it can be seen how the different velocities present at the outlet of the different HEPA filters of the ceiling diffuser increases the sweeping effect of the airflow towards the peripheral parts of the critical zone of the OT. Furthermore, even in this section, it can be seen the presence of the recirculation vortexes, due to the absence of the exhaust grilles in the middle of the vertical walls of the OT. The presence of the narrow slits of the two doors, slightly influences the size and the shape of the recirculation vortexes which arise

close to the vertical walls of the OT along the x-axis of the reference system used in this simulation. Evidence of this influence can be seen in Figure 5.22. The airflow rate flowing out through those two narrow slits is a small amount in comparison with the supply flow rate, but sufficient to maintain the differential pressure between the OT environment and the adjacent ones. More in detail the exfiltration flow rate through the doors is equal approximately to $300m^3/h$ ($\approx$ 3 % of the total supply air) in agreement with the designed and measured values.

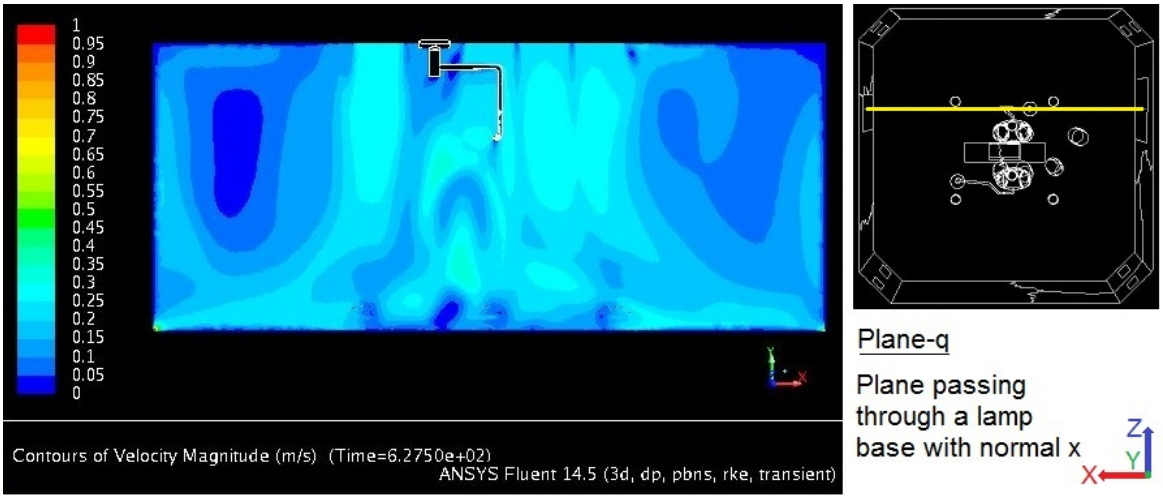

Figure 5.22: Velocity contours on the plane called q, according to the figure on the right, for the case A1

Particle concentration within the OT is an important parameter for the safety of patient and personnel. In case A1 , with the external contamination layout, the level of air contamination over the table, is almost equal to zero. Presence of particle contamination can be detected and seen beneath the table, with higher concentration in the zone near by the head of the patient where there is the presence of the surgical equipment and the anesthetist. Of coarse, higher concentration is also presence in the upper part of the room due to the already mentioned recirculation vortexes. Figure 5.23 and Figure 5.24 better explains what afore mentioned.

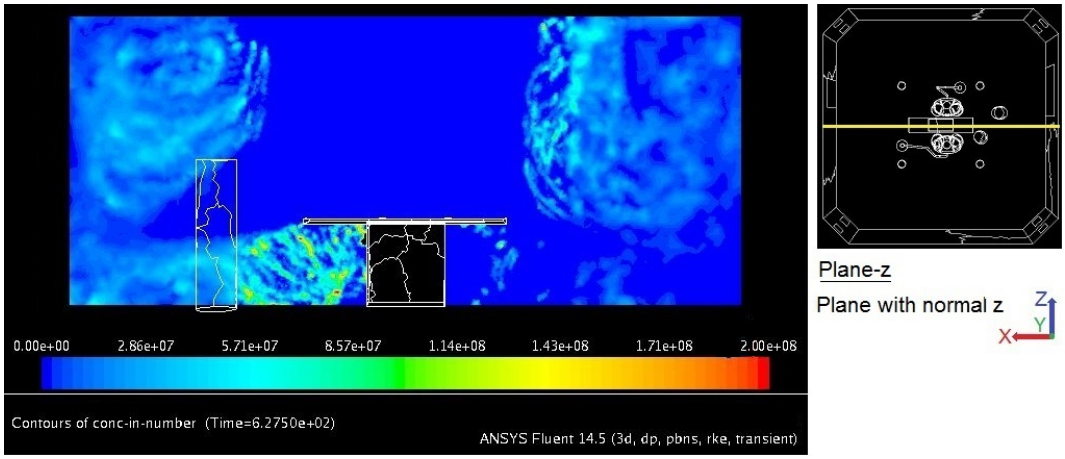

Figure 5.23: Concentration contours (in pp/m^3) on the plane called z, according to the figure on the right, for the case A1

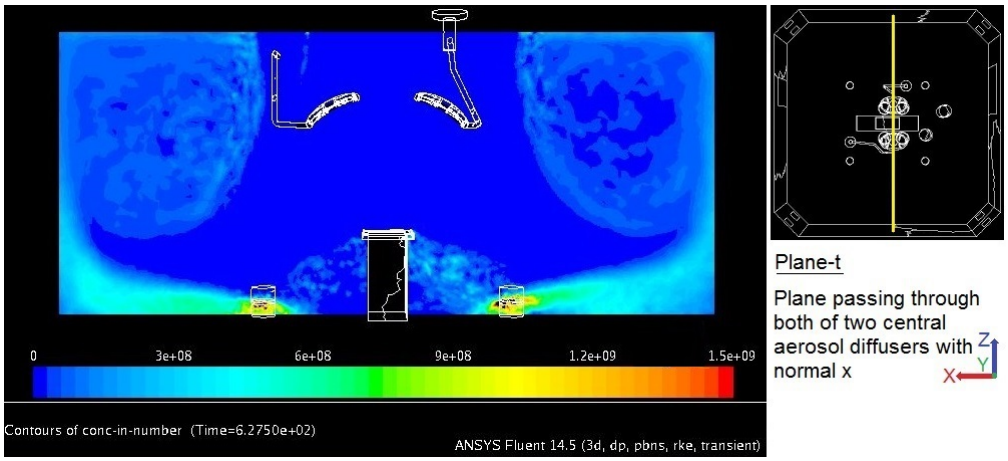

Figure 5.24: Concentration contours (in pp/m^3) on the plane called t, according to the figure on the right, for the case A1

The results of the aforementioned CFD simulation, case A1, should be validated with a real experimental measurements of the same OT environment under the same conditions. For lack of time and availability of the operating theater, for this case, there is only a comparison between the results found out during the experimental test for the calculation of the protection class and those found out in the simulation. The Table 5.3 shows the results of particle concentrations in the three positions indicated by the German regulation on the operating table, data obtained during a real experimental test. Moreover, in the table it is also present the results of the calculation

of the protection class SG, according to the equation 5.3, and the mentioned comparison between the experimental value of SG and the simulated one. In addition, there is a ISO class calculation, obtained with the experimental data, according to UNI EN ISO 14644-1 [20].

Table 5.3: Case A1: Airborne particle concentration from experimental test. Comparison of simulated and measured SG value. ISO class number calculation

SG CALCULATION

A1		Particle concentration		Particle concentration		Experimental results		Simulated results
Number of measure	Location	≥0.5 µm pp/m^3	≥1.0 µm pp/m^3	Average ≥0.5 µm pp/m^3	Average ≥1.0 µm pp/m^3	SG 0.5 µm	SG 1 µm	SG 0.5 µm
1	HEAD	0	0	0	0	5	5	5
2	HEAD	0	0					
3	HEAD	0	0					
4	HEAD	0	0					
5	HEAD	0	0					
1	THORAX	1327.8	113	1438	113	4.4	4.6	5
2	THORAX	1511.5	113					
3	THORAX	1172.4	113					
4	THORAX	1907	113					
5	THORAX	1271.3	113					
1	FEET	0	0	0	0	5	5	5
2	FEET	0	0					
3	FEET	0	0					
4	FEET	0	0					
5	FEET	0	0					

ISO CLASS NUMBER CALCULATION

	≥0.5 µm pp/m^3	≥1.0 µm pp/m^3
Average on the table	479.3	37.7
Maximum on the table	1438.0	113.0
Minimum on the table	0.0	0.0
Standard deviation	830.2	65.2
Concentration ISO on surgical table	1869.4	146.9
ISO Class on surgical table	4.7	< ISO 4

How it can be seen in Table 5.3, the concentration on the operating table is, with good approximation, equal to zero. In the region of the thorax there are some particles which are due to the presence of the dummies. In fact, the technical nonwoven material are in part deteriorated. In order to verify this hypothesis, a particular test just with the dummies switched on (without the artificial aerosol) has been carried out, as mentioned in the introduction on the experimental campaign. However, the protection class (SG) is completely satisfactory and corresponds with the simulated results. The ISO class number calculation attests the air quality within the critical area.

Case A2

Case A2 deals with the standard lay-out of the OT with the internal contamination setting, according to DIN 1964-4 [32]. Figure 5.27 shows the entire OT with the particle traces colored by different concentration from the CFD simulation of this case, according to the setting parameters introduced in Chapter 4. In this figure it is possible to see a large amount of particle concentrated under the table, because of the presence of the two aerosol diffusers just tangent to the central dummies representing the surgical staff.

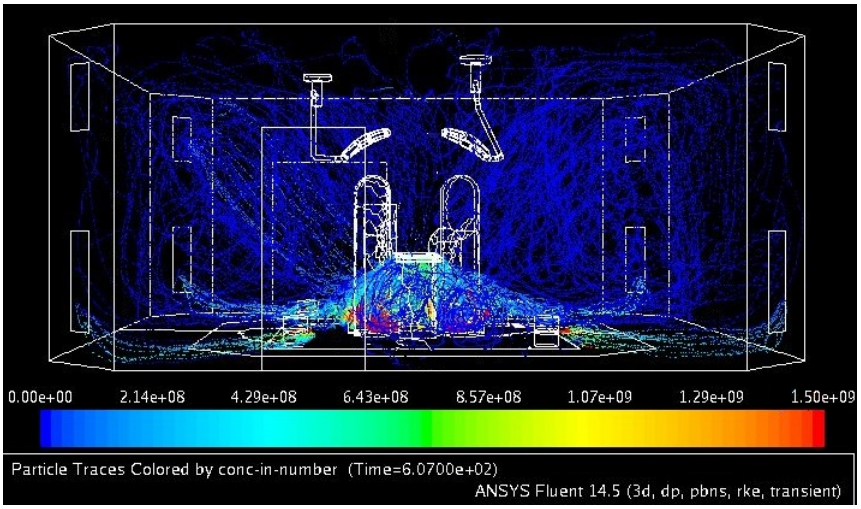

Figure 5.25: Particle traces within all the space of the OT, colored by concentration (in pp/m^3), for the case A2

The intent of the Figure 5.26 is to show that the behavior of the air streams is almost the same of the previous case, A1. It is possible to see the recirculations present under the surgical lamps, and the two large vortexes in the zone around the critical area.

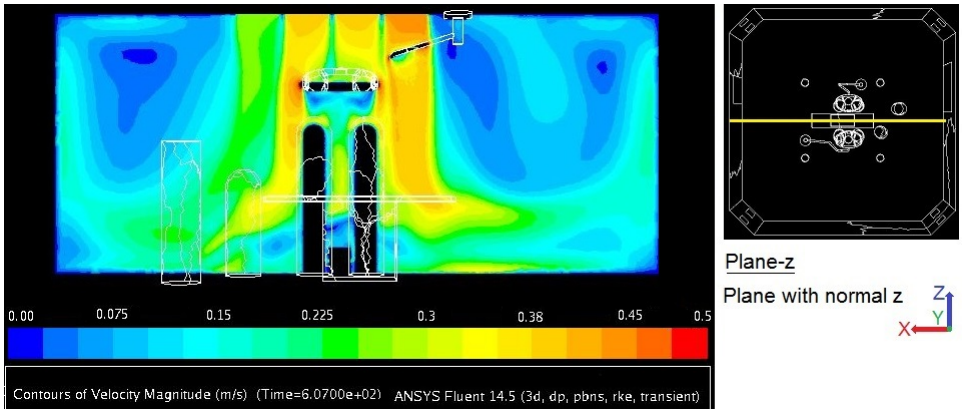

Figure 5.26: Velocity contours on the plane called z, according to the figure on the right, for the case A2

As introduced before, the main difference between this case and the previous one is the presence of the two central aerosol diffusers in the critical area. This fact provokes an high level of contamination under the table.

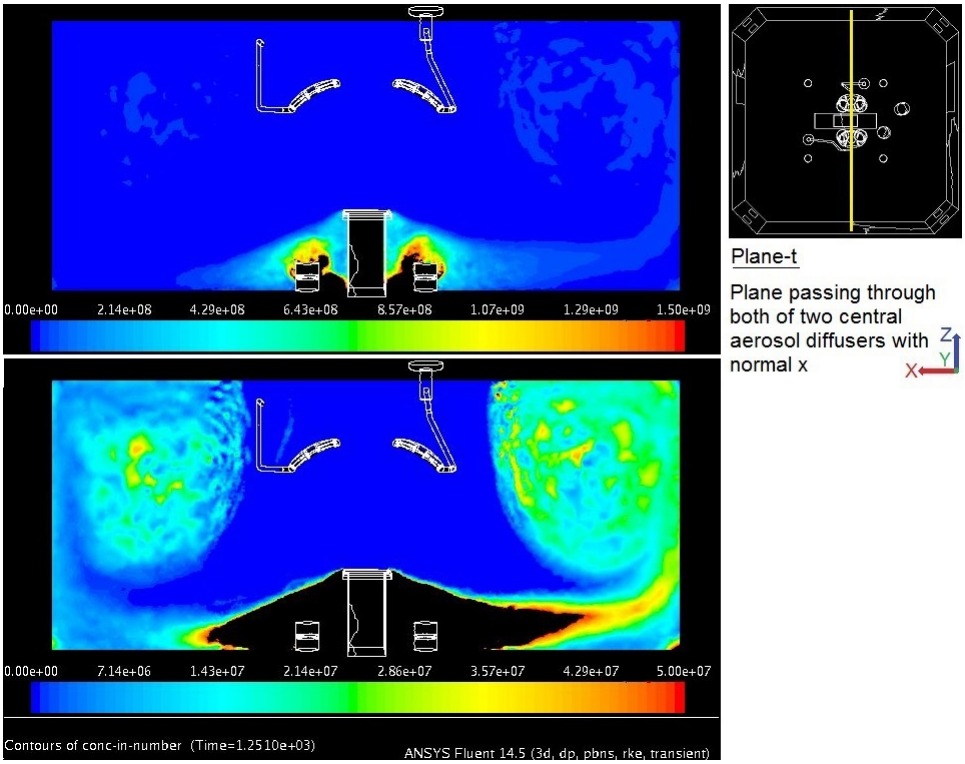

Figure 5.27: Concentration contours (in pp/m^3) on the plane called t, according to the figure on the right, with two different scales, case A2

The Figure 5.27 shows, on the same plane, the contours of contamination, in pp/m^3, for two different reference scales. In fact, in order to visualize the contamination distribution in the part outer the critical zone, it is necessary to decrease the maximum value of the scale. The black zone has a greater contamination concentration than the others. In this way it is possible to observe the presence of the contamination also in the two big vortexes in the periphery of the critical zone. The Figure 5.29 shows the contamination contours in another plane. It is possible to observe a large contamination presence in proximity of the main door. In fact, in this region, there are the anesthetist and the medical equipment and their presence strongly influences the airflow path and creates turbulence.

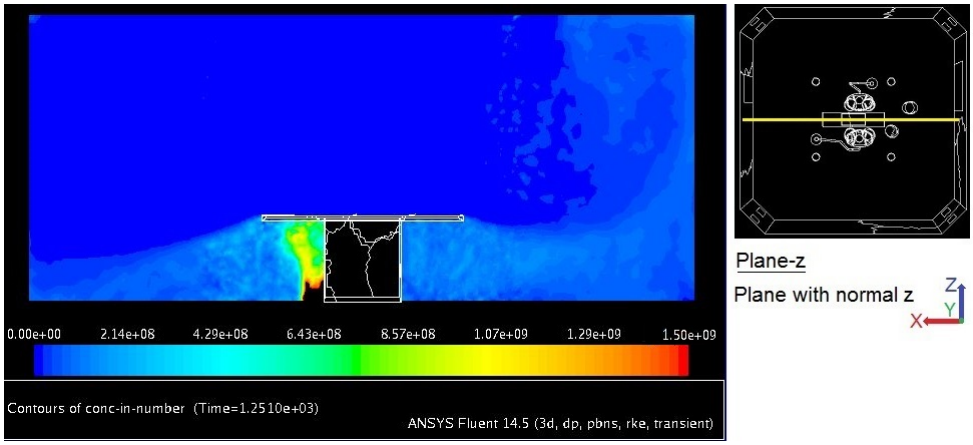

Figure 5.28: Concentration contours (in pp/m^3) on the plane called z, according to the figure on the right, for the case A2

For this configuration it was possible to conduct experimental measurements directly in the OT. In particular, it has been measured the value of the properties and physical quantities in the points introduced in Figure 5.16. Thanks to this fact, it was possible to conduct the central part of the CFD model validation. In the Table 5.4 and 5.5, there is a comparison between experimental data and simulated one. It is important to underline that, in order to do a good validation study, the boundary conditions used in the simulation A2 corresponds to the values sampled during the experimental campaign. For lack of time and availability of the operating theater this comparison has been done only for this configuration.
The temperature values of experimental data and of the value found out from the simulation are very similar. In fact, it can be seen in Table 5.4 the error percentage is much less than 3% . For the velocity the interpretation is more complex, in fact it is necessary to add some consideration. During the exper-

imental campaign, within the room, there were other surgical equipment and surgical supports and arms installed on the ceiling around the air diffuser, not included in the German regulation.

Figure 5.29: Frontal photo of the real OT at the end of the test. On the left the corner called 2 and on the right the corner 3

These tools do not represent total negligible aspects for the study of the airflow streams and their velocity. In fact the comparison between experimental and simulated data highlights some different, slightly (less than 10%) where the fluid is less influenced by the obstacles presence, while, in the direction of these 'barrier' the differences between experimental and simulated data are between the 15-20 %. In particular, the additional arms, functioning as supports for other medical equipment during the operations, have been positioned near the ceiling between the exhaust grilles called 2 and 3. This fact, is reflected in a calculated error between 15-20 % for the values of the velocity on the upper exhaust grilles at the corner called 2 and 3. On the other hand, the percentage error of the velocity calculated on the lower grilles is around 10 % there where the airflow was undisturbed, while, for the lower grilles at the corner 4, where has been present another not modeled medical equipment, the error is approximately equal to 20 %. On the surgical table, especially in proximity of the thorax, the gap between experimental and simulated results is between 20 and 30%. These values are not totally unexpected. In fact, the surgical table was found located approximately 10 *cm* out of the axis of the three high speed filters in the center of the ceiling diffuser. To compensate this situation, during the test the two surgical lamps were located in order to be, as much as possible, in axis with the high speed filters. The problem it was partially compensated but not totally. Furthermore, while the other velocity measurements have been sampled with the vane anemometer, the velocity measurements on the surgical table have

been taken with the hot-wire anemometer. This measurement instrument is more affected by error possibility, than the other one.

Table 5.4: Comparison between experimental and simulated data of the velocity and temperature values and percentage error

	VELOCITY			TEMPERATURE		
	Experimental results	Simulated results		Experimental results	Simulated results	
Points of measurements	Velocity m/s	Velocity m/s	Velocity error m/s	Temperature °C	Temperature °C	Temperature error %
M01	0.31	0.25	0.18	21.4	21.7	0.01
M02	0.31	0.21	0.31	21.5	21.7	0.01
M03	0.24	0.28	0.18	21.3	21.7	0.02
M11	0.44	0.34	0.24	22.1	21.7	0.02
M12	0.43	0.37	0.14	21.9	21.7	0.01
M13	0.43	0.36	0.16	21.5	21.7	0.01
RB1	1.07	1.32	0.24	22.6	21.8	0.03
RT1	1.53	1.30	0.15	22.5	22.1	0.02
RB2	1.23	1.32	0.07	22.3	21.8	0.02
RT2	1.73	1.31	0.24	22.3	21.8	0.02
RB3	1.19	1.31	0.11	22.3	21.7	0.02
RT3	1.57	1.30	0.17	22.3	21.7	0.02
RB4	1.07	1.32	0.23	22.3	22.1	0.01
RT4	1.49	1.30	0.13	22.4	22.6	0.01

In the Table 5.5 there is a comparison between experimental and simulated value of particle concentration and the calculation of the error.

Table 5.5: Comparison between experimental and simulated data of the particle concentration values and percentage error

	PARTICLE CONCENTRATION		
	Experimental results	Simulated results	
Points of measurements	Concentration pp/m^3	Concentration pp/m^3	Concentration error pp/m^3
R1_15B	17'195'873.7	20'581'255.0	0.2
R1_15T	21'028'068.3	20'937'532.0	0.0
R2_15B	15'291'398.0	6'720'506.0	0.6
R2_15T	9'541'985.7	5'857'432.0	0.4
R3_15B	9'286'924.3	3'176'340.2	0.7
R3_15T	3'576'857.0	7'006'761.4	1.0
R4_15B	30'349'914.0	26'465'254.0	0.1
R4_15T	11'101'648.8	46'633'256.0	3.2
M01	0.0	0.0	0.0
M02	0.0	0.0	0.0
M03	1'572.7	0.0	1.0
M11	0.0	0.0	0.0
M12	0.0	0.0	0.0
M13	0.0	0.0	0.0
MC12	16'057'587.3	5'114'135.2	0.7
MC34	7'649'744.3	1'176'096.1	0.8

The conclusions about gap between simulated and experimental value for the concentration are very similar to the velocity one. In fact, the main differences are in the zones where the airflow streams are mainly disturbed by the extra medical equipment present. Especially, in the upper exhaust grille at the corner called 4, where one of the obstructions is present, there is a strong variation of the value of contamination. In this area probability there are sac of dirty air which recirculates. As highlighted for the velocity, also the upper exhaust grille at the corner called 3 has some consistent differences of correspondence between simulated and real values. This is caused, as mentioned before, for the present or an additional surgical arm used during the operating and not modeled. The other values have not so strongly differences. In any case it is necessary to add some considerations. Concerning the measurements of particle concentration, since they are strongly conditioned by the cleanliness of the operating theater, it is possible to do a limited comparison. In fact the conditions of cleanliness of the room were not ideal indeed, like the ones in the simulations. In the real operating theater there were some aspects to consider: the lateral walls presented evident signs of not good cleanliness and, not of secondary importance, the surgical table resulted installed approximately 10 cm out of the central axis of the room in the direction of the three central filters. This fact is not irrelevant: in fact the three central high speed filters have been conceived to be located perfectly above the surgical table, in order to cover completely the surface where the surgical operation takes place. To overcome this problem, as mentioned before, some expedients were taken. Furthermore, for the measurements near the exhaust grilles, it must do another observation. These measures were taken at the end of the experimental campaign when, therefore each operator wore the proper technical clothes, the operating theater results dirtier than the initial stages of the campaign. The remark about the quality of the dummies material has been done before. About those, it is important just to add that they are maintained in their shape thanks to a fan on the base which draws air from the low. This mechanism, unites with the deterioration of the paper, tends to provoke a particle release from the dummies which are very close to the surgical table and therefore to the probes.
Also for this configuration, as it is prescribed by the German regulation, it has been carried out the test for the evaluation of the protection class. The following table 5.6 shows the results of particle concentrations in the three positions indicated by the German regulation on the operating table, data obtained during a real experimental test. Moreover, in the table it is also present the results of the calculation of the protection class SG, according to the equation 5.3, and the mentioned comparison between the experimental value of SG and the simulated one. In addition, there is a ISO class cal-

culation, obtained with the experimental data, according to UNI EN ISO 14644-1 [20].

Table 5.6: Case A2: Airborne particle concentration from experimental test. Comparison of simulated and measured SG value. ISO class number calculation

SG CALCULATION

A2		Particle concentration		Particle concentration		Experimental results		Simulated results
Number of measure	Location	≥ 0.5 µm pp/m^3	≥ 1.0 µm pp/m^3	Average ≥ 0.5 µm pp/m^3	Average ≥1.0 µm pp/m^3	SG 0.5 µm	SG 1 µm	SG 0.5 µm
1	HEAD	0	0	0	0	5	5	5
2	HEAD	0	0					
3	HEAD	0	0					
4	HEAD	0	0					
5	HEAD	0	0					
1	THORAX	1568	70.6	1576.44	118.66	4.4	4.6	5
2	THORAX	1596.2	113					
3	THORAX	1440.8	84.8					
4	THORAX	1892.9	211.9					
5	THORAX	1384.3	113					
1	FEET	0	0	0	0	5	5	5
2	FEET	0	0					
3	FEET	0	0					
4	FEET	0	0					
5	FEET	0	0					

ISO CLASS NUMBER CALCULATION

	≥ 0.5 µm (p/m^3)	≥ 1.0 µm (p/m^3)
Average on the table	525.5	39.6
Maximum on the table	1576.4	118.7
Minimum on the table	0.0	0.0
Standard deviation	910.2	68.5
Concentration ISO on surgical table	2049.4	154.3
ISO Class on surgical table	4.8	< ISO 4

How it can be seen the ceiling filtering system ensures a good protection level, according to the DIN 1964-4 [32].

5.3.4 Analysis of the case configurations B2, C2, D1, D2

This section illustrates how can be used a validated model in order to highlight the behavior of the ventilation system when it is used improperly or to test other configurations of the filtering system.
It will be described the choice of each arrangement investigated; in particular we want to study three cases called: B and C, with the aerosol diffusers disposed to create the contamination coming from inside the critical zone, and D, with the aerosol diffusers disposed to create the contamination coming from both outside and inside the critical zone.

Case B2: Behavior of the ventilation system with two exhaust grilles obstructed

The B2 configuration takes into account the situation for which one corner of the OT has both of the two exhaust grilles completely obstructed. In particular, the exhaust grilles, at corner called 2, are completely closed (see Figure 5.31). It was chosen these two grilles because their obstruction is the most critical for the room. In fact, this is the location where, during the surgical operation the surgical personnel tends to collect the additional tools useful for conduct the operation (see Figure 5.30).

Figure 5.30: Two photo of the exhaust grilles obstructed by surgical equipment during an inspection in the studied operating theater

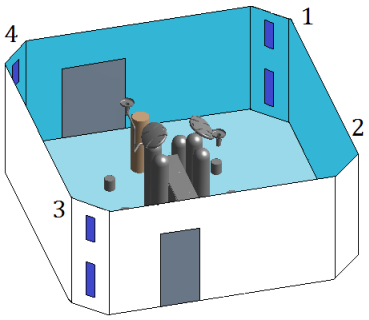

Figure 5.31: The placement of the obstructed exhaust grilles for case B2

For this case, only the simulation stage has been carried out. In the following figures there are the main aspects whom it is important to underline. In Figure 5.32 there are the pathlines, representing the air streams coming out from the ceiling filter diffuser, colored by the velocity value. It is important to note that, in the corner where the exhaust grilles are obstructed, the pathlines are obliged to recirculate there. In fact, the red color due to the high outlet velocity are absent in the corner where the exhaust grilles are closed.

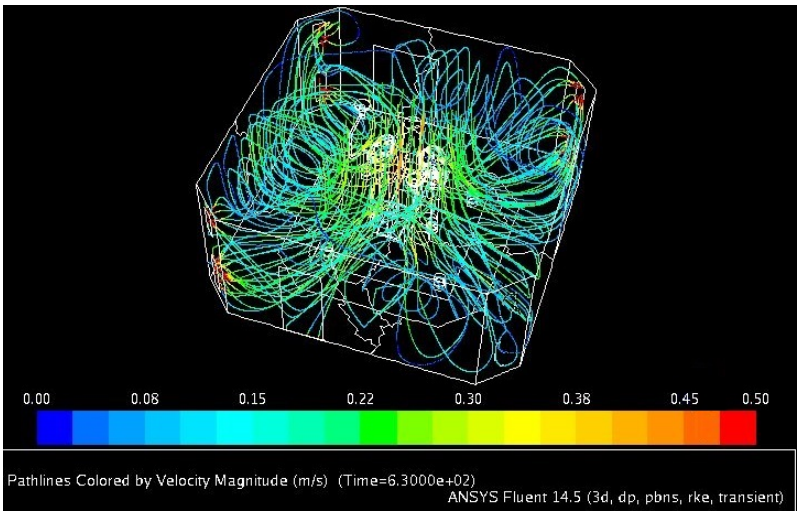

Figure 5.32: Pathlines colored by velocity magnitude within all the space of the OT, for the case B2

Figure 5.33 shows the contours of velocity in a plane which passes through the corner where both of the exhaust grilles are obstructed and through the opposite one, as represented on the right side of the figure. It is possible to note the absence of velocity on the wall without the exhaust grilles and an incomplete throw of the air coming from the ceiling diffuser in that side.

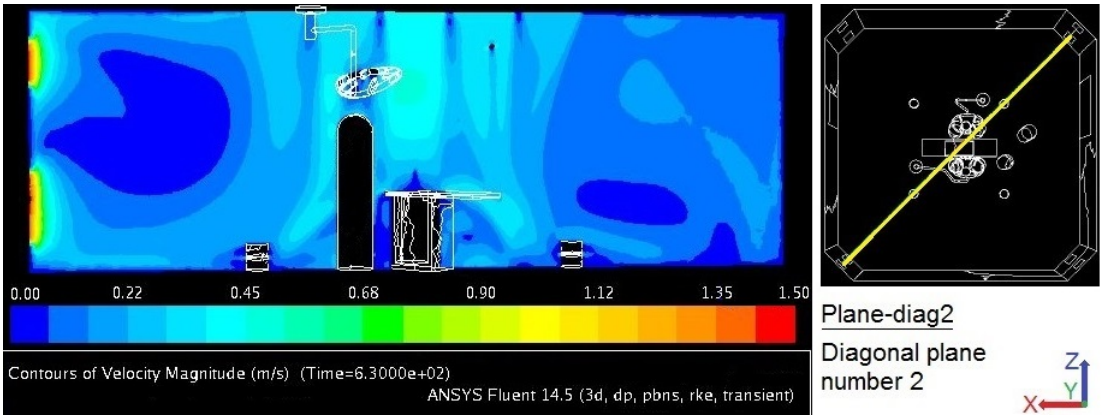

Figure 5.33: Velocity contours on the plane called diag-2, according to the figure on the right, for the case B2

Because of the closure of the two exhaust grilles there is an increase of particle presence in proximity of the other corners, even though, near the corner obstructed there is a presence of a particle recirculation, as it can be seen in Figure 5.34. In fact the air flow prefers outcomes through this way, more than remain within the room.

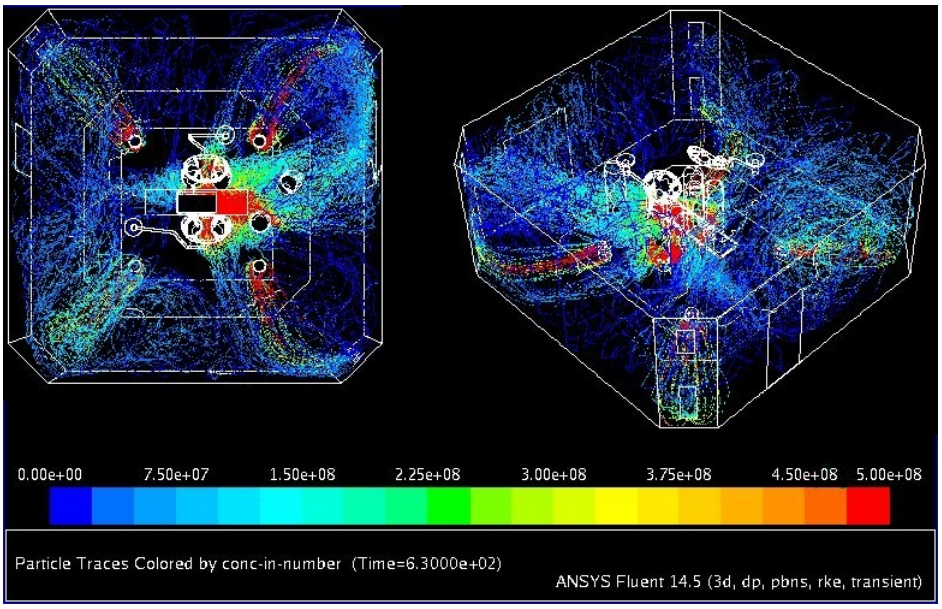

Figure 5.34: Plant and isometric view of the particle traces within all the space of the OT, colored by velocity magnitude within, for the case B2

Figure 5.35 illustrates the concentration on the diagonal plane described before. It is possible to observe the particle recirculation afore mentioned

just in proximity of the corner with the two exhaust grilles obstructed. In the opposite side the particle concentration is less than there and it is not possible to see in the figure because of the reference scale.

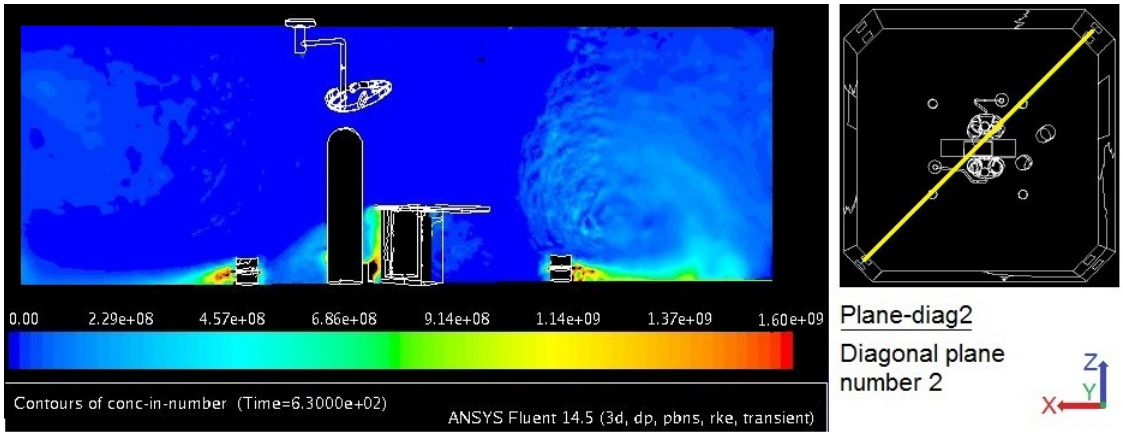

Figure 5.35: Concentration contours (in pp/m^3) on the plane called diag-2, according to the figure on the right, for the case B2

Even though the absence of two exhaust grilles, the ceiling diffuser is designed in way to assure a concentration value on the surgical table, equal to zero.

C2: Behavior of the ventilation system with the main door open

The C2 configuration take into account the situation for which the main door is open. In general this situation is enough common during the surgical operations.
Even though door opening during an operation must be reduced as much as possible (due to hygienic requirements and hospital policy), it is found that up to approximately 100 door openings during one operation may occur. The high number of door openings observed during several operations is obviously a source of concern. Thus, it is important to have an indication of the importance in terms of potential bacteria transport from inside and outside the critical zone to the patient's wound where it may cause infections [52]. For this reason it was decided to consider this situation and verify the behavior of the ceiling filtering system in respect on these events. In Figure 5.36 there are the pathlines of the airflow entering in the room from the ceiling diffuser. It is possible to observe the pathlines coming out towards the adjoined rooms, through the main sliding door.

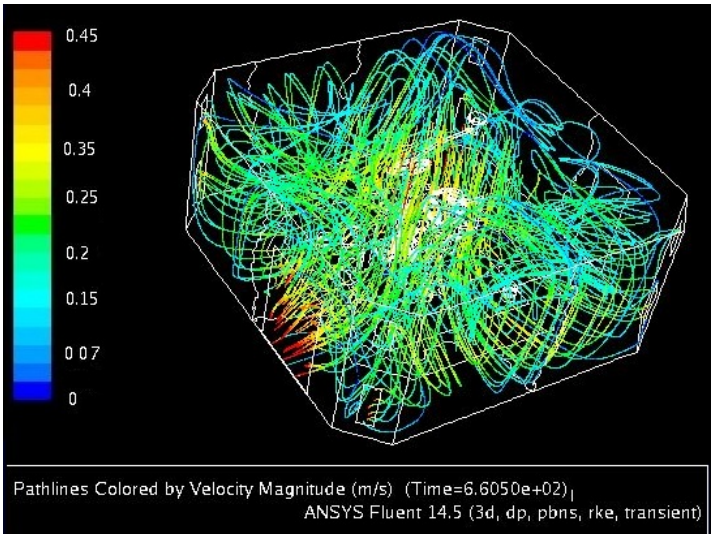

Figure 5.36: Pathlines colored by velocity magnitude within all the space of the OT, for the case C2

The velocity vectors in Figure 5.37, helps to note the airflow direction towards the open door, and the Figure 5.38 evidences the influence of the door opening on the ceiling diffuser throw. In fact, it can be seen in Figure 5.38 the airflow coming into the OT is like pushed out of the it and it is mainly true for the air coming from the external filters. For this reason, on the table the particle concentration measured in the points of interest is always equal to zero.

Figure 5.37: Velocity vectors on the plane called q, according to the figure on the right, for the case C2

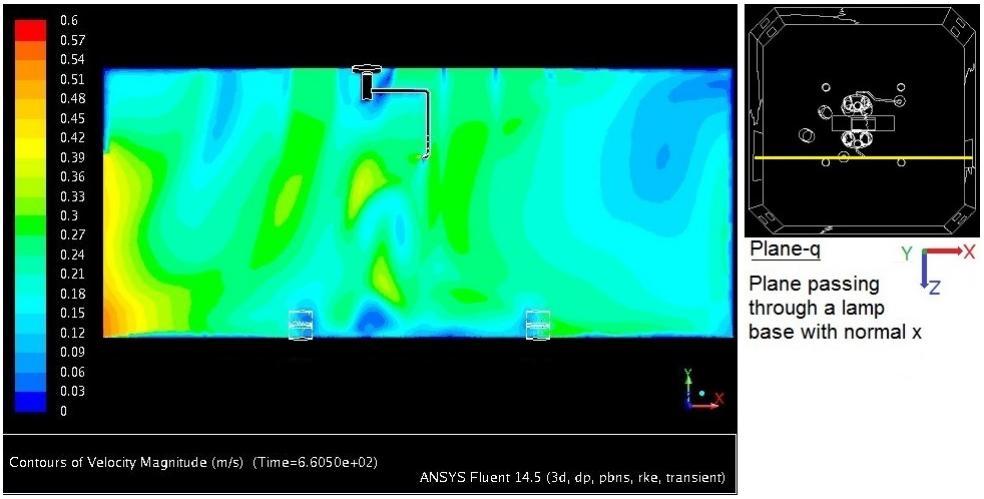

Figure 5.38: Velocity contours on the plane called q, according to the figure on the right, for the case C2

D1 and D2: A new configuration of the ceiling filtering system and lamps

The OT configurations treated in this section are different from the other cases discussed before. In this cases, the main aim is the study of the airflow path behavior over the operating table and critical area when the arms of the two surgical lamps are attached exactly at the center of the ceiling diffuser. The ceiling diffuser layout of these configurations was already described in Figure 4.20 in Chapter 4. As it can be seen in Figure 4.20, the new ceiling diffuser has two extra low-speed filters and one high-speed filter less than before. The high-speed filter missing is the central one.

In the following part of this section will be discussed the results of the CFD simulations delivered with the external (case D1) and internal (case D2) contamination layout of the critical area in order to evaluate some possible differences with the standard layout used in the previous simulation.

Case D1

Due to the different positions of the surgical lamp arms, and the missing of the central high speed velocity filter in which now it is positioned the lamp joint, the airflow path in the critical area, and in particular over the operating table, has a different behavior. Figure 5.39, clear shows how the absence of the central high speed filter creates a low velocity area just in the center of the critical area.

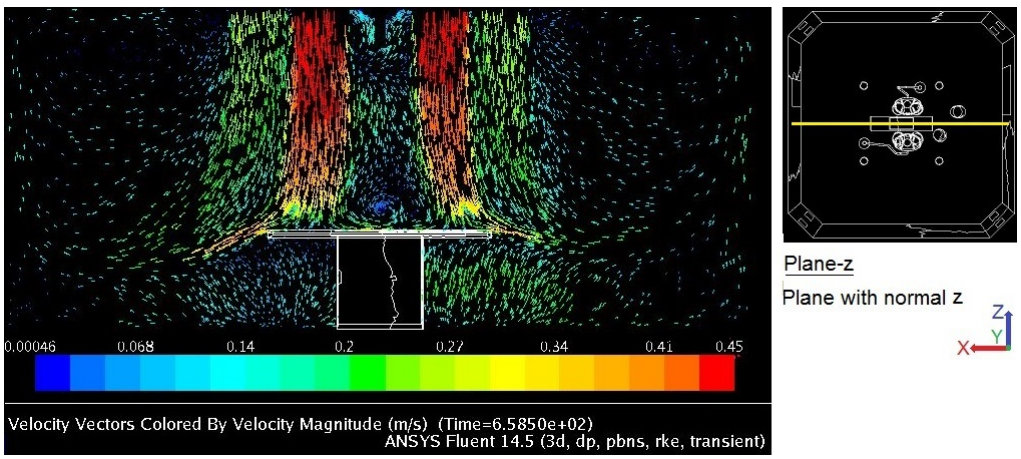

Figure 5.39: Velocity vectors on the plane called z, according to the figure on the right, for the case D1

The presence of the two high speed filters adjacent to the central arm joint plus the presence of the particle sampling probe over the table, creates some turbulence over the operating table in the area on the thorax. This weak central airflow, just in the near by of the thorax area, may causes some problems during the operation. Figure 5.40, clearly explains what before mentioned. In addition, the connenction of the surgical lamps with the ceiling diffuser, in this configuration, creates a stagnant area with turbulence just beneath the ceiling.

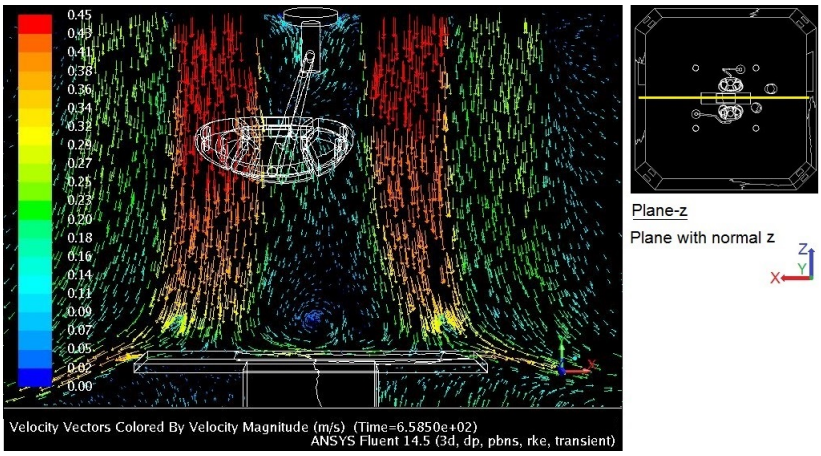

Figure 5.40: Detail of velocity vectors on the plane called z, according to the figure on the right, for the case D1

This configuration, as shown in Figure 5.40, tends to creates a weak contamination protection in the central area of the operating table close

to the thorax area. In the zone close to the feet and head of the table, the protection class offered by the aiflow is acceptable and almost equal to the other configuration simulated. Another important element of air flow disturbance, due to the central surgical lamp joints, as in case D1 and D2, is the obstruction of the vertical airflow caused by the two arms of the lamps as shown in Figure 5.41.

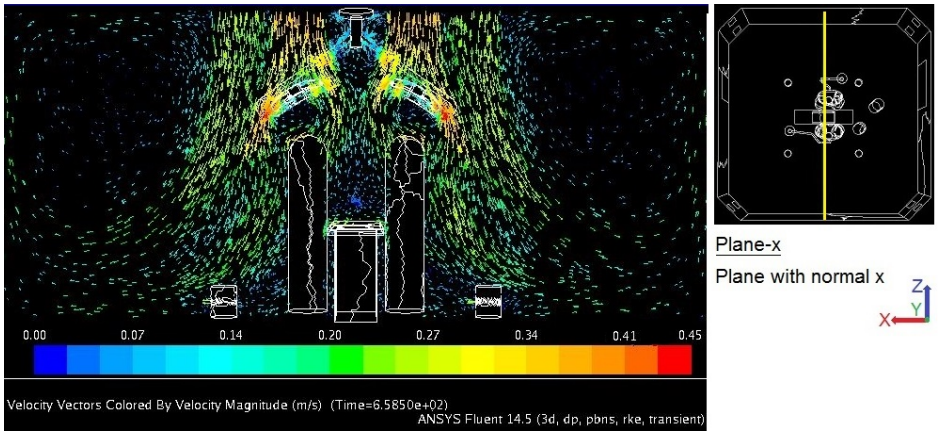

Figure 5.41: Velocity vectors on the plane called x, according to the figure on the right, for the case D1

In this case many airflow turbulence and deviations can easily be detected close to the arms and under the lamps, as shown in Figure 5.42.

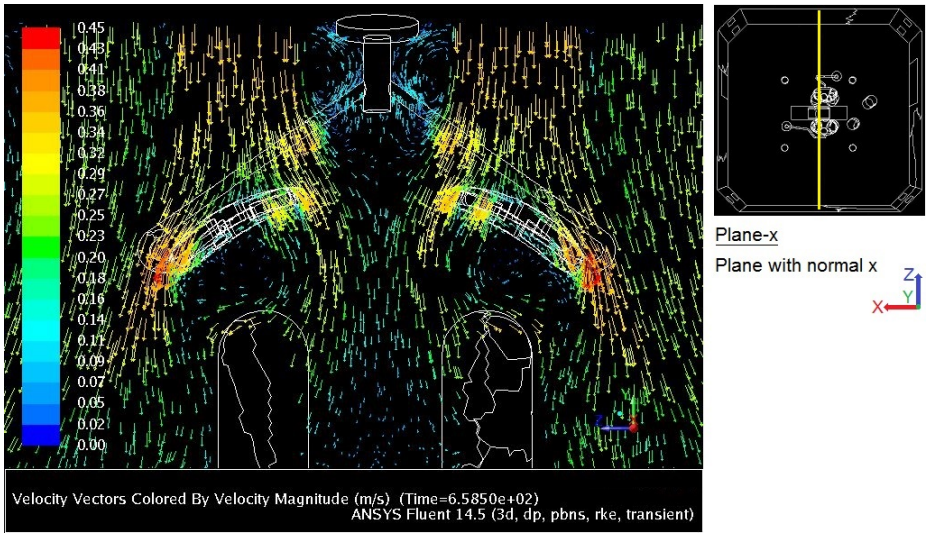

Figure 5.42: Detail of velocity vectors on the plane called x, according to the figure on the right, for the case D1

Even though the presence of many disturbances in the airflow path over the operating table with respect to the other cases simulated, also in this case, the airborne particle concentration measured over the operating table at the three sampling points simulated, is equal to zero in all the three points. In fact, the particle concentration distribution seems mot to affect the critical area as shown in Figure 5.43 and 5.44.

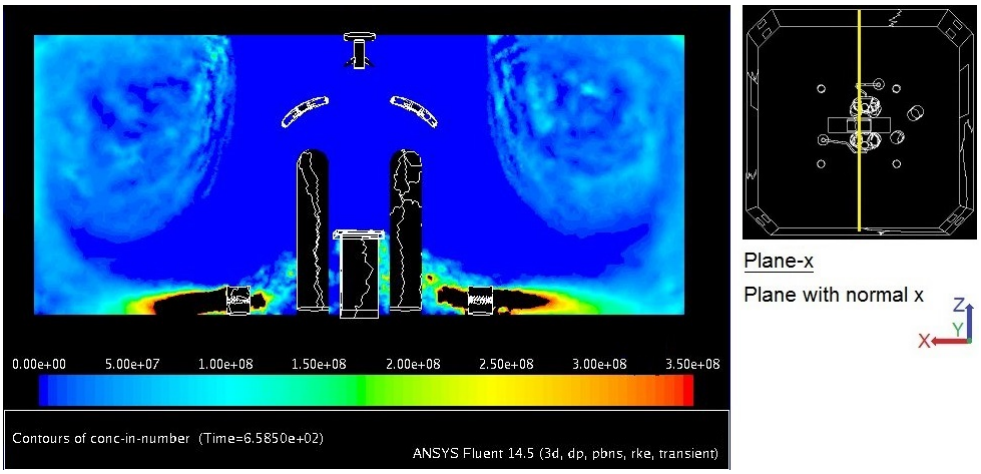

Figure 5.43: Concentration contours (in pp/m^3) on the plane called x, according to the figure on the right, for the case D1

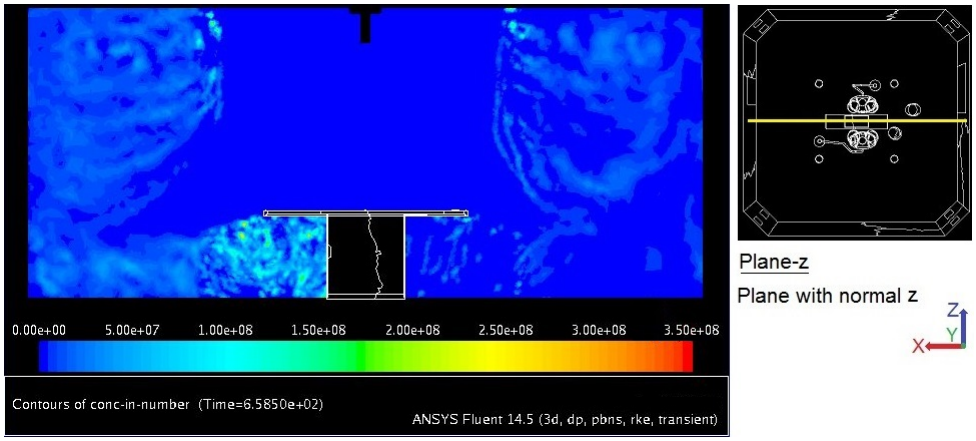

Figure 5.44: Concentration contours (in pp/m^3) on the plane called z, according to the figure on the right, for the case D1

The presence of the two large recirculation vortex close to the vertical walls and the ceiling has the same shape and behavior of the other cases simulated.

Case D2

Case D2 was run with the internal contamination layout. The macroscopic behavior of airflow stream is the same as for the case D1, as how it can be seen in Figure 5.45 and Figure 5.46.

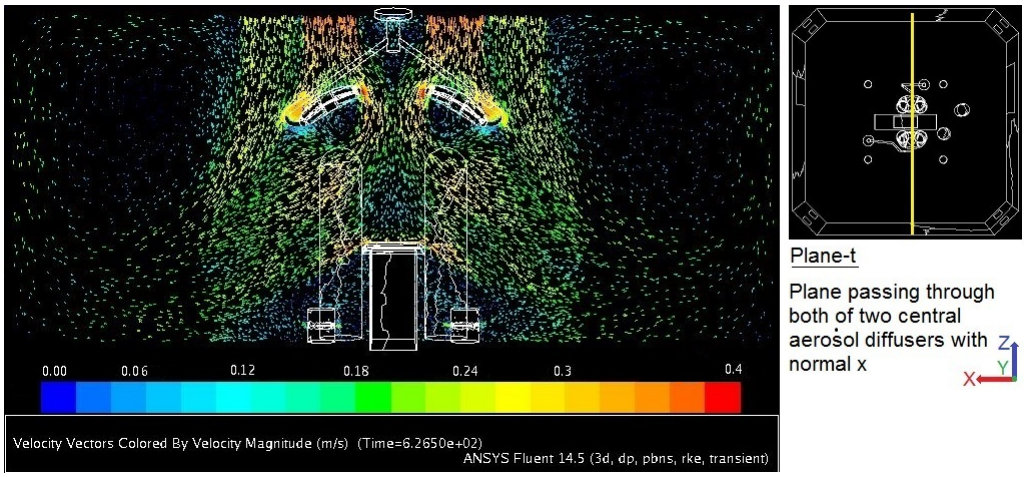

Figure 5.45: Velocity vectors on the plane called t, according to the figure on the right, for the case D2

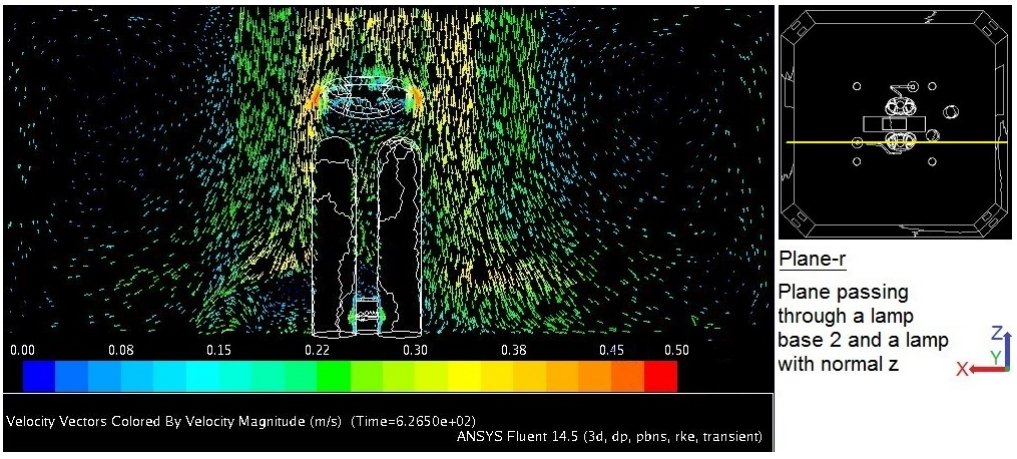

Figure 5.46: Velocity vectors on the plane called r, according to the figure on the right, for the case D2

The main differences, instead, are present in the distribution of airborne particles, especially close to the anesthetist and between the two couples of dummies, as shown in Figure 5.47.

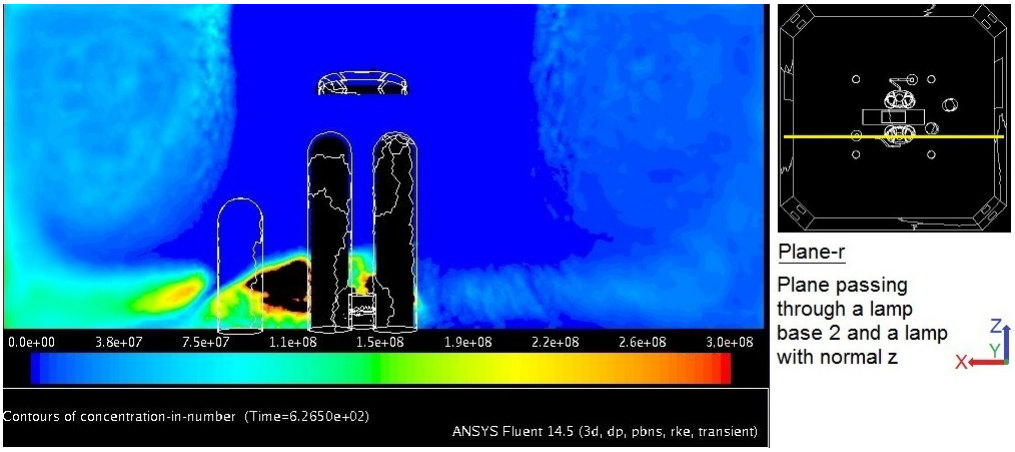

Figure 5.47: Concentration contours (in pp/m^3) on the plane called r, according to the figure on the right, for the case D2

The conclusion of this case is, even though the simulated values of particle concentration above the surgical table are equal to zero, the vortex present in the there is very dangerous in case of presence of contamination which, if it enter in this vortex, may remain there endangering the health of the patient and the surgical staff.

Chapter 6

Conclusions

This master thesis work is focused on the study of a simulated model for the evaluation of the protection class of the ventilation system installed in operating theaters and its subsequent validation through standardized experimental measurements. The need of a safe and clean environment in operating room is an important aim for both the protection of surgical staff and patients. Surgical staff within an operating room are commonly considered one of the main source of contaminants but in the same way, depending on the type of surgical operations and of ventilation systems, may also be affected by the contamination generated during the operations. Therefore, an accurate evaluation of the protection class from airborne contamination given by the ventilation system, and in particular of the ceiling diffuser, is of great importance. As mentioned in chapter 3, many standards and technical documents have been released regarding the design, construction and performance test of operating rooms and contamination control. Although, the great amount of material on this topic, nowadays there is no a clear and unique procedure or standard for the implementation of a real experimental performance test on the protection class (SG) of the ventilation system of an operating room. This lack, is mainly due to the great variance of the layout and setting which an operating room may have during its usage. Even though, an operating room may be compared for certain instance with a cleanroom, some differences clearly arise. Within an operating room, movements of people, medical equipment and drugs have standardized path and procedure which most of the time are not respected because of the uncertainties which rely on surgeons, patients and the consequences of the ongoing operations. Therefore, an operating room rarely has a fixed layout or procedure. This aspect influence a lot the way of designing and testing the protection class performances of an OT HVAC system. Among all the standards and procedures discussed in this work, related with the way of performing experimental tests of the

protection class, the German standard DIN 1964-4 [32] was chosen as the reference one. This choice was adopted because the experimental procedure suggested by this standard has seemed to be the one with the most detailed and simple setting specifications for a quantitative and repetitive tests. The experimental tests were conducted in a real operating room which has the necessary characteristics as specified by the German standard. The real OT chosen, moreover, is equipped with a differential velocity H14 HEPA filtered ceiling diffuser which makes the study even more interesting. So, after having chosen the standard to be followed and the real OT in which carrying out the tests, were also decided the various layout setting of the operating rooms for which the CFD simulation have been conducted. Six different OT scenarios were evaluated via time variant CFD simulations with the aim to investigate the performance and the behavior of the OT ventilation and diffusion systems. Chapter 3 gives all the necessary informations on the model and settings used for the implementation of the CFD software simulation used, in this case ANSYS Fluent. In more detail, it was investigated how the airborne contaminants and the air flow path behavior change with respect of different boundary conditions imposed in the CFD simulation model. The first two simulations, case A1 and A2, followed exactly the specifications imposed by the DIN standard. Results obtained by the simulated scenarios gave interesting results which in large part agree with the experimental results. In particular, the values of airborne particle concentration over the operating table have almost the same values, with only a gap for the values at the thorax area. However, as discussed in Chapter 5, those gaps at thorax area may not be considered because of the uncertainties of the fabric of the real dummies used during experimental tests. In fact, even though the differences, the protection class evaluated via CFD model and the measured one have a difference of 12 % for both case A1 and A2 for the thorax area, and zero for the feet and head area. Moreover, the velocities, temperature and airborne particle concentrations measured on field during the experimental tests diverge from the values obtained from the simulated scenarios, case A1 and A2, of at maximum 24 %. Large errors between simulated and measured points have been encountered for some areas of the OT environment which with good approximation are caused by a different layout setting from the ones simulated in the CFD model, e.g. presence of extra surgical arms, medical and experimental equipment in OT as amply described in chapter 5. This extra presence of objects within the OT environment has perturbed the fluid dynamics of the air flow from the one simulated and therefore also the original measurements. The validation process of the simulated scenarios was only carried out for the first two cases, briefly for A1 and mainly for A2, due to time restriction in having available a real OT room equipped. How-

ever, the good results obtained from the validation of the first two cases, give the possibility to assume that the results of the other cases simulated, B2, C2, D1 and D2, can also be considered validated. This assumption, even if strong, can be supported by the procedures, settings and fluid dynamic models used for the implementation of the other 4 cases which are equal to the first two cases. Case B2, was run in order to evaluate how the contamination level within the OT behaves when one corner of the OT room is without air exhaust grilles. In this scenario it is evident the particle recirculation caused by the absence of the exhaust grilles in corner called 2. The ventilation system, however, is able to sweeping away the contamination and especially the presence of the high speed filters assure a good level of cleanliness in the critical zone. The removal of particles in the room is assign to the other three corners where the particle presence became consistent (mainly in the return grilles at the opposite corner of the number 2) because the air flow prefers outcomes through this way, more than remain within the room. In case C2, the emphasis is concentrated to the response of the ventilation system to a door opening. This simulation is carried out assuming that the main sliding door is completely open. The simulation shows a trend mainly for the air streams out-coming from the peripheral filters to be carrying out through the door, due to the less velocity of these streams. The air wall creates by the airflow patter is less strong than the other configurations but is still assure a good protection against the contamination. Case D1 and D2, as mentioned before, have been evaluated only via CFD , with a large difference with respect to the other cases in order to study how the different position of the surgical lamps may influence the fluid dynamic in the nearby of the operating table under the same layout setting of the DIN standard used for the other cases. The absence of the central high speed filter and the presence of the two lamp arms under the medium speed filters provokes the appearance of vortexes over the operating theater, exactly in the most critical area. Hence, from the simulation it is suggest to locate the lamp joints in the periphery of the ceiling diffuser, in order to have the high number of undisturbed filters on the most demanding zone, over the surgical table, and to bring down the contamination.

In conclusion, it can be said that the work done in this master has in many parts fulfilled the initial aims. The CFD simulations of the different scenarios of the real OT room chosen as reference has given interesting results. The experimental tests of case A1 and A2 well agree with the results of the correspondent CFD simulations. The evaluation of the protection class of the OT room calculated by means of the standard DIN 1964-4 [32] has given almost same results for both numerical and real calculations. Based

on these last assumptions, it can be stated that in the future, for cases with similar conditions to these used in this work, OT room performances may be evaluated via CFD and numerical tools with a good grade of accuracy. However, dealing with OT rooms where the safety and health of humans are at risk, and it is necessary to refine many aspects of the simulation taking also into account humans and random uncertainties and failures which CFD simulations cannot yet discover. Future improvements must be done from the validation side, in fact it is necessary to develop less invasive test conditions using tools which ensure almost zero release of particles, and, from the simulation point of view, in meshing process, modeling of the boundary conditions and interaction phenomena between two or more phases, e.g. fluid-particle, in order to have a wider and more accurate simulation of the real phenomena.

Nomenclature

A_0	Constant	$[-]$
A_{ref}	Reference area covered by unidirectional flow	$[m^2]$
A_p	Particle area	$[m^2]$
C_n	Maximum allowed concentration for the class n	$[pp/m^3]$
C_{Aer}	Particulate concentration in the aerosol	$[pp/m^3]$
C_d	dispersed-phase mass concentration	$[kg_d/kg_c]$
C_μ	Is a $\kappa - \varepsilon$ model parameter (usually 0.09)	$[-]$
C_{ref}	Reference concentration	$[pp/m^3]$
C_x	Particle concentration measured in the x-location	$[pp/m^3]$
c_p	Specific heat at constant pressure	$[J/kg\,K]$
D	Particle diameter	$[m]$
d_p	Particle diameter	$[m]$
F	Different types of forces	$[N]$
g	Acceleration of gravity	$[m/s^2]$
h	Convective heat transfer coefficient	$[W/K\,m^2]$
κ	Turbulent kinetic energy	$[J/kg]$
k	Thermal diffusivity	$[W/K\,m]$
L	Average particle spacing	$[m]$
l	Lenght	$[mm]$
$\dot{m}$	Mass-flow rate	$[kg/s]$
m_p	particle mass	$[kg]$
P	Pressure	$[Pa]$
Q_{ref}	Referemce source strenght	$[pp/h]$
R_{ij}	Component of the Reynolds stress tensor	$[m^2/s^2]$
s_{ij}	Component of the tensor of deformation rate of a fluid element	$[1/s]$

S_{ij}	Mean component of local strain rate	$[1/s]$
SG_x	Protection class	$[-]$
S_p	Source termm for particulate	$[kg/m^3 s]$
Stk	Stokes number	$[-]$
T	Temperature	$[K]$
u_i, u_j	Velocity component	$[m/s]$
u_i', u_j'	Turbulent fluctuation component of velocity	$[m/s]$
U_i, U_j	Mean velocity component	$[m/s]$
u^+	Dimensionless velocity	$[-]$
u_τ	Friction velocity	$[m/s]$
$\mathbf{v}$	Air velocity vector	$[m/s]$
v	Velocity	$[m/s]$
V_{Aer}	Aerosol volumetric flow	$[m^3/h]$
V_c	Continuous phase volume	$[m^3]$
V_d	Dispersed phase volume	$[m^3]$
δV	Infinitesimal volume	$[m^3]$
v_{ref}	Outlet air velocity of unidirectional flow	$[m/s]$
w	Width	$[mm]$
x_i, x_j	Component of vector coordinate	$[m]$
y^+	Dimensionless distance from the wall	$[-]$
Z	Ratio between particle mass flowrate and air massflowrate	$[-]$

Greek Letters

α_d	Dispersed phase volume fraction	$[-]$
α_c	Continuous phase volume fraction	$[-]$
δ_{ij}	Kronecker delta	$[-]$
ε	Rate of dissipation of turbulent kinetic energy	$[m^2/s^3]$
θ_R	Reference temperature	$[K]$
μ	Fluid viscosity	$[Pa\,s]$
μ_t	Turbulent viscosity	$[kg/m\,s]$
ν_t	Turbulent kinematic viscosity	$[m^2/s]$
ρ	Fluid density	$[kg/m^3]$
ρ_d	Bulk density	$[kg/m^3]$
ρ_c	Continuous phase density	$[kg/m^3]$

ρ_m	Mixture density	$[kg/m^3]$
σ	Standard deviation of particle pluctuation velocity	$[m/s]$
τ_{ij}	Component of shear stress tensor	$[N/m^2]$
τ_v	Relaxation time of the particle	$[s]$
τ_F	Characteristic fluid time	$[s]$
Φ	Mean value of generic parameter	$[of\ parameter]$
φ	Value of generic parameter	$[of\ parameter]$
φ'	Turbulent fluctuation component of generic parameter	$[of\ parameter]$
ω	Eddy "turn-over" frequency	$[1/s]$
ω_k	Angular velocity	$[rad/s]$
$\tilde{\Omega}_{ij}$	Mean rate-of -rotation tensor	$[1/s]$

Acronyms

AFNOR	Association Francaise de Normalisation
AHU	Air Handle Unit
AMC	Airborne Molecular Contamination
ANSI	American National Standards Institute
AR	Aspect Ratio
ASHE	American Society for Healthcare Engineering
ASHRAE	American Society of Heating, Refrigerating and Air Conditioning Engineers
ASM	Algebraic Stress Model
ASMM	Algebraic Slip Mixture Model
CEN	Comité Européen de Normalisation
CFD	Computational Fluid Dynamics
CFU	Colony Forming Unit
DEHS	Di-Ethyl-Hexyl-Sebacat
DIN	Deutsches Institut für Normung
DOP	Di-Octyl Phthalate
DNS	Direct Numerical Simulation
DPM	Discrete Phase Model
EE	Eulerian-Eulerian
EN	European Standard

EWT	Enhanced Wall Treatment
FT	Front Tracking
HAI	Hospital Acquired Infections
HTM	Health Technical Memorandum
HVAC	Heating, Ventilating and Air Conditioning
INAIL	Istituto Nazionale Assicurazione contro gli Infortuni sul Lavoro
ISO	International Organization for Standardization
ISPESL	Istituto Superiore Per La Prevenzione E La Sicurezza Del Lavoro
LES	Large Eddy Simulation
LEV	Local Exhaust Ventilation
LS	Level Set
MPPS	Most Penetrating Particle Size
NEWF	Non-Nquilibrium Wall Function
OT	Operating Theater
RANS	Reynolds-Averaged Navier-Stokes
RSM	Reynolds Stress Model
SG	Schutzgrades
SIS	Swedish Institute of Standardization
SSI	Surgical Site Infection
SWF	Standard Wall Function
SWKI	Schweizerischer Verein von Warme- und Klimaingenieuren Sekretariat
TLV	Threshold Limit Value
ULF	Unilateral Flow
UNI	Ente Nazionale Italiano di Unificazione
UCV	Ultra-clean Ventilation
VAC	Ventilation and Air-Conditioning
VCCC	Ventilation and air-Conditioning system for Contamination Control
VOF	Volume Of Fluid

Bibliography

[1] S. H. Ho, L. Rosario e M. M. Rahman, *Three-dimensional analysis for hospital operating room thermal comfort*, Applied Thermal Engineering, vol. 29, pp. 2080–2092, 2009

[2] A. E. Andersson, *Patient Safety in the Operating Room - Focus on Infection Control and Prevention*, Work of Thesis, pp. 7-18, University of Gothenburg, 2013

[3] Z. Rui, T. Guangbei e L. Jihong, *Study on biological contaminant control strategies under different ventilation models in hospital operating room*, Building and Environment, vol. 43, pp. 793–803, 2008

[4] T. T. Chow e X. Y. Yang, *Ventilation performance in the operating theatre against airborne infection: numerical study on an ultra-clean system*, The Journal of Hospital Infection, vol. 59, pp. 138–147, 2005

[5] E. G. Dascalakia, A. Lagoudib, C. A. Balarasa, A. G. Gaglia, *Air quality in hospital operating rooms*, Building and Environment, vol. 43, pp. 1945–1952, 2008

[6] C. Méndez, J.F. San José, J.M. Villafruela, F. Castro, *Optimization of a hospital room by means of CFD for more efficient ventilation*, Energy and Buildings, vol. 40, pp. 849–854, 2008

[7] A. Stacey, H. Humphreys, *A UK historical perspective in ioerating theatre ventilation*, The Journal of Hospital Infection, vol. 52, pp. 77-80, 2002

[8] J. Charnley, N. Eftekhar, *Postoperative infection in total prosthetic replacement arthroplasty of the hip-joint. With special reference to the bacterial content of the operating room*, The British Journal Surgery, vol. 56, pp. 641-9, 1969

[9] W. Whyte, R. Hodgson, J. Tinkler, *The importance of airborne bacterial contamination of wounds*, The Journal of Hospital Infection, vol. 3, pp. 123-35, 1982

[10] C. Balaras, E. Dascalaki e A. Gaglia, *HVAC and indoor thermal conditions in hospital operating rooms*, Energy and Buildings, vol. 39, pp. 454–470, 2007

[11] UNI 11425:2011, Impianto di ventilazione e condizionamento a contaminazione controllata (VCCC) per il blocco operatorio - Progettazione, installazione, messa in marcia, qualifica, gestione e manutenzione, UNI, Ente Nazionale Italiano di Unificazione, Milan, Italy, 2011

[12] Decreto del Presidente della Repubblica, Italy, 14th Genuary 1997

[13] T.T. Chow, L. Zhang, B. Wei, *The integrated effect of medical lamp position and diffuser discharge velocity on ultra-clean ventilation performance in an operating theater*, Indoor and Built Environment, vol. 15, pp. 315-331, 2006.

[14] B. F. Friberg, S. Burman, L. G. Lundholm, R. Ostersson, *Inefficiency of upward displacement operating theater ventilation*, The Journal of Hospital Infection, vol. 33, pp. 263-72, 1996

[15] T. T. Chow e X. Y. Yang, *Ventilation performance in operating theatres against airborne infection: review of reserch activities and practical guidance*, Journal of Hospital Infection, vol. 56, pp. 85–92, 2004

[16] UNI EN 1822 - parts 1-4, *Filtri per l'aria ad alta efficienza (EPA, HEPA e ULPA)*, UNI, Ente Nazionale Italiano di Unificazione, Milan, Italy, 2010

[17] UNI EN 779, *Filtri d'aria antipolvere per ventilazione generale. Determinazione della prestazione di filtrazione*, UNI, Ente Nazionale Italiano di Unificazione, Milan, Italy, 2012

[18] C.M. Joppolo, F.Romano, *Diffusione dell'aria in sala operatoria: simulazione CFD e progetto di un laboratorio di test*, Report of a research study, Milan, December 2012

[19] C. M. Joppolo, F. Romano e L. Sabatini, *Camere bianche e tecniche di controllo della contaminazione*, April 2012

[20] UNI EN ISO 14644 - parts 1-10, *Cleanrooms and associated controlled environments*, UNI, Ente Nazionale Italiano di Unificazione, Milan, Italy, 2011

[21] F. Martelli, C. Petrigni, S. Iudicello, R.Scarabotti, A. Fadda, Notiziario dell'Istituto Superiore di Sanità, *Una nuova norma UNI: Impianti di ventilazione e condizionamento a contaminazione controllata (VCCC) per il blocco operatorio*, vol. 25, pp. 3-6, October 2012

[22] EU-GMP-Guide to Good Manufacturing Practice, *Annex 1, Manufacture of Sterile Medicinal Products*, European Committee, Brussels, BE, 2008

[23] FDA-Food and Drag Administration-Current Good Manufacturing Practice, European Draft Guidance, Rockville, Maryland, USA, 2008

[24] *Linee guida sugli standard di sicurezza e di igene del lavoro nel reparto operatorio*, ISPESL, Istituto Superiore per la Prevenzione E la Sicurezza del Lavoro, Rome, Italy, 2009

[25] Health Technical Memorandum 03-01: *Specialised ventilation for healthcare premises. Part A: Design and validation*, Department of Health / Estates and Facilities Division, Leeds, England, November 2007

[26] ISO 21501-4, *Determination of particle size distribution — Single particle light interaction methods: Light scattering airborne particle counter for clean spaces*, ISO, t International Organization for Standardization, Geneva, Switzerland, 2007

[27] SIS-TS 39:2012, *Microbiological cleanliness in the operating room - Preventing airborne contamination - Guidance and fundamental requirements*, SIS, Swedish Standard Institute, Stockholm, Sweden, 2012

[28] NF S90-351, *Établissements de santé — Zones à environnement maîtrisé — Exigences relatives à la maîtrise de la contamination aéroportée*, AN-FOR, Association Francaise de Normalisation, Paris, France, 2013

[29] UNI EN ISO 14698:1-2, *Camere bianche ed ambienti associati controllati: Controllo della biocontaminazione*, UNI, Ente Nazionale Italiano di Unificazione, Milan, Italy, 2004

[30] Standard 170-2013, *Ventilation of health care facilities*, ANSI/ASHRAE/ASHE, TuIlie Circle, Atlanta, United State of America, 2013

[31] SWKI 99-3E, *Heating, ventilation and air-conditioning system in hospitals*, Schweizerischer Verein von Warme- und Klimaingenieuren Sekretariat, Schonbuhl, 2004

[32] DIN 1964-4, *Ventilation and air conditioning, Part 4: Ventilation in buildings and rooms of health care*, Deutsches Institut für Normung, Berlin, December 2008

[33] O. Di Marino, A. M. Capra, C. Rossi, *Test di sale operatorie in condizioni operative simulate - metodo di prova, risultati e criticità*, Ascca News, vol.1, pp.21-27, January 2011

[34] H. Versteeg e W. Malalasekra, *An Introduction to Computational Fluid Dynamics*, Second Edition, Pearson Education, 2009

[35] Z. Sun, S. Wang, *A CFD-based test method for control of indoor environment and space ventilation*, Building and Environment, vol. 45, pp. 1441–1447, Hong Kong, 2010

[36] J. Swift, E. Avis, B. Millard, T. M. Lawrence, *Air distribution strategy impact on operating room infection control*, Proceedings of Clima 2007 WellBeing Indoors, Helsinki, Finland, 2007

[37] F. Memarzadeh, A. Manning, *Comparison of operating room ventilation systems in the protection of the surgical site*, ASHRAE Transactions, vol. 108, 2002

[38] F. Memarzadeh, Z. Jiang, *Effect of Operation Room Geometry and Ventilation System Parameter Variations on the Protection of the Surgical Site*, IAQ, 2004

[39] R. Kameel, E. E. Khalil, *Simulation of flow, heat transfer and relative humidity chararacteristics in air-conditioned surgical operating theaters*, 41st Aerospace Sciences Meeting and Exhibit, Reno, Nevada, January 2003

[40] H. Brohus, M. L. Hyldig, S. Kamper, U.M. Vachek, *Influence of disturbances on bacteria level in an operating room*, Proceedings of Indoor Air 2008: The 11th International Conference on Indoor Air Quality and Climate, Copenhagen, Denmark, 2008

[41] D. Shuyun, T.Guangbei, C. Rongguang, Y. Zhenfeng, *Numerical study on effects of door-opening on airflow patterns and dynamic cross-contamination in an ISO class 5 operating room*, Transactions of Tianjin University, vol.15, pp. 210-215, Tianjin, China, 2009

[42] Y.C. Tung, Y.C. Shih, S.C. Hu, *Numerical study on the dispersion of airborne contaminants from an isolation room in the case of door opening*, Applied Thermal Engineering, vol. 29, pp. 1544–1551, 2009

[43] J. Srebrica, V. Vukovica, G. Heb, X. Yang, *CFD boundary conditions for contaminant dispersion, heat transfer and airflow simulations around human occupants in indoor environments*, Building and Environment, vol. 43, pp. 294–303, 2008

[44] W.A.C. Zoon, M.G.L.C. Loomans, J.L.M. Hensen, *Testing the effectiveness of operating room ventilation with regard to removal of airborne bacteria*, Building and Environment, vol. 46, pp. 2570-2577, 2011

[45] P. V. Nielsen, F. Allard, H. B. Awbi, L. Davidson, A. Schalin. *Fluidodinamica computazionale applicata alla progettazione della ventilazione*, Dario Flaccovio Editore, Palermo, 2009

[46] F. Inzoli, Politecnico of Milan, *Notes from lessons about Computational Fluid dynamics*, a.a. 2012-2013

[47] M. Chmielewski, M. Gieras, *Three-zonal Wall Function for $k-\varepsilon$ turbulence models*, Computational Methods in Science and Technology, vol. 19, pp. 107-114, 2013

[48] L. Marocco e A. Mora, *CFD modeling of the Dry-Sorbent-Injection process for flue gas desulfurization*, Separation and Purification Technology, vol. 108, pp. 205–214, 2013

[49] T. T. Chow and X.Y. Yang, *Performance of ventilation system in a non-standard operating room*, Building and Environment, vol. 38, pp. 1401 – 1411, 2003

[50] T.-H. Shih, W. W. Liou, A. Shabbir, and J. Zhu. , W. W. Liou, T. H. Shih, A. Shabbir e J. Zhu, *A New k- epsilon Eddy-Viscosity Model for High Reynolds Number Turbulent Flows - Model Development and Validation*, Computers Fluids, vol. 24, pp. 227-238, 1995

[51] P. J. Roache, *Perspective: A Method for Uniform Reporting of Grid Refinement Studies*, Journal of Fluids Engineering, vol. 116.3, pp. 405-413, Albuquerque (NM), United States of America, 1994

[52] H. Brohus, M. L. Hyldig, S. Kamper and U. M. Vachek, *Influence of disturbances on bacteria level in an operating room*, International Conference on Indoor Air Quality and Climate, 2008